

# The Recovery of Kish Graphite from Secondary Sources

---

By Robert Frost

Thesis submitted to the University of Birmingham for the Degree of Master of Research

School of Chemical Engineering

College of Engineering and Physical Sciences

December 2014

UNIVERSITY OF  
BIRMINGHAM

**University of Birmingham Research Archive**

**e-theses repository**

This unpublished thesis/dissertation is copyright of the author and/or third parties. The intellectual property rights of the author or third parties in respect of this work are as defined by The Copyright Designs and Patents Act 1988 or as modified by any successor legislation.

Any use made of information contained in this thesis/dissertation must be in accordance with that legislation and must be properly acknowledged. Further distribution or reproduction in any format is prohibited without the permission of the copyright holder.

## **Abstract**

With the worldwide demand of graphite increasing, so the availability, cost and quality of graphite is under renewed scrutiny - with the vast majority of graphite being mined from primary mineral resources, and with these mines located in only a few significant countries, considerations of availability and sustainability have led to an increasing dependence on synthetic graphite to meet industrial needs. However, the production of synthetic graphite is costly and time-consuming, so other potential sources are keenly sought after for strategic and economic reasons.

One potential source is the recovery of 'kish' graphite from the steel making process: It has been observed that present within the dust produced as waste in steel plants, graphite flakes are found in varying quantities, sizes and purity. Seven samples taken from different locations in Tata Steel's Scunthorpe steel plant were analysed, and the two from the desulphurisation plant were found to contain enough graphite to warrant further testing. This testing (broadly) consisted of two goals: Separating the kish graphite from the excess waste dust, and refining and purifying the separated graphite to a degree that renders it usable (typically >95% Carbon content).

Froth flotation was found to be an extremely effective way of achieving this, with purities of >90% being achieved from a single flotation for the larger flake sizes (>500µm, under optimal frothing conditions). For the smaller flake sizes (<500µm), multiple froth floats were found to be needed in order to achieve the desired purity, but due to impurities embedded on the flakes themselves, there was found to be a limit where an acid cleaning was needed in order to achieve a >90% graphite sample.

A saleable product was produced and a technical-economic assessment was made for a 10,000 tonne per year process plant.

## Acknowledgments

I would like to extend my thanks and appreciation for all the help offered to me in the undertaking and completion of this project. In particular, my thanks extend to Ayekame Tseja and Jennifer Omigie for their assistance and hard-work in the majority of the project, and to Rajesh Gurung for his further assistance in the latter stages of the project. My thanks also go to Zubera Iqbal for her help with the XRF processing of the kish material. For the greater project, I extend my thanks to the Technology Strategy Board for funding this project, and in particular Jon Aumonier, Alex Daily and his colleagues at Morgan PLC for their assistance and insight offered – special thanks go to my project supervisor Prof. Neil Rowson for his guidance, help and advice, and most importantly his patience. Finally I extend my thanks to my friends and family for their constant badgering to finally get this thesis completed.

## Contents

### CHAPTER 1 – PRELIMINARIES AND BACKGROUND

1.1 Introduction.....	8
1.2 Graphite.....	10
1.3 Important properties of Graphite.....	11
1.3.1 Flake Size and Aspect Ratio.....	11
1.3.2 Separation and Sorting.....	14
1.3.3 Types of Natural Graphite.....	15
1.3.4 Impurities within flakes and the Structure of Flake Edges.....	17
1.4 Uses of Graphite in Industry.....	19
1.4.1 Graphite as a Writing Implement.....	19
1.4.2 Graphite as a Lubricant.....	20
1.4.3 Graphite as a Conductor.....	21
1.4.4 Graphite as a Thermal Resistor/Propagator .....	22
1.5 Summary.....	23

### CHAPTER 2 – NATURAL, SYNTHETIC AND KISH GRAPHITE

2.1 Types of Graphite.....	25
2.1.1 Natural Graphite.....	25
2.1.2 Synthetic Graphite.....	25
2.1.3 Kish Graphite.....	27
2.2 Summary.....	28

### CHAPTER 3 – EXTRACTION OF KISH GRAPHITE FROM STEEL WASTAGE

3.1 Project Brief.....	30
3.2 Literature Review.....	31

### CHAPTER 4 – APPARATUS, EXPERIMENTAL METHODS AND MATERIALS

4.1 Initial Samples.....	36
4.2 Primary Methodology.....	37
4.2.1 Sample Preparation.....	37

4.2.2 Mechanically Agitated Sieving.....	38
4.2.2.1 Wet Sieving.....	39
4.2.2.2 Magnetic Separation.....	40
4.2.3 Froth Flotation.....	41
4.2.4 Filtration.....	42
4.2.5 Drying.....	43
4.2.6 Acid Leaching.....	44
4.2.7 Loss on Ignition.....	45
4.3 Characterisation Methods.....	46
4.3.1 XRF Spectrometry.....	46
4.3.2 Thermal and Electrical Conductivity (Morgan).....	47
CHAPTER 5 – RESULTS	
5.1 As Received Reference Samples.....	48
5.2 Preliminary Experiments.....	53
5.2.1 Size Separation – Wet Sieving.....	53
5.2.2 Selection of the Dusts.....	54
5.2.3 X-Ray Fluorescence (XRF) Analysis.....	56
5.2.2 Magnetic Separation.....	57
5.3 Primary Experiments.....	57
5.3.1 Physical Separation through Mechanically Agitated Dry Sieving.....	58
5.3.2 Physical Separation through Froth Flotation.....	60
5.3.2.1 Desulph 1.....	60
5.3.2.2 Desulph 2.....	65
5.3.3 Chemical Cleaning through Acid Leaching.....	67
5.3.4 Top-up Bags (Desulph 1 $\beta$ & 2 $\beta$ ) and Additional Samples.....	69
5.4 Processing of minus 180 micron fraction.....	72
5.5 Thermal and Electrical Conductivity (Morgan PLC).....	75
5.6 Cost Analysis.....	76
5.7 Results Summary.....	78

## CHAPTER 6 – FUTURE RECOMMENDATIONS

6.1 Post-results Outline.....	80
6.2 Meta-analysis of Results.....	80
6.3 Scaling–up to Industrial Quantities.....	82
6.4 Future research and Conclusions.....	83

## BIBLIOGRAPHY

References.....	85
Images.....	88

## WORD COUNT

Word Count.....	90
-----------------	----

## APPENDICES

Appendix A – XRF Analysis.....	91
Appendix B – Cost Analysis.....	107
Appendix C – Sub-180 micron Raw Results.....	111
Appendix D – Morgan PLC Data.....	124
Appendix E – Lab Safety.....	130

## Figures and Tables

Table 1: Minerals and metal resources considered critical to the EU.....	8
Figure 1.1: Diagram illustrating various materials and their corresponding supply risk and economic importance.....	9
Figure 1.2: The Atomic Structure of Graphite.....	11
Figures 1.3 and 1.4: A variety of different flake sizes are used in industry, ranging from a few millimetres to just a few microns in size.....	12
Figure 1.5: A flake of kish graphite – note the shape is not uniform.....	13
Figures 1.6, 1.7 and 1.8 (clockwise from top left): Examples of flake, amorphous and lump (vein) graphite.....	16
Figures 1.9 and 1.10: Sometimes the edges can become distorted .....	18
Figure 1.11: A proportional breakdown of the industries that use graphite.....	19

Figure 1.12: Graphite and a Pencil containing it.....	20
Figure 1.13: A selection of graphite electrodes.....	22
Figure 1.14: A blast furnace such as this is likely lined with graphite.....	23
Figure 2.1: A sample of synthetic graphite.....	26
Figure 2.2: A sample of carborundum.....	26
Figure 2.3: Some flakes of kish graphite.....	28
Figure 2.4: A schematic representing the types of graphite.....	29
Figure 4.1 - Sample Preparation.....	38
Figure 4.2 - Agitated Dry Sieving Set-up.....	39
Figure 4.3: An example of the kish slurry formed.....	40
Figure 4.4: The wet magnetic separator used.....	41
Figure 4.5: Left to Right - A Denver flotation cell; 2 minute froth conditioning; 3 minutes scraping.....	42
Figure 4.6: Left - Vacuum Filtration Unit; Right - graphite Froth in collection tray before filtration.....	43
Figure 4.7: Carbolite Burn-off Furnace with extractor hood.....	45
Figure 4.8: LOI test furnace with door open to allow cooling of crucibles.....	46
Figures 4.9 and 4.10: An XRF spectrometer (left), and a typical XRF results display (right).....	47
Figure 5.1: A schematic of the steel-making process, with manual additions as to where the kish dust was collected (provided by Tata Steel).....	49
Figure 5.2: A microscope image of the Eastern Secondary Vent sample.....	50
Figure 5.3: A microscope image of the Ladle Arcs 1 & 2 sample.....	50
Figure 5.4: A microscope image of the Ladle Arc 3 sample.....	51
Figure 5.5: A microscope image of the ladle arc cyclone sample.....	51
Figure 5.6: A microscope image of the convertor ladle additions sample.....	52
Figure 5.7: A microscope image of the Desulph 1 sample.....	52
Figure 5.8: A microscope image of the Desulph 2 sample.....	53
Figure 5.9: A graph detailing the particle size distribution of the samples received from Tata Steel.....	55
Table 2: Loss on Ignition – Tata Steel samples.....	56
Figure 5.10: A representation of the processes needed to refine the graphite.....	58

Figure 5.11: A Graph Detailing the Particle Size distribution after Sieving of Desulph 1 and Desulph 2.....	59
Table 3: The carbon content of the different size fractions.....	61
Figure 5.12: A Graph Detailing the effect of varying frother additions on yield for the 180µm Desulph 1 sample.....	61
Figure 5.13: A Graph Detailing the effect of varying frother additions on yield for the 355µm Desulph 1 sample.....	62
Figure 5.14: A Graph Detailing the effect of varying frother additions to the Carbon Content for the 355µm and 180µm Desulph 1 sample.....	63
Figure 5.15: A Graph Detailing the effect of varying diesel oil to the Carbon Content for the 355µm and 180µm Desulph 1 sample.....	64
Figure 5.16: A Graph Detailing the effect of varying frother additions on yield for the 335µm and 180µm Desulph 2 sample.....	65
Figure 5.17 & 5.18: A Graph Detailing the effect of varying frother additions to the Carbon Content for the 180µm and 355µm Desulph 2 sample.....	66
Table 4: The different Carbon Contents of the samples after varying cleaning treatments.....	68
Table 5: The revised Carbon Content of the larger flake sizes of Desulph 1 after froth flotation.....	69
Figure 5.19: Comparison of particle size distribution for Desulph 1 & 1β, 2 & 2β.....	70
Table 6: The Loss on Ignition data comparison for Desulph 1 & 1β, 2 & 2β.....	71
Table 7: The Loss on Ignition of Miscellaneous samples Supplied by Tata Steel.....	72
Table 8: The Carbon Content of the non-treated sub-180 micron samples tested.....	74
Table 9: The final Carbon Content achieved on some of the sub-180 micron samples tested.....	75

## Chapter 1 – Preliminaries and Background

### 1.1 Introduction

The demand on the world's natural resources is constantly growing due to an ever increasing population and need for these materials in a number of growing markets (Schoolerman, 2011).

One such market affected by this growth in demand is the minerals industry – with a finite amount of natural resources available and only a fraction of used materials being recycled (even once, let alone multiple times), there is a growing necessity to investigate alternate ways to harvest these resources and produce more sustainable methods of obtaining these material.

In 2010, *The British Geological Survey's* publication '*Critical Raw Materials for the European Union*' highlighted a selection of minerals and metal resources which were considered highly critical to the European Commission (Table 1). Alongside the expected platinum group minerals and the rare earth metals, graphite was listed (Note – for the remainder of this thesis whenever the country China is mentioned this is to be taken as the Peoples Republic of China, as opposed to Taiwan):

**Table 1: Minerals and metal resources considered critical to the EU (The British Geological Survey, 2010)**

<b>Element</b>	<b>Relative Risk Index</b>	<b>Leading Producer</b>
<b>Antimony</b>	8.5	China
<b>Platinum group elements</b>	8.5	South Africa
<b>Mercury</b>	8.5	China
<b>Tungsten</b>	8.5	China
<b>Rare earth elements</b>	8.0	China
<b>Niobium</b>	7.5	Brazil
<b>Strontium</b>	7.0	China
<b>Bismuth</b>	7.0	China
<b>Thorium</b>	7.0	India
<b>Bromine</b>	7.0	USA
<b>Graphite</b>	7.0	China

Indeed, the European commission included graphite among the 14 materials it considered high in both Economic importance and Supply risk (Fig 1.1):

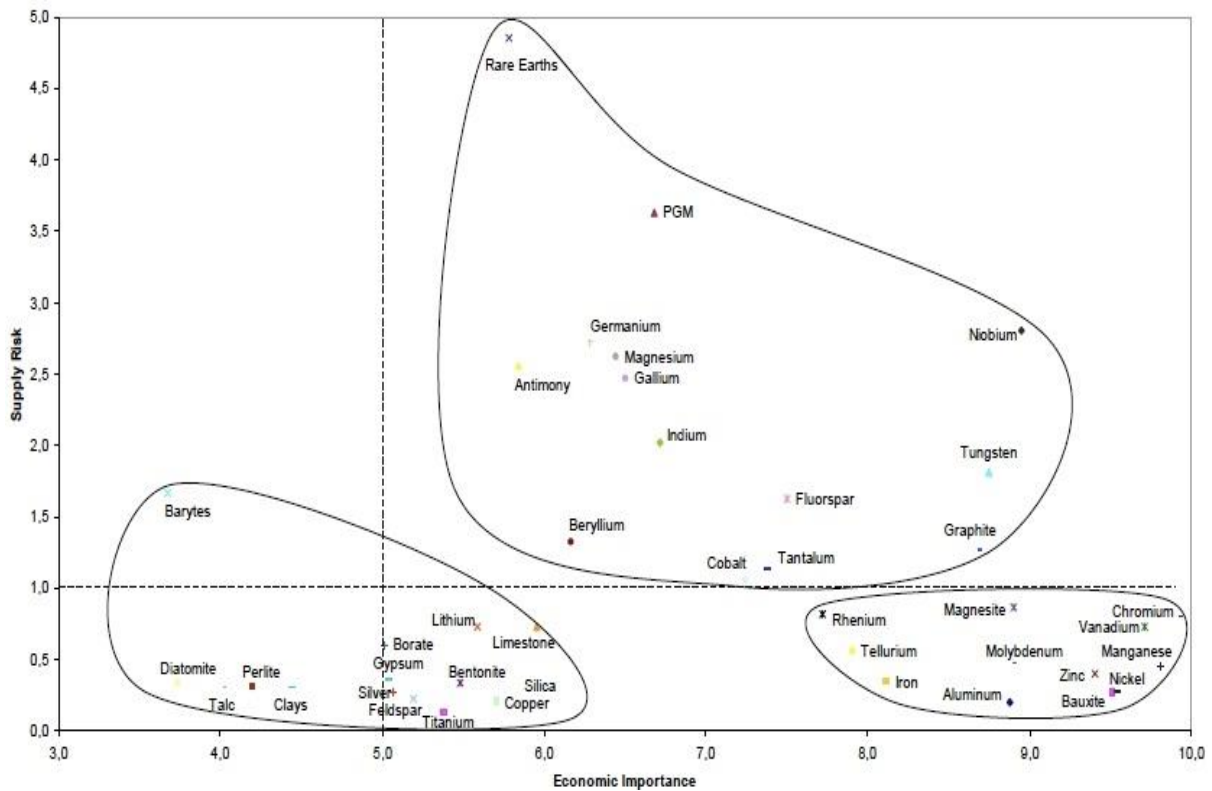


**Figure 1.1: Diagram illustrating various materials and their corresponding supply risk and economic importance (European Commission, 2010: 6)**

Whilst graphite has been extensively used in a multitude of industries for a number of years, it is only relatively recently that it has been viewed as a key strategic material: This is due to the growth of industries such as the development of electric cars (where graphite is an essential material used in the construction of the anode for the batteries), and the excitement and vast amount of research and development into the ‘super-material’ graphene (which is derived from graphite). Due to this increased demand, the supply risk readily becomes apparent – the majority of the world’s graphite is mined in a few countries. With this increased demand on these finite reserves of natural graphite, coupled with the great time, energy and cost associated with the creation of synthetic graphite

(Acheson (1896), Mersen), a heavy emphasis is placed on the development of alternative sources of graphite recovery at a manageable cost.

This chapter will outline the micro and macro properties of graphite as a material, highlighting the important aspects to consider when putting the product to market, and then give a brief summary of the uses of graphite, which industries it is used in, and just why its properties make it so suited to these applications in industry.

## **1.2 Graphite**

Graphite, alongside diamond, is one of the two principle naturally occurring forms of pure, crystalline carbon, located in different mineral deposits around the earth (other crystalline forms of carbon such as Buckminster fullerene do exist, but are found naturally in far less abundance (Kroto *et al.*, 1985).

The structure of graphite is essentially that of a stack of carbon 'sheets' (Dresselhaus *et al.*, 1998). These single, one atom thick sheets are comprised of carbon atoms covalently bonded to each other in a honeycomb lattice. This means that each carbon atom is bonded to three other carbon atoms (with the angle of separation being  $120^\circ$ ), which when repeated forms the familiar honeycomb pattern (Fig 1.2):

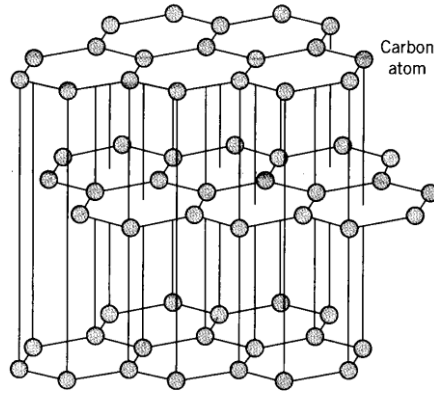


**Figure 1.2: The Atomic Structure of Graphite (Battery Blog)**

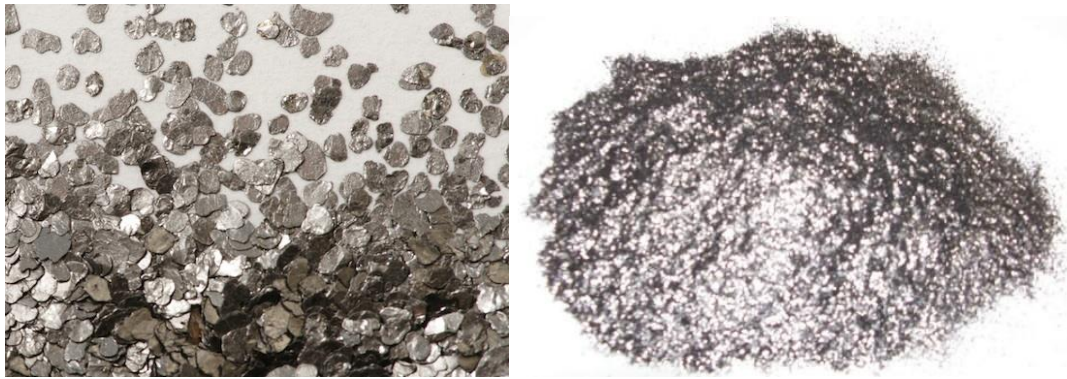
Given carbon possesses six electrons (with four being located in its outer shell), when a carbon lattice is formed through covalent bonding one electron for each carbon atom present remains un-bonded, and as such can be considered 'free'. This is of particular importance when the sheets of the lattice are 'stacked' - comprising the graphite as a whole (Graphene - the single sheet variant of graphite - is under particular scrutiny in the scientific community at present). Once this stacking occurs, the sheets are held together by weak Van der Waal interactions, and the environment between the sheets allow the 'surplus' electron in each carbon atom to become delocalised and free to move in the plane between the sheets. It is precisely due to this delocalisation that graphite has its effective, but specifically limited ability as an electrical conductor. In fact, it is this stacking of layers in graphite that is the key factor responsible for its properties.

### **1.3 Important properties of Graphite**

#### **1.3.1 Flake Size and Aspect Ratio**

Whilst the core physical properties of graphite are dependent on its properties at an atomic level, the way in which graphite operates and performs as a functional material is equally dependent on the micro (and occasionally macro) properties of the material obtained.

First amongst these is that graphite is often found in the form of flakes (Figs 1.3 & 1.4). One of the main (and certainly most noticeable) properties of graphite is the variance in flake size. In general, flake graphite ranges in size from 1mm to 25mm with an average size of 2.5mm (Mitchell, 1993). However, for use in industry, typical flake sizes are generally of the order of microns, with flake sizes of over 180µm being classified as coarse, and anything under being classified as fine. The fine flake graphite is further divided into medium flakes (100-150µm), fine flakes (75-100µm) and powder (<75µm). Flake graphite is typically not used when the flake sizes are less than 45µm in size – this is due to the increased difficulty in separating the graphite from the impurities, and the loss of performance due to flake size (Mitchell, 1993).



**Figures 1.3 and 1.4: A variety of different flake sizes are used in industry, ranging from a few millimetres to a few microns in size (Canada Carbon/smokechemicals)**

As a general indicator, the larger the flake size the more pronounced the properties as the natural structure is preserved and not forced into an artificial arrangement. For this reason, larger flake sizes typically retail at a higher price than their smaller counterparts as properties such as their thermal and electrical conductivity are better (something of importance in the refractory industry, where graphite's thermal properties are of key importance in the building of components). The industrial consumption of the different sizes of flake is varied as well – whilst almost all flake sizes on sale are used for refractory materials, brake linings and other lubricants, the smaller, powder graphite tends to be used as an additive for various materials, where the larger flake sizes tend to be

used in for more specialised applications such as electronic components, pencil leads and explosives (Mitchell, 1993). However, whilst there is a general increase in utility as the flake size increases, this can be offset with the ability to manipulate the flakes and put them towards the purpose intended – for instance, graphite is often used to create crucibles for the refractory industry: For this to be done, the graphite needs to be pressed in a mould, and the flakes aligned to create the crucible. For larger flake sizes (>1mm) (Fig 1.5), this alignment is harder to achieve, and as such the product is less stable. For these types of considerations, graphite flakes are often milled to reach the size required, yet without sacrificing their intrinsic properties too much – there is a trade-off between the flake size and the ability to manipulate it that must be considered within industry.

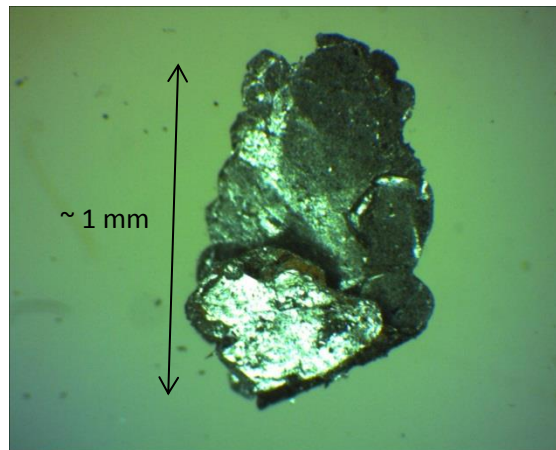


**Figure 1.5: A flake of kish graphite – note the shape is not uniform**

Related to their size is the aspect ratio of the graphite flakes. This, too can be an important factor in the performance of the graphite product, and has its own considerations and uses within industry (Ledbetter and Datta, 1989). The aspect ratio again can have a pronounced effect on the properties of the graphite, influencing factors such as the electrical and thermal conductivity, and mechanical properties such as the Young's modulus and internal friction (Kuvardina *et al.*, 2013). For these reasons it is of paramount importance in industry to be able to effectively sort the graphite flakes into their corresponding sizes and geometries.

### 1.3.2 Separation and Sorting

A multitude of separation techniques that are standard practices in the minerals Industry can and have been used with variable degrees of success in graphite separation (a few notable examples are listed below):

- **Magnetic Separation:** Since graphite is non-magnetic, and the impurities present with it are generally non-magnetic as well, magnetic separation as a sorting technique is rarely used. In fact, even when the graphite is encountered in amongst magnetic material (such as the case with kish graphite – see sections 3.2 and 5.2.4), magnetic particles can get embedded in the flake itself, rendering it a de facto magnetic particle, and the separation technique less efficient.
- **Electrostatic separation:** This works marginally better but there are some issues with the impurities which further limit the effectiveness of this technique (Lipson, 1942). Principally, this is due to the relative softness of graphite, and the sometimes considerable flat surface area of the flakes – because of this it is quite easy for a flake to be ‘coated’ in impurities, rendering a purely mechanical separation as ineffective.
- **Centripetal separation:** Again, this technique (whilst effective in a general sorting) will not adequately separate the impurities which have ‘stuck’ to the flakes themselves.
- **Gravimetric separation:** Much the same issues are encountered here – a purely mechanical separation is ineffective at achieving the results desired.

The common denominator for each of these methods is that the flakes are too readily ‘coated’ in impurities, and as such the flakes will not be separated adequately without some sort of cleaning element. As such, the below method is often considered one of the most effective:

- **Froth Flotation:** This need for a cleaning element, combined with the high degree of hydrophobicity that graphite possesses renders froth flotation as the ideal technique to

further refine the graphite (Bennett *et al.*, 1997). The method essentially works by mixing the graphite into a suspension, and then injecting air into the vessel. Any hydrophobic materials (such as the graphite) will attach themselves to the air bubbles and float, whilst the rest of material will remain dispersed in the agitated suspension. The aerated material floats to the surface as a froth, where it can be physically removed for further processing. Not only is this extremely effective at separating the graphite (particularly smaller flake sizes) from the associated impurities (with it being the most widely used way of achieving this with graphite, and being used extensively in the minerals industry for other materials), the process actually includes a cleaning element (due to agitation from the cell rotor) which helps remove any impurities which may have attached themselves to the flake's surface. This process is discussed more thoroughly in the literature review (chapter 3).

### **1.3.3 Types of Natural Graphite**

Given one of the main considerations of the use of graphite in industry is the purity of a given sample (with grades ranging from 70% to over 99% pure being needed for different applications (Mitchell, 1993)), an important requirement in processing the graphite is to ascertain the impurity content of the given sample. As such, it is useful to know where the graphite comes from: The majority of the world's graphite naturally occurs in metamorphic and igneous rocks and is also occasionally found in meteorites. Although it is essentially a form of coal, it is relatively sparsely located, and is only significantly recovered (as a percentage of the world's graphite) from mines from a few countries, such as China, India, Brazil, North Korea and Canada (Brown, 2011). From these mines, graphite is normally recovered from three different types of ore deposit, and as such is generally split into three classifications (Mining Turkey, 2012):

The first is flake graphite (Fig 1.6) – this is where the graphite is found as isolated, hexagonal flakes, which are highly valued as the flake size directly influences the performance of the end product, and as such is treated appropriately to avoid size degradation.

The second is amorphous graphite (Fig 1.7) – this is where the graphite is either irregular or ‘misshapen’ in nature, or the flake size is so small as to not reap the benefits of being treated as fully fledged flake graphite. This type of graphite is typically milled into a fine powder, to be used in a number of industries (see section 1.4).

The third is lump (or vein) graphite (Fig 1.8) – this occurs as large deposits of material, and is a true vein mineral as opposed to a seam mineral. As such, this is generally the most valuable form of natural graphite (Canada Carbon).



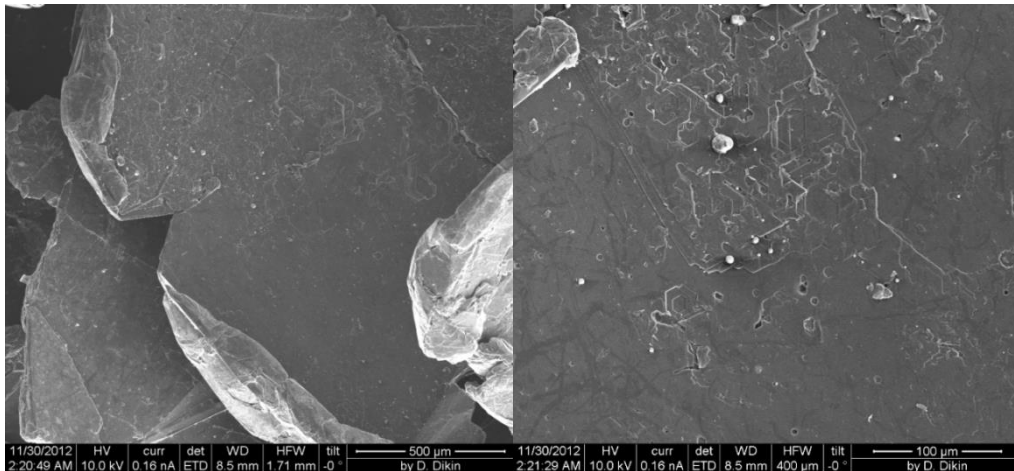
**Figures 1.6, 1.7 and 1.8 (clockwise from top left): Examples of flake, amorphous and lump (vein) graphite (made-in-china/grupolandfer/saintjeancarbon)**

All three of these types of graphite are mined and as such the purities obtained from the ore alone are rarely of a high enough grade to not require further purification (synthetic graphite can be produced but this is a very costly and time-consuming process – more on this in chapter 2 (Acheson, 1896). As such, further refinement to the graphite flakes is often required due to the impurities that are present within a given graphite sample (see section 1.3.2). Whilst a simple sorting can be performed (for example, by sieving the material), it is often not enough to achieve the higher purities and for the smaller flakes (such as powder graphite and fine graphite) the finer impurities are harder to separate because they are of a comparable size.

#### **1.3.4 Impurities within flakes and the Structure of Flake Edges**

Whilst the types of separation (and classification) detailed above goes some way to purifying the graphite by removing the impurities from a given sample of graphite, occasionally impurities can embed themselves within the graphite flake itself (both as a naturally included part of the flake, and also with the act of processing the flakes - this is especially true of kish graphite). Given that the graphite flakes can and do have imperfections embedded within the surface of the flakes themselves, and that in order to achieve the desired purity of graphite these may need be removed, further issues are encountered. Since these impurities can lower the overall grade of the graphite obtained, it is beneficial to remove them – the most effective (or at least widely used) method is to dissolve the impurities via acid leaching (Olson, 2004). A major problem is that the acid damages the surface structure of the flakes altering the desirable characteristics *i.e.* electrical and thermal conductivity. This is especially true of the edges of a graphite flake, which if damaged may further impact these characteristics, and other properties such as the packing of the flakes. For this reason it is important to assess whether it is beneficial to further purify by this method, if a desirable grade has been reached. For instance, in Figs 1.9 & 1.10 (below), clear distortion of the edges of a graphite

flake and pores present in the surface of the flake can be seen – both could be a direct consequence of the acid leaching process.



**Figures 1.9 and 1.10: A graphite flake with distorted edges, and a graphite flake with pores in its surface**

When acid leaching is applied to remove particulate impurities a pore is created in the surface of the flake that disturbs the laminate structure and as a consequence its properties. This disturbance at the surface not only affects the geometric properties, (i.e. shape, surface area, density etc.) but also affects its electrical, thermal and lubricating properties (though not as severe as when the impurity was present (Abel *et al.*, 1999; Feiyu *et al.*, 2002; Nishi *et al.*, 2002; Giesche, 2006). The pores can have an effect on the lubrication due to it changing the laminar nature of the graphite, and potentially allowing more liquid between layers. For the electrical properties, having an effective gap in the sheet acts as an impedance to the flow of electrons, and as such lowers the electrical conductivity. Likewise, the anisotropic properties of the graphite are affected when the hexagonal lattice is broken, effectively allowing heat to propagate *through* the layers. Given this anisotropy can be fundamental to the performance of the graphite, identifying and quantifying these pores can be integral to the grade of obtained.

## 1.4 Uses of Graphite in Industry

A breakdown of the industries in which graphite is utilised are presented in the following pie chart (Fig 1.11).

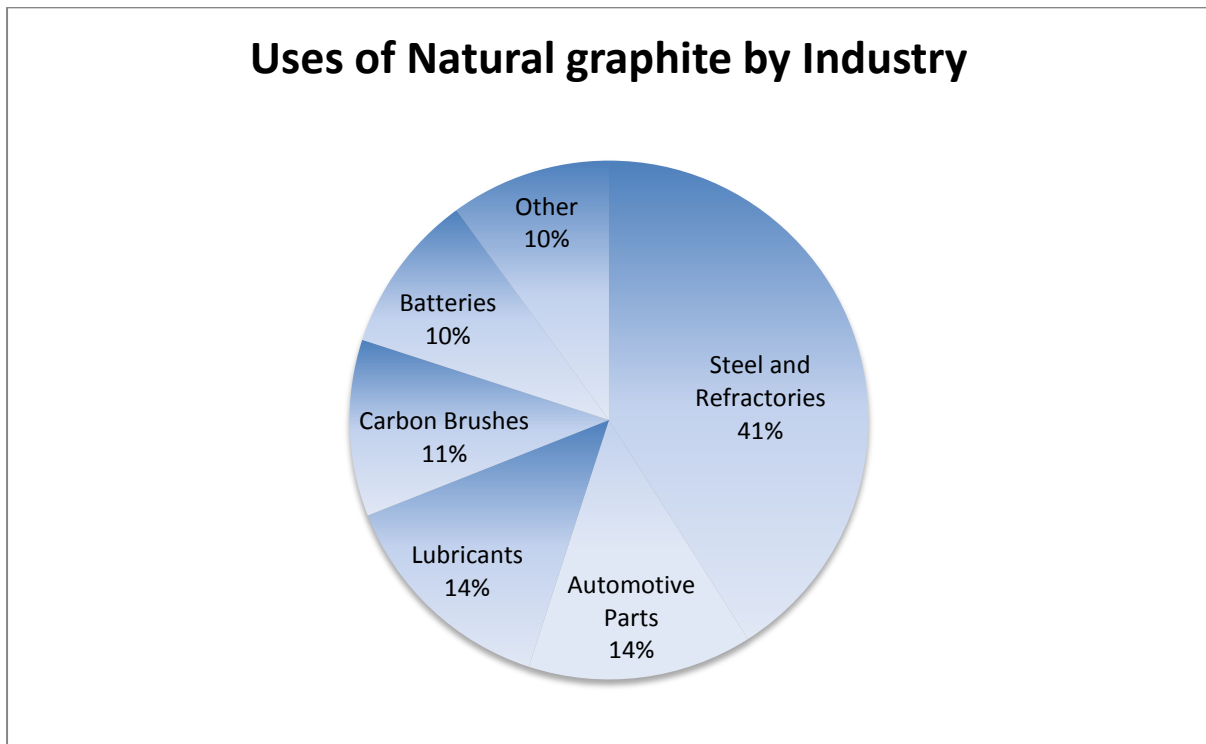


**Figure 1.11: A proportional breakdown of the industries that use graphite (Mining Turkey, 2012)**

### 1.4.1 Graphite as a Writing Implement

The most identifiable use of graphite is as the 'lead' in standard pencils to make marks. The graphite derives its meaning from the ancient Greek 'graphō' which translates as 'to draw/write'. In this original form, blocks of natural graphite were literally carved from the natural reserve into a rod and inserted into the pencil linings (Fig 1.12). The reason it is so effective in transferring marks is due to the layering of the material – since the layers are only held together by relatively weak Van der Waal forces, only a small shear stress need be applied in order to separate the layers, hence leaving a layer on the writing medium, making a mark.



**Figure 1.12: Graphite and a Pencil containing it (Wikipedia)**

With regards to the micro structure influencing the use of graphite in this manner, as has already been mentioned this requires a fairly specialised grade of graphite, with high purity and larger relative flake size – this is because the function of the lead in a pencil is highly dependent on the shearability of the graphite, which in turn will increase with flake size and the reduction of imperfections in a sample.

This is a basic way of using graphite, as the greater utility that graphite affords spreads far further than this. However, whilst the usages of graphite have greatly expanded since its discovery, it is still used for this purpose, with around 4% of natural graphite mined being used in this way (Mining Turkey, 2012).

#### **1.4.2 Graphite as a Lubricant**

Due to the ease with which graphite's layers can be sheared, a natural extension for its uses is for it to be used as a lubricant. Of particular interest is the fact that graphite is a dry lubricant and has the ability to self-lubricate – these properties make it ideal as a lining for moveable, mechanical parts such as gears, or as the coating for containers in high temperature environments, such as foundries (Mitchell, 1993) (the lubrication eases the separation of objects from the moulds, when cooled).

The lubricant properties have previously been attributed to the ease with which the Van der Waal interactions between layers can be overcome, but it has been shown (Lavraka, 1957) that in a vacuum environment the separation of graphite layers is not nearly as easy as in a standard environment. This led to the conclusion that graphite's ability to shear its layers is actually highly dependent on fluids (whether gaseous or liquid) being present between the layers via adsorption from the general environment, which aid the slipping effect that enables lubrication to take place. Whilst this strays from the traditional interpretation of graphite's properties, the process is still highly dependent on the specific structure of graphite (in fact the specific way in which graphite has this property has been shown to be unlike other layered, dry lubricants, affording graphite a proportion of uniqueness on this front (Lavrakas, 1957), and as such still differentiates graphite from other lubricants. With regards to the microstructure, this is perhaps where the largest variation of graphite quality comes in, with only particularly high performance mechanisms requiring the best grades of graphite.

### **1.4.3 Graphite as a Conductor**

As mentioned in section 1.2, the layering effect gives graphite useful electrical properties. In fact, it is classified as a semi-metal (Dreselhaus *et al.*, 1988) - this is due to the fact that one electron from each carbon atom is delocalised, creating an extremely hospitable environment in which a current can run through. Whilst graphite is an effective electrical conductor, this property is restricted to along the sheets that form the structure. The passage of electrical current between the layers encounters significant resistance and as a consequence the flow of current, propagated by the delocalised electrons, occurs along the parallel layers. This is why the importance of impurities embedded within the flake can have a pronounced effect on the performance of the electrical 'layers' – with the breaking of the graphite sheets by the impurity (or pore if it has been removed), the electrical properties can be disrupted, and the performance of the graphite effected. Due to

these electrical properties, graphite is often used as a semiconductor material, and as a major component of the anode on batteries, in particular of the Lithium ion variety (Li-ion batteries are a major component in the production of electric and hybrid cars. As the demand for these types of cars increases – as is happening – so the demand for more readily available and affordable graphite increases also (Industrial Minerals, 2010)). For use as a higher performance electrical component graphite of a higher grade and greater flake size is generally required (Deprez *et al.*, 1988) (Fig 1.13).



**Figure 1.13: A selection of graphite electrodes (robotroom)**

#### **1.4.4 Graphite as a Thermal Resistor/Propagator**

As a consequence of graphite's high thermal anisotropy in conjunction with high thermal conductivity, due to its layer like structure, it is an ideal material for certain high temperature metals, such as blast furnace linings. The fact that the layers themselves are covalently bonded makes the graphite extremely durable with regards extreme heat – it has a high melting point (>3600°C (Dreselhaus *et al.*, 1988)). Again, as with the electrical properties, the uniform nature of the layers and the packing of the graphite as it constitutes the constructed material is of paramount importance. This durability combined with its anisotropic properties means it can be used in a way

that controls heat propagation, which is extremely useful if containing heated substances – by having the multiple layers of graphite sheets expanding radially out from the container, the heat is contained more efficiently as it encounters resistance crossing the layers, consequently making graphite highly suitable for blast furnace linings (Fig 1.14).



**Figure 1.14: A blast furnace such as this is likely lined with graphite (wikipedia)**

### **1.5 Summary**

The key properties that make graphite such a useful and sought after resource are fundamentally reliant on the atomic arrangement of the carbon atoms, and how they interact with each other – this in turn dictates the graphite’s thermal, mechanical and electrical properties that are characteristic of it. However, with regards to the actual use of graphite within industry, it is the micro properties that are essentially modifying these characteristic properties that dictates how the graphite performs:

The flake size and aspect ratio is first and foremost amongst these, but the performance and quality of the graphite is dictated by other factors such as flake graphite’s shape, adherence to other materials and hydrophobic nature. To this end, it is essential that any processing of graphite designed for its marketability should ensure that the physical structure of the flakes is maintained

and therefore minimising their degradation whilst handling and processing – the limiting of destruction to the graphite flake is of paramount importance, and is treated as such with respect to this project.

## Chapter 2 – Natural, Synthetic and Kish Graphite

### **2.1 Types of Graphite**

Broadly speaking graphite can be split up into two categories: Natural and synthetic. However, whilst the variations in natural graphite have already been discussed, the variations in synthetic graphite have not been extensively covered. Whilst it is beyond the scope of this project to analyse all these variations in detail, one such variation – namely ‘kish’ graphite – is central to this project’s aims.

#### **2.1.1 Natural Graphite**

As was previously mentioned in section 1.3.2, natural graphite is found in three forms: Flake, amorphous and lump (vein), and is mined in bulk. However, the exploitable graphite ore reserves are concentrated in only a few countries with 70% of the known reserves being located in the China. As a consequence of these countries domination of the reserves they are able to exert undue influence over the supply, and consequently price of graphite. In the event that demand for graphite exceeds production due to manipulation of the market then alternative sources of graphite, such as synthetic and recycled, will become more important.

#### **2.1.2 Synthetic Graphite**

Synthetic graphite is essentially any graphite that has not been obtained through a mining process, whether it is from the direct creation of the graphite artificially, the harvesting and refining of graphite as a by-product of other industrial processes, or the actual recycling of graphite (including natural graphite) from processes and objects which are no longer needed.

In general, there are a number of different ways in which synthetic graphite can be created (Fig 2.1), but all essentially rely on the same method.



**Figure 2.1: A sample of synthetic graphite (Graphiteproduct)**

This method typically takes the form of the superheating of carborundum (silicon carbide – Fig 2.2) – because this mineral is made up of silicon and carbon, when heated to above 2,600°C (Carolina Biological Supply Company) , the silicon vaporises, leaving behind only the carbon (Bellis, Mersen). This carbon in turn, takes the form of high-quality graphite that is almost pure in nature. However, due to the high temperatures required, and the typically long periods of time that these temperatures need to be maintained, the energy consumption alone can seriously jeopardise the economic viability of producing graphite this way.



**Figure 2.2: A sample of carborundum (Wikimedia)**

There are also inherent issues with regards the recycling of graphite, as most is taken from components such as graphite electrodes and crucibles. Whilst some of this is reused into producing

more graphite (as detailed above), most is used as either a carbon raiser (literally something that when added increases the carbon content of a material to a specified level) in the steel making industry, or as a repair material for objects such as furnaces.

In general, whilst there are many ways in which synthetic graphite can be produced, there are several issues with many aspects of the final product: The quality may not be of a standard required for high-grade usage (as from the recycled graphite), the process may not be cost effective (it can take many months for the heating and storing to be completed, and at a significant cost due to the temperatures maintained over this time period), and the materials needed (such as the carborundum) can be extremely rare in themselves. This is why there is a constant search for more cost effective ways of obtaining synthetic graphite of a high quality – if a way to produce high quality graphite that does not require rare materials or significant time and cost could be found, then this would be a major boon to the industry.

### **2.1.3 Kish Graphite**

In the initial stages of the steel making process, a large amount of powdered waste product, known as kish, is produced (Bennett *et al.*, 1997). Kish is a general term for the waste material that collects on the surface of molten iron, after it is tapped from a blast furnace (with the term 'kish' having thought to be derived from the German 'kies' for gravel (Dictionary.com)). As steel cools it becomes supersaturated with carbon that then comes out of solution as flakes of graphite that float to the surface of the steel alongside iron, lime-rich slag and other trace materials. So desulphurisation of hot metal by injecting a mixture of magnesium and lime or calcium carbide and lime produces a lime rich slag that mixes with the graphite resulting in kish graphite (Fig 2.3). Through relatively non-intensive refining, a relatively pure form of flake graphite can be obtained from this waste material (as will later be shown). The way it is formed is due to similar processes as detailed in section 2.1.2, but due to the fact it is a by-product of an already essential process, a significant amount of cost is curtailed, rendering it economically viable. Additionally kish graphite is a potential source of carbon

that is widely distributed geographically, the initial cost is low and the resource is not currently exploited.

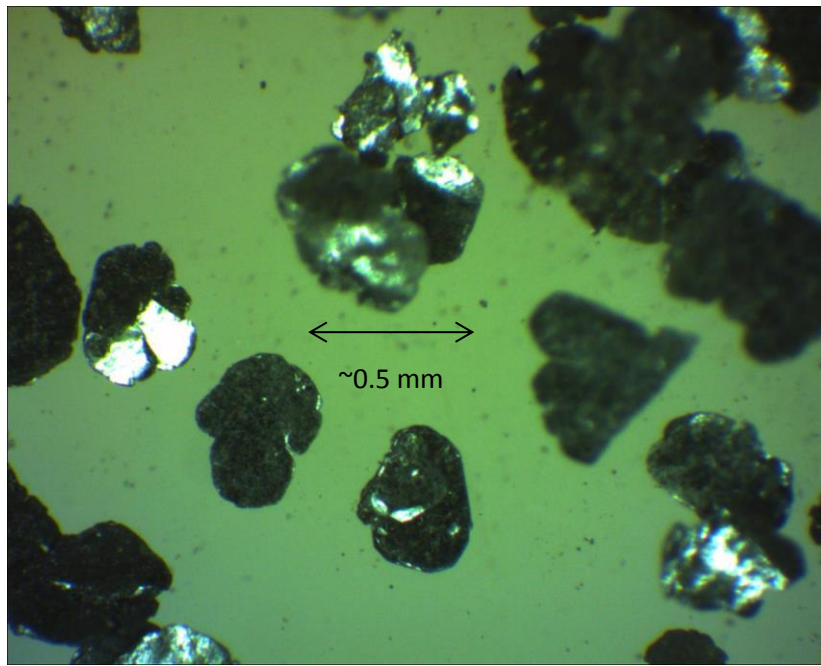


**Figure 2.3: Some flakes of kish graphite**

## **2.2 Summary**

The majority of the world is reliant on a finite resource of natural graphite (current estimates put this at over 800 million tonnes (Focus Graphite) that is controlled by only a few countries, with the remainder being produced by costly and time consuming synthetic methods. However, as part of the steel making process, potential reserves of 'kish' graphite (produced via a similar mechanism to the synthetic graphite, but as a by-product) have been identified in the waste stream. As such the different 'types' of graphite can be roughly represented by the schematic below (Fig 2.4):

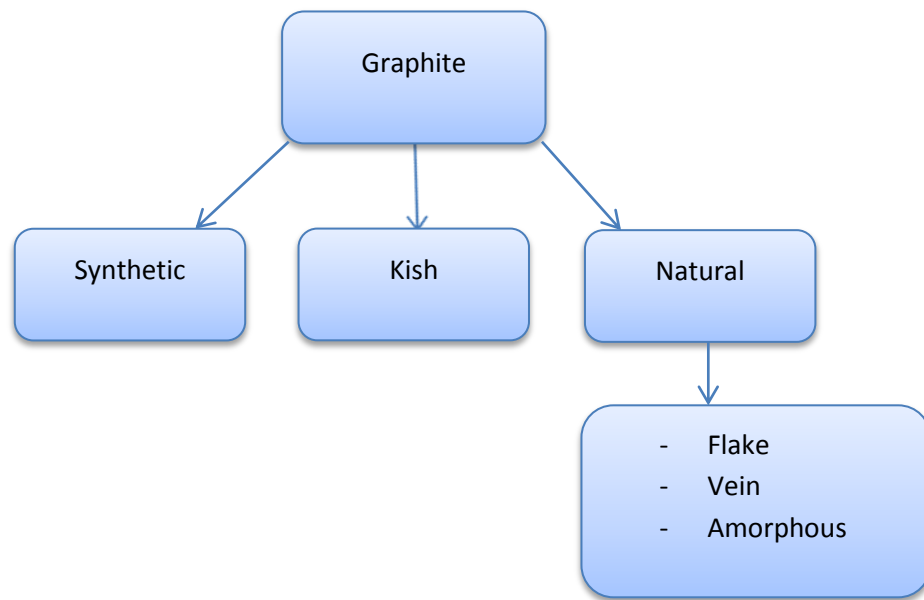


**Figure 2.4: A schematic representing the types of graphite resource**

The potential to exploit this untapped source of graphite represents the prospect of reducing the reliance on limited, potentially unreliable sources of natural graphite and expensive to produce synthetic graphite.

## Chapter 3 – Extraction of Kish Graphite from Steel Wastage

### **3.1 Project Brief**

The project's main aim was to assess the physical and economic viability of obtaining market grade kish graphite from the dust produced (and currently largely considered a waste) as part of the steel making process. In this instance, the figure given as typical kish dust wastage produced for the TATA steel plant in Scunthorpe was 10,000 tonnes per year. This was undertaken by the isolation of the potential sources of graphite, and the refinement of the kish dust through physical separation, using methods such as wet and dry sieving, magnetic separation and froth flotation, which were considered due to their widespread use throughout the minerals processing industry. Where further refinement was required, possible chemical cleaning via acid leaching was considered.

It was intended that once this initial characterisation, testing and process development had been accomplished that a cost analysis would be conducted based upon the costs of a typical steel plant. This assessment was then to be used to evaluate the viability of constructing a pilot plant based upon the process developed.

The characterisation of the dust samples was the first stage of the experimental process. A total of seven different dust samples (all taken from different operational areas of the steel plant) were assessed for their graphite content. Due to the fact that the graphite flakes desired are typically a number of orders of magnitude larger than the other constituents of the kish dust, and that the graphite is easily distinguishable from the kish dust, the process of mechanical separation via sieving was considered an effective method to assess whether a given dust sample had potential for future refinement. Whilst qualitative assessment of the various dust samples was performed, dusts found to have potential underwent XRF analysis and loss on ignition testing to determine the elemental content and amount of graphite contained, respectively.

The samples that were found to have an acceptable graphite content underwent various physical tests to separate the graphite. The various methods were assessed and appraised for their effectiveness, with promising methods undergoing further optimisation to maximise the yield. Once a successful method for graphite extraction was developed that satisfied the desired purity specified, the final testing was to construct a process which produces the best way of extracting the graphite given the various considerations.

### **3.2 Literature Review**

In terms of the methodology and the general goals of the project (namely the separation of the graphite from the kish dust as a whole), similar studies have been documented before. What distinguishes this project from the remainder of the available literature is that this has the specific goal of producing a cost-effective and practical method of graphite recovery from a present and well defined starting product. Also, whilst many of the methods used in this project are functionally similar to the already investigated methods, many of the specifics differ rendering this research as legitimately novel.

There are very few academic papers detailing the specifics of liberating graphite from kish dust, and a number of different sources detailing the efficacy of some of the processes used in this project. The three specific papers considered are a study conducted by the US Bureau of Mines (Lavery *et al.*, 1990), a US patent concerning the liberation of graphite from kish (Bennett *et al.*, 1995), and a paper concerning the beneficiation of kish using froth flotation cells (Kazmi *et al.*, 2008). The other relevant literature primarily concerns the operation of flotation cells (which are of critical importance in this project), and will be mentioned in more detail below.

The scope of the research by the US Bureau of Mines is wider in extent than that of this project, and as such is less concerned with the refinement of the processes involved in liberating the graphite from the kish dust, and more in detailing the relevant efficacies of various different methods with

regards their ability to liberate the graphite. Their primary concern is the physical beneficiation of the graphite from the kish stream – the methods utilised included air and foam elutriation, magnetic separation, froth flotation, and hydraulic classification. The air elutriation study examined the effect of changing air velocity on graphite recovery and grade: It was found that by increasing the air velocity the amount of feed as overflow product (along with the coarse graphite content *in* the overflow) increased also. However, it was also found that this increase directly lead to a decrease in carbon content and increased contamination in any specific fraction of the overflow. Their data showed that there was a general decrease in carbon content with decreasing size of the product, and as such it was decided to discard any material below 149 microns (100 U.S. mesh), reasoning that at such purities, the amount of acid required to successfully leach the product to the required grade was too much, and as such the economics were untenable. Reasoning that for the overflow above this size the method was successful, they would develop a secondary stage to complement this.

Alongside the air elutriation, foam elutriation was considered as the primary process using kerosene and tetradecyltrimethyl ammonium bromide as conditioning reagents. Compared with the air elutriation, they observed that whilst a cleaner overall product was produced, the throughput for similarly sized systems was less than one fifth of the air version, making it economically less viable in comparison. However, due to the improved cleaning capabilities, it was considered that combining the two processes (air elutriation to process the kish dust followed by foam elutriation to clean it) would produce a more attractive overall mechanism.

The notion of combining processes was extended to magnetic separation as a consequence of the high iron content of the kish dust (typically upwards of 30%, according to initial XRF analysis (Appendix A)). However, this was rejected as, in preliminary experiments, whilst a distinct separation was visually obtained the relative graphite concentrations of both the feed and products remained relatively unchanged. A microscopic examination of the products revealed the presence

of particles of iron embedded in the surface of the graphite flakes rendering them de facto magnetic particles.

Due to the known high hydrophobicity of graphite, froth flotation was also considered, with various frothing agents. Initially considered was a standard pine oil frother, but due to the extremely hydrophobic nature of the graphite, iron rich slag with small, undesirable flakes of graphite attached were found in the resultant froth. Using a more selective frother such as Methyl Isobutyl carbinol (MIBC), the efficiency was increased with the addition of kerosene (Lavery *et al.*, 1990).

Using a Denver flotation vessel operating at 800rpm and varying the MIBC, kerosene and conditioning time, it was found that they could produce a concentrate high in carbon and low in contaminants. Where low carbon recovery was encountered, this was attributed to the fact that only around 51% of the recoverable carbon was in the form of free graphite – the rest was locked in iron particles. In addition, it was found that use of kerosene along with MIBC resulted in increased amounts of contaminants in the flotation concentrate, compared with the concentrate produced using only MIBC (Lavery *et al.*, 1990).

The purity of graphite they achieved was around 70% compared to a saleable grade of 94%, and consequently more purification was required. To achieve this, they decided to put the feed through a chemical process, via acid leaching. Originally they used sulphuric acid, but whilst this was successful in removing the majority of contaminants from the sample, any calcium present in the sample precipitates as gypsum, attaches to the graphite flakes, and as such lowers the potential purity (the purity they achieved was 88%). As an alternative, hydrochloric acid was used – whilst it was thought that this alone would be enough to produce a carbon content of 95%, due to the flakes floating to the top of the surface (preventing total leaching of the flakes) the leaching needed to be performed in stirred vessels (25rpm for 2 hours). This produced a 95%-97% product. A further 2 hour leaching stage using hydrofluoric acid raised this to >99%.

Whilst the U.S. Bureau of Mines study was fairly broad in scope (with the availability of resources and wider-reaching project aims enabling them to try a number of approaches), other work on the topic has been more focussed in its approach (as is this project). The Bennett *et al.* (1996) text is a patent focussing on a process designed to chemically purify the kish dust post beneficiation. The starting grade they were using for the process was a 35%-C kish concentrate. The process involved taking the starting concentrate and froth floating it to upgrade the purity to 70%. This was then screened, selecting the +74 micron fraction. Taking this fraction, it was milled for 5-20 minutes under conditions that were designed to further liberate the graphite from the kish dust, whilst minimising the damage done to the flakes themselves – this resulted in a concentrate containing 95% C. Reasoning that to further purify the graphite would require the removal of particles embedded on the flake itself, the flakes were then mixed with dilute acid (HCl being preferred, at <7.5% conc.) in order to weaken the bonds attaching the impurities to the flakes. To remove the graphite from the acidic slurry, it was then fed into an attrition scrubber (essentially a machine that scrubs high solid density particles together, resulting in polishing and disintegration) to which silica sand as an attrition adjuvant (an additive that helps make the process more efficient) was added producing a slurry of 55% solid concentrate (the weight ratio of concentrate to attrition adjuvant to acidic water is approximately 1:2:2.5). This material was then washed and further froth floated (again using fuel oil or MIBC) producing an eventual graphite product (when dried) of over 99% C content.

The Kazmi paper focusses on the methodology of froth flotation on kish dust with regards to beneficiation. Using a Denver D-12 flotation vessel, with 1-7 minutes of conditioning and 10-25 minutes collecting the froth, the study showed that under simple 'rougher' conditions, a 65% C pre-concentrate is upgraded to 81% C product at 97% recovery. An additional concentration stage increased the grade to 92% C. Using this as a starting point, the study then examined the various parameters that the flotation can be performed under, such as pH, pulp density, collector, frother, gangue, iron depressant, and impeller speed. Testing the variance of these parameters, the ideal

conditions they found were a pulp pH of 7.5, pulp density of 15%, frothing aids of kerosene 0.05kg/tonne and pine oil 0.05kg/tonne, sodium silicate 0.02kg/tonne and starch 1.5kg/tonne of the feed collectively. The cleaning stages were performed with no further additives.

As mentioned above, any other relevant literature largely concerns the operation of flotation cells in an industrial setting. Foremost amongst these is *Hydrodynamic characterisation of a Denver laboratory flotation cell* (Sung-Su (2003)), which is a study of the performance of test flotation cells and the optimisation of them for an industrial setting. Factors investigated were the effect of superficial gas velocity of the aspirated air, frother concentration, solids content, bubble size and impeller speed. Focussing mainly on the scaling up of laboratory conditions to industrial specifications, it was shown that increasing the speed of the impellers in the flotation cells increased the amount of aspirated air – to the extent it was shown that higher impeller speeds than are usually encountered in test cells (1400-2300rpm as opposed to 800-1200rpm) reproduced a closer match to the gas velocities found in industrial practice (0.5-2.0 cm/s). As such, it was concluded that in order to better represent industrial conditions in a laboratory setting, higher impeller speeds are recommended. A number of other observations are made, with other studies (Schubert, 1978; Liu, Roper Jr 1991; Cho and Laslowski, 2002) fleshing out the nomenclature more – but for the purposes of this project, the main relevant points have been covered. For more on the operation of a flotation cell, please see section 4.2.3.

To summarise the existing literature, it is clear that not only has the use of flotation cells in an industrial setting (a key component of this project) been thoroughly researched, with the specification for their optimisation been investigated extensively, but the extraction of graphite from kish wastage has been previously attempted. Of these attempts, it appears that there exist a number of methods which are successful in purifying the product (and consequently a number of unsuccessful methods), but regardless of the physical beneficiation it appears that in order to achieve a carbon concentration of over 99% some sort of chemical cleaning stage is needed.

## Chapter 4 - Apparatus, Experimental Methods and Materials

### 4.1 Initial samples

Originally, seven different kish dust samples from around the Tata Steel Scunthorpe steel processing plant were selected for testing (these were selected by operators at the plant with considerations of areas where a large amount of kish dust was produced and particular focus on potential areas where high graphite levels are observed in the kish dust) – they were labelled as follows, in accordance with the area they were obtained:

- Eastern Secondary Vent
- Ladle arcs 1 & 2
- Ladle arc 3
- Ladle arc cyclone
- Convector Additions

Two samples were taken from the desulphurisation plant, Desulph fall out and Desulph dust – these were designated as (in respective order):

- Desulph 1
- Desulph 2

The majority of the project was performed with these materials, but later in the project replacements for the Desulph fall out and Desulph Dust were received (denoted as Desulph 1 $\beta$  and Desulph 2 $\beta$  respectively), and a number of other samples for basic testing were received (with various names). These, and the characterisation of the dusts will be discussed in length in the next chapter.

## **4.2 Primary Methodology**

This section details the methods and procedures used for the bulk of the project (Note – for considerations of reading, any mention of basic laboratory equipment has been omitted, and only unusual equipment or equipment used in an unconventional way has been listed).

### **4.2.1 Sample Preparation**

The samples in general were very easy to handle with minimal dust issues. Dust masks were used but not essential in the preparation of the samples, as it primarily consisted of pouring the dust into a container and having it weighed for further testing.

#### ***Method***

The bulk dusts were stored in the bags they arrived in. Smaller, more easily handled sample bags were collected and from these samples were taken to be weighed. Using an accurate balance, a portion (normally 500g) of the dust was transferred into a glass beaker using spatulas for precision (Fig 4.1). Whilst technically a grab sample was taken (for ease and speed of processing), the kish dust itself (barring any anomalous object found in the larger size ranges) was on visual inspection fairly homogenous, and as such it was decided that this was enough justification for sampling in this manner. This reasoning was applied for all further sampling of the kish dust.



**Figure 4.1 - Sample Preparation**

#### **4.2.2 Mechanically Agitated Sieving**

##### ***Materials and Equipment***

- 4 BS410 Endecotts lab test sieves (Aperture range: 1000 $\mu$ m, 500 $\mu$ m, 355 $\mu$ m, 180 $\mu$ m, later an additional 2500 $\mu$ m sieve; Stainless steel mesh material, brass frame)
- BS410 Endecotts bottom collector pan
- Smooth stainless steel beads (9mm diameter)
- Retsch VS1000 Vertical agitator

##### ***Method***

After the relevant sample had been weighed, it was placed at the top of a sieve tower (with sieves in descending aperture size and a collecting pan at the bottom, and approximately 10 agitation beads placed within the mesh layers). This sieve tower was then placed on a mechanical agitator which operated at 30Hz vibrating at 30 second intervals. The time period selected was 20 minutes per 500g feed which was ascertained to be sufficient to size the sample as no further significant material discharged through the screen after this time (Fig 4.2).



**Figure 4.2 - Agitated Dry Sieving Set-up**

#### **4.2.2.1 Wet Sieving**

##### ***Materials and Equipment***

- 4 BS410 Endecotts lab test sieves (Aperture range: 1000 $\mu$ m, 500 $\mu$ m, 355 $\mu$ m, 180 $\mu$ m; Stainless steel mesh material, brass frame)

##### ***Method***

The tested sample was mixed in a large bucket with water to an approximate 1:3 ratio (by volume) to form a slurry. This slurry was periodically passed through the relevant sieve aperture with constant flowing water to wash it, and the resultant underflow was then collected in another bucket (Fig 4.3). The process was then repeated for the various aperture sizes. The wet sample was then dried and collected as per the above methods.



**Figure 4.3: An example of the kish slurry formed**

#### **4.2.2.2 Magnetic Separation**

##### ***Materials and Equipment***

- Wet High-Intensity Magnetic Separator (Boxing Mag BHW Separator)

##### ***Method***

The sample to be tested was mixed with water to approximately 10% w/w suspension. The magnetic separator was then turned on and the current adjusted to give the required magnetic field (0.04 Tesla/400 Gauss). The suspension was then passed through the magnetised matrix and separated, whilst the paramagnetic particles were attracted to the matrix and retained. The non-magnetic particles pass through the matrix unaffected by the magnetic field and were collected in a beaker. The external magnetic field was then switched off and the magnetics were flushed with water from the separator. Both fractions were then filtered, dried and analysed for loss on ignition testing (Fig 4.4).



**Figure 4.4: The wet magnetic separator used**

#### **4.2.3 Froth Flotation**

##### ***Materials and Equipment***

- Laboratory scale *Denver D12* flotation cell (H:20cm, B: 13.5cm, W: 14cm; Fill height: 15cm)
- Froth scraper (old credit card)
- Tee frother (frothing agent)
- Diesel oil (optional)

##### ***Method***

In general, (unless there was a shortage of material) 50g of the kish sample was weighed out into a beaker and deposited in the flotation cell. This was then filled almost to the brim with tap water and for the specific experiments the required amount of tee froth and diesel oil was measured with a pipette and deposited into the cell. The impeller would then be carefully lowered into the cell and turned on (rotating at a rate of 1500rpm – as per the recommendations from the literature) – this was then left for around 2 minutes in order for the mixture to homogenise (this time was determined from observation). In order to create the froth, the air sparger was turned on and the

valve gradually released until a froth naturally starts to form. At this point the froth starts to overflow into the collection tray, and this assisted by actively scraping it. This was carried out for 3 minutes as it was observed that the majority of the visible graphite has been removed from the froth - this process was assisted with the use of a wash bottle to prevent graphite flakes from sticking to the cell walls. Once the three minutes expired, the air sparger valve was closed, and the impeller turned off and removed. What was collected was considered the graphite product and what remained in the flotation cell was considered to be the tailings (Fig 4.5).



**Figure 4.5: Left to Right - A Denver flotation cell; 2 minute froth conditioning; 3 minutes scraping**

#### **4.2.4 Filtration**

##### ***Materials and Equipment***

- Vacuum filtration unit consisting of a 3000 ml vacuum filtering flask, electric vacuum pump, ceramic Buchner funnel, connection tubing and a rubber stopper.

## **Method**

The equipment was set up in the configuration as per Figure 4.6 and filter paper was placed on the funnel until it was completely covered. The vacuum was turned on and the filter paper wetted in order to form a seal. The post-froth flotation graphite product was then carefully poured in and allowed to drain. Once completely drained any material stuck to the ceramic walls was removed with the wash bottle, the vacuum was turned off and the filter paper removed (with the graphite material on it) for drying. The remaining liquid was then discarded and the process repeated for the tailings sample (Fig 4.6).



**Figure 4.6: Left - Vacuum Filtration Unit; Right - Graphite Froth in collection tray before filtration**

## **4.2.5 Drying**

### **Materials and Equipment**

- Small size paint brush

### ***Method***

The coated filter paper from the filtration stage was placed on a tray and left to dry in a drying oven (operating temperature 20°C -240°C) at 80°C (preferably overnight, but a few hours was sufficient). Once completely dry, the trays were removed and left to cool and the resulting graphite product was transferred from the filter paper into a labelled sample bag using the trowel spatula and brush. The paper was then discarded and the resultant product weighed.

### **4.2.6 Acid Leaching**

#### ***Materials and Equipment***

- Dilute Hydrochloric acid, HCl (5% wt concentration)
- Ultrasonic bath
- Vacuum filtration unit consisting of a 500ml vacuum filtering flask, electric vacuum pump, ceramic Buchner funnel, connection tubing and a rubber stopper.

#### ***Method***

Around 2g of the sample (enough so that a satisfactory amount for LOI testing could be retrieved) was placed in a beaker with enough acid (or water in case b) to fully submerge it and underwent one of three treatments:

- a. Magnetically stirred for 20 minutes
- b. Agitated in an ultrasonic water bath (water sample) for 20 minutes
- c. Agitated in an ultrasonic water bath (acid sample) for 20 minutes

Once the time period expired, the samples cleaned with acid were washed with water to stop the reaction, and the all three samples were filtered, dried, and bagged as per the previous methods.

#### 4.2.7 Loss on Ignition Test (LOI)

##### **Materials and Equipment**

- Bench top *Carbolite* Burn-off Furnace (Maximum operating temperature: 1200 °C) (Fig 4.7).

##### **Method**

Using a precision balance, the weight of a crucible was taken and around 0.2-0.5g of sample was added (enough to coat the bottom of the crucible). This was then re-weighed and placed into the furnace. This was then heated up to 900 °C, and remained at this temperature for three hours (in order for all of the combustible material to be burnt). Once this time period expired, the furnace was then turned off and the doors opened in order to allow it to cool. Once the crucible(s) were cooled, they were re-weighed (in order to calculate the mass of burnt material) and the remaining sample bagged and labelled (Figs 4.7 & 4.8).



**Figure 4.7: Carbolite Burn-off Furnace with extractor hood**



**Figure 4.8: LOI test furnace with door open to allow cooling of crucibles**

### **4.3 Characterisation Methods**

Whilst not essential to the project, a number of characterisation procedures were performed as described below.

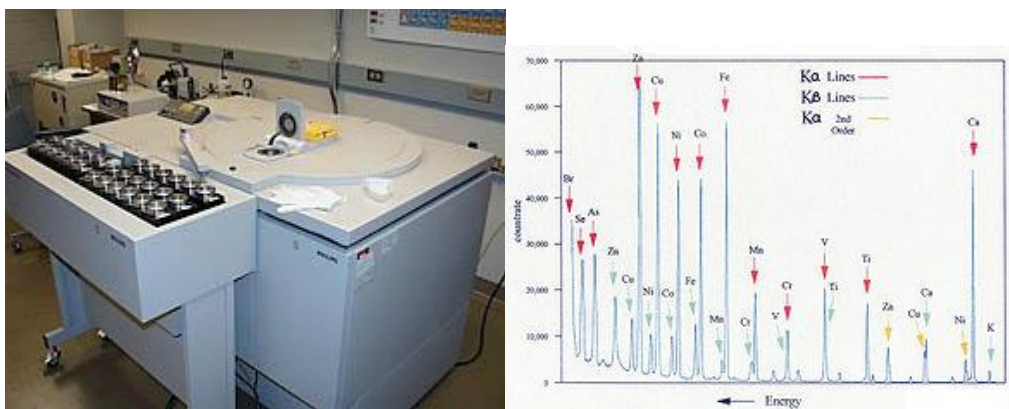
#### **4.3.1 X-Ray Fluorescence (XRF) Spectrometry**

##### ***Materials and Equipment***

- University of Birmingham X-Ray Fluorescence Spectrometer
- Powder Compressor
- Powder binder

## Method

0.1g of the sample (enough to create the tablet) was mixed with a known amount of binder into a homogenous powder. This powder was then placed into the powder compressor in order to create a tablet. This tablet was then placed into the XRF spectrometer, which then analysed the elemental content. Once completed the tablet was bagged for repeat testing (if required). For a more in-depth breakdown of the preparation of specimens for XRF analysis, please see Burhke *et al.* (1998). For an explanation as to the mechanisms behind XRF analysis, please see Appendix A.



**Figures 4.9 and 4.10: An XRF spectrometer (left), and a typical XRF results display (right)**  
**(Carleton/Wikipedia)**

### 4.3.2 Thermal and Electrical Conductivity (Morgan PLC)

A number of thermal and electrical conductivity tests were performed with selected samples by one of the project's industrial partners, Morgan plc, details of which are presented in Appendix D.

## Chapter 5 – Results

### **5.1 As Received Reference Samples**

*Note: Unless otherwise specified, if a singular number for a size fraction is listed, it is to be taken that this represents the size fraction greater than that number, but less than the corresponding larger size fraction. For example, by 355 $\mu$ m, this is to be taken as the size fraction of +355 $\mu$ m, -500 $\mu$ m.*

As specified in section 4.1, seven different dusts were sampled from Tata's Scunthorpe steel processing plant (Fig 5.1), from different areas where the iron and steel (or rather the products that eventually become the steel) is processed: These included samples taken from (and named after) the following locations:

- Eastern Secondary Vent
- Ladle arcs 1 & 2
- Ladle arc 3
- Ladle arc cyclone
- Convector Additions

And the two samples from the desulphurisation plant:

- Desulph 1
- Desulph 2

These areas were singled out by site engineers as areas where the kish dust is likely to occur.

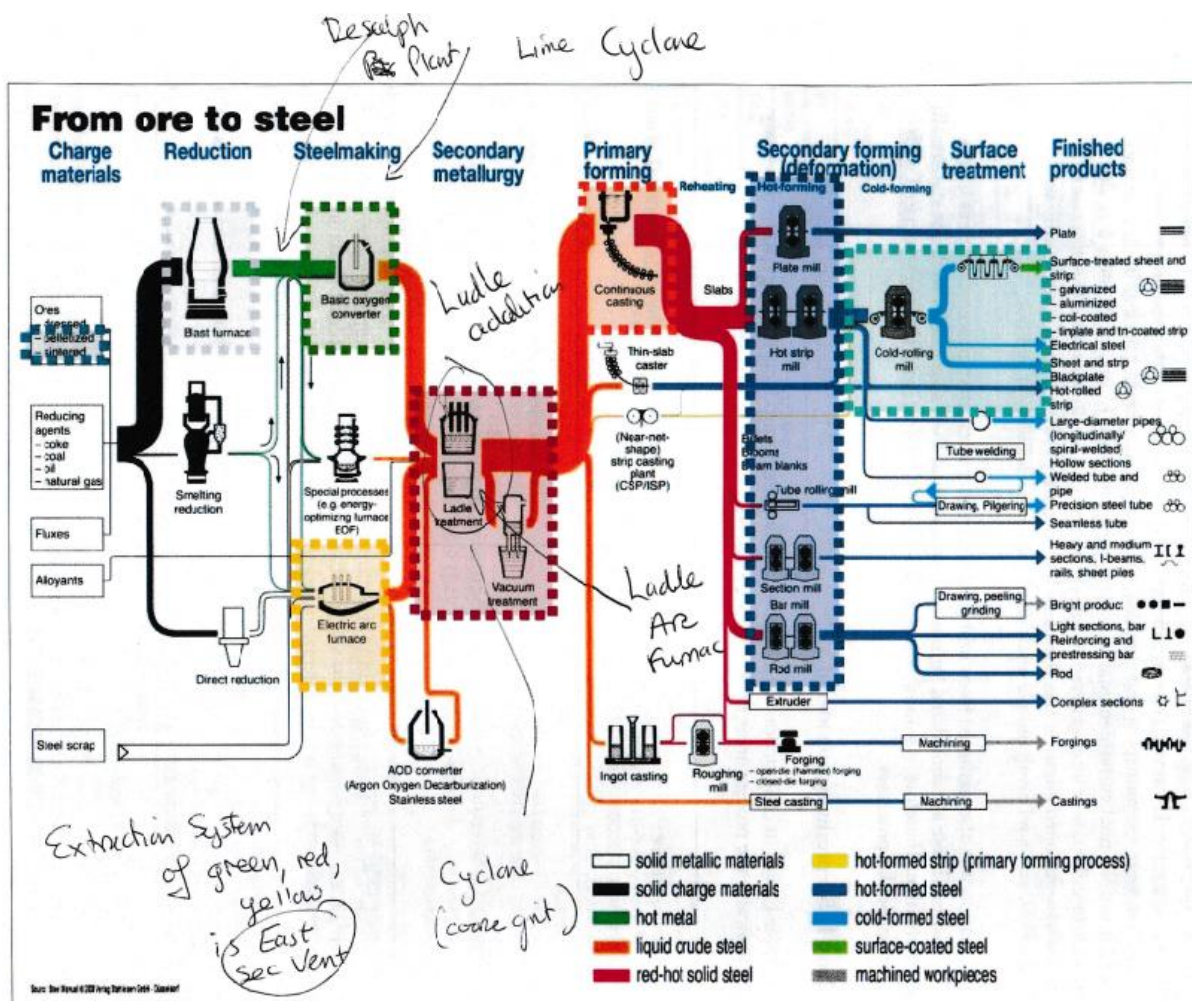
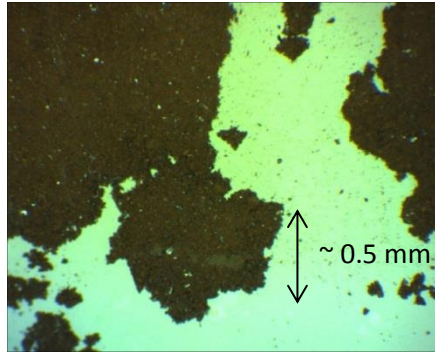


Figure 5.1: A schematic of the steel-making process, with manual additions as to where the kish dust was collected (provided by Tata Steel)

Initial testing involved characterisation of the different dusts and their properties – after testing the carbon content and size distributions each would be assessed on their potential for graphite recovery. The dusts were qualitatively assessed as follows:

**Eastern Secondary Vent** – This was a fine brown powder with a relatively low cohesion. Small impurities appeared to be present and flakes of kish graphite are noticeable, but occur in small quantities (Fig 5.2).



**Figure 5.2: A microscope image of the Eastern Secondary Vent sample**

**Ladle Arcs 1 & 2** – A fine brown powder, but with a far higher cohesion causing the dust to clump together into agglomerates. Possibly due to this clumping, the appearance of impurities and graphite flakes appear more sparsely under microscopic examination (Fig 5.3):

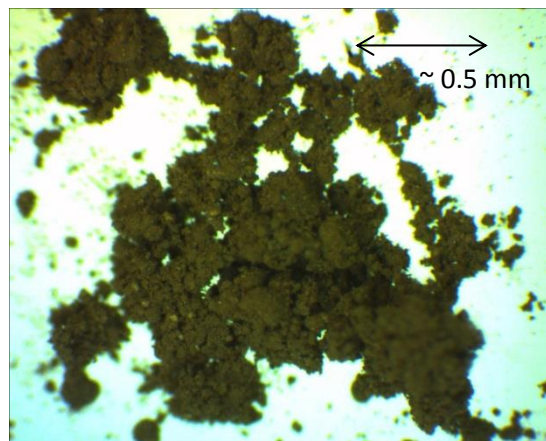


**Figure 5.3: A microscope image of the Ladle Arcs 1 & 2 sample**

**Ladle Arc 3** – largely indistinguishable from the collections taken from Ladle Arcs 1 & 2 (Fig 5.4).

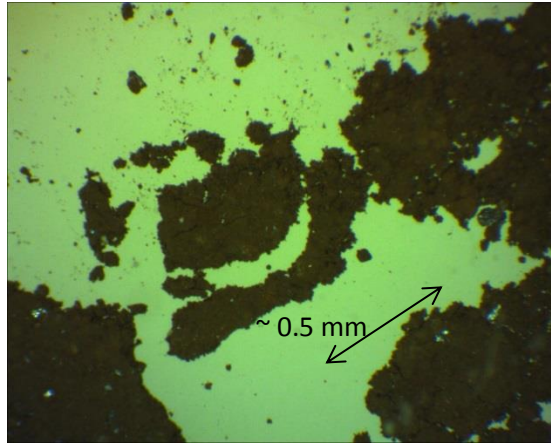


**Figure 5.4: A microscope image of the Ladle Arc 3 sample**

**Ladle Arc Cyclone** – This was a largely grey, grit-like material with a varying degree of impurities and graphite flakes visible. Low to no cohesion with the particles, but larger particles generally coated with a finer grey dust (Fig 5.4).

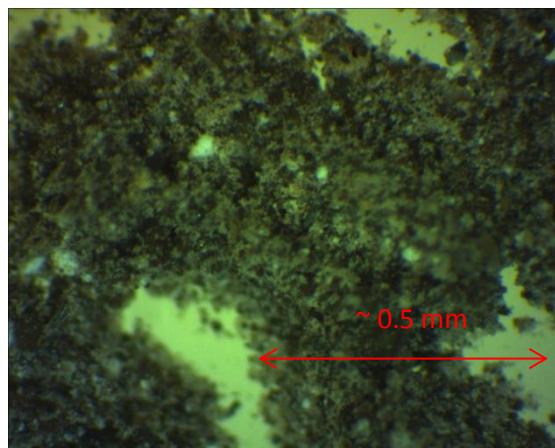


**Figure 5.5: A microscope image of the ladle arc cyclone sample**

**Convertor Ladle Additions** – This was the densest material, and consisted of very fine black particles with little to no cohesion. There did not appear to be many impurities present, rather each particle was roughly a small black ball in shape, but there did appear to be fairly significant amounts of graphite present. However, this may have been emphasised by the contrast between the shiny graphite flakes and the black powder (Fig 5.6).

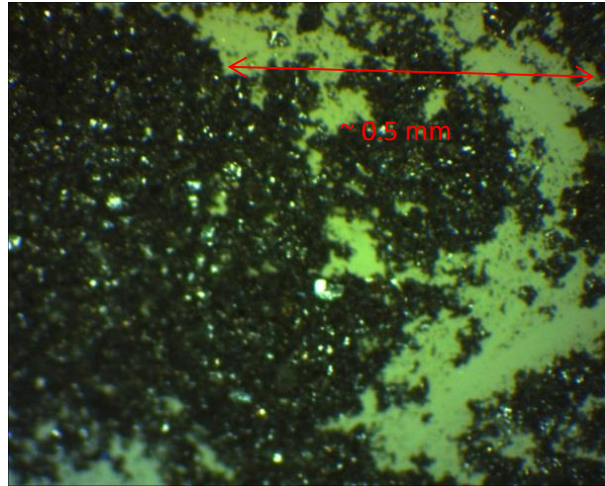


**Figure 5.6: A microscope image of the converter ladle additions sample**

**Desulph Fallout (Desulph 1)** - This was immediately singled out as the most promising source of graphite from observation alone. Taken from the sweepings of the desulphurisation plant, this sample mainly consisted of a largely grey dust of mid to low cohesion, with a wide range of grit-like impurities. Also present was a high proportion of graphite flakes in the sample (Fig 5.7).

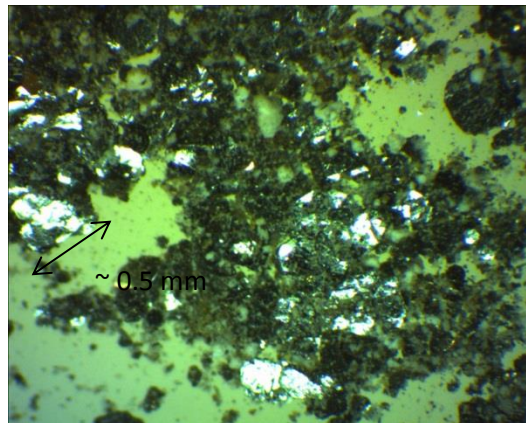


**Figure 5.7: A microscope image of the Desulph 1 sample**

**Desulph Dust (Desulph 2)** – Also immediately recognised for its potential, this was again taken from the desulphurisation plant. As opposed to Desulph 1 dust, this was largely brown in colour, and whilst the same sorts of large impurities were present, they appear to be less frequent. Like the

Desulph 1, it appeared to have a mid to low cohesion, and a clearly promising concentration of graphite was present in the sample (albeit less than Desulph 1) (Fig 5.8).

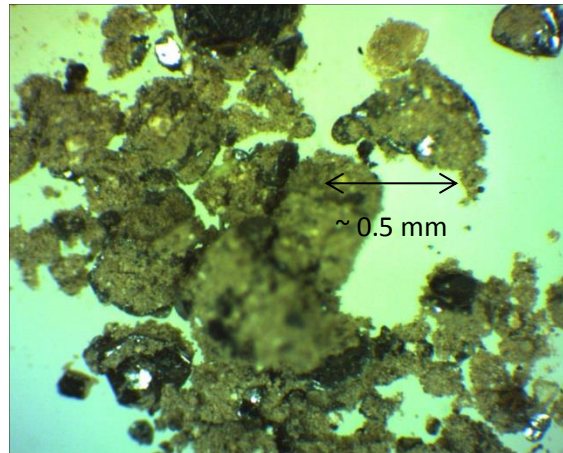


**Figure 5.8: A microscope image of the Desulph 2 sample**

## **5.2 Preliminary experiments**

In order to assess the different samples' viability for the recovery of graphite, two key factors were determined: The size distribution of the dust and the carbon content. It is evident there is no point in pursuing further a product with a low concentration (<10%) of Carbon (and consequently graphite). However, the relative importance of the size distribution is less clear as for example, even if there were a high concentration of graphite, if it were all of the order of a few microns its desirability is severely reduced to industry (as detailed in Chapter 1, as a general rule of thumb, the larger the flake size the more desirable the graphite). As such, for the initial stages of the project it was decided that in order for the dust to be worth investigating further, it needed a carbon content of over 10% and an appreciable proportion of its mass in the >180 $\mu$ m size range.

### **5.2.1 Size Separation – Wet Sieving**

Due to its availability, ease of use and cost, it was decided that physical separation via sieving would be a suitable mechanism to separate the size fractions, with the distinction between wet and dry

sieving yet to be decided. The perceived benefits to wet sieving was that in addition to separating the size fractions, by converting the dust(s) into a suspension, it would minimise losses (and risk to health by inhalation) and would have the added bonus of acting as a cleaning agent to the graphite flakes. To test its suitability, the wet sieving of one sample of dust was performed, but the results were found to be unsatisfactory due to the volumes of water used and the need for subsequent drying.

Dry sieving was consequently tried, and found to be far more suited to requirements; the dust(s) were all found to be easy to handle (with minimal dispersion to the atmosphere), and whilst the effectiveness of separating the size fractions varied due to the cohesiveness of some of the dusts, it was shown to effectively liberate the graphite flakes from the wider mass of dust.

### **5.2.2 Selection of the Dusts**

The seven samples were placed on a sieve tower and mechanically agitated until no more separation was observed (the mesh sizes used were 1000 $\mu\text{m}$ , 500 $\mu\text{m}$ , 355 $\mu\text{m}$  and 180 $\mu\text{m}$ ). The distributions of masses in the samples are illustrated below in Fig 5.9:

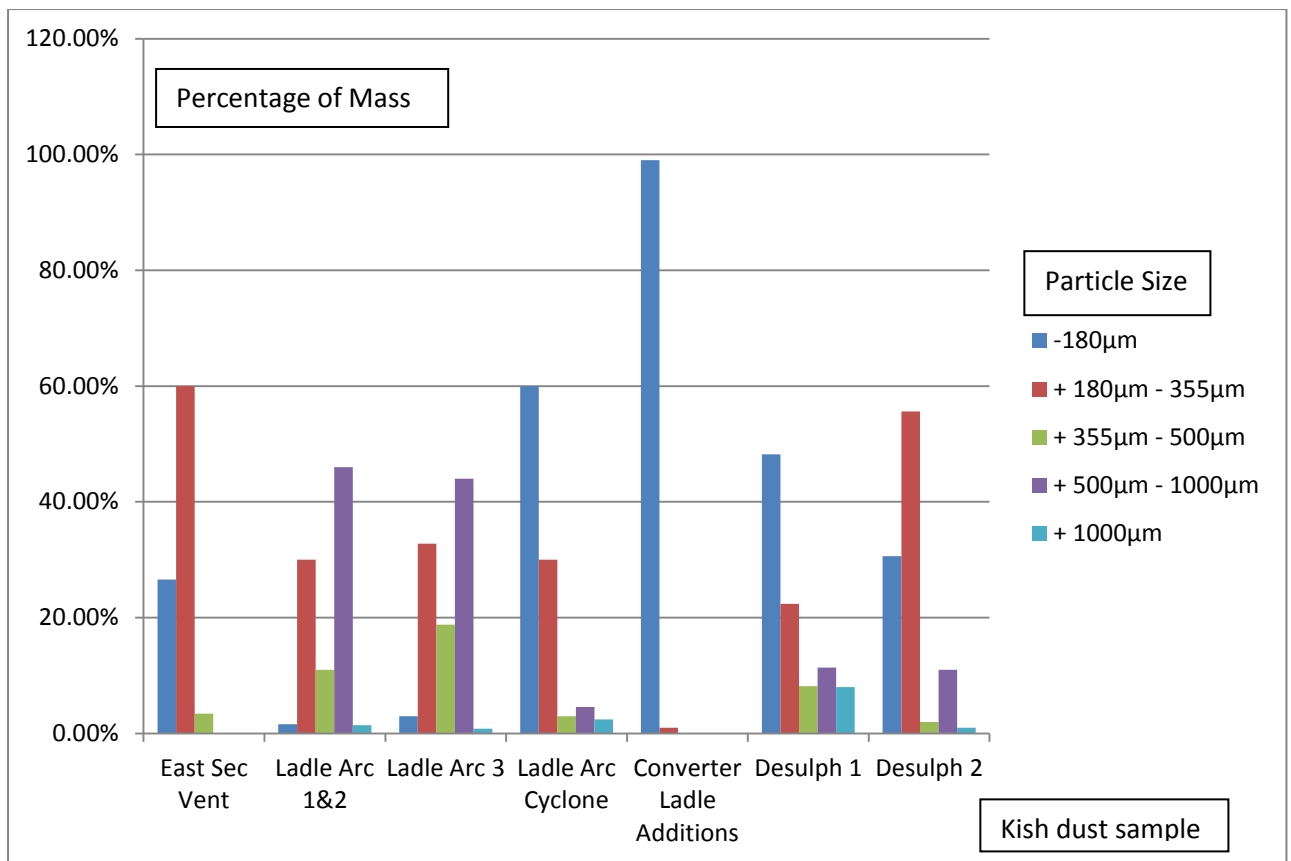


**Figure 5.9: A graph detailing the particle size distribution of the samples received from Tata Steel**

As can be seen, the majority of the mass in the samples is found below the 355µm size range – the exceptions to this being the Ladle Arc samples. However, this was a misleading result, as the Ladle Arc dusts were highly cohesive, and as such formed clumps that were not suited to sieving – as such, a more realistic result would likely show the majority of the mass of both of these samples to be in the sub 180µm fraction. Given this additional information, the dusts of promise at this point were Desulphs 1 & 2, and the Ladle Arc Cyclone collections. Even without the considerations of carbon content, the convertor ladle additions were rejected on the basis of the size of the particles, with 99% of the mass belonging to the sub 180µm range.

Loss on Ignition analysis was also performed on the dusts to ascertain their carbon content – the results were as follows (Table 2):

**Table 2: Loss on Ignition – Tata Steel samples**

<b>Dust Sample</b>	<b>Carbon Content (%)</b>
Eastern Secondary Vent	3.9
Ladle Arc 1&2	6
Ladle Arc 3	4.5
Ladle Arc Cyclone	8.5
Convertor Ladle Additions	0
Desulph 1	32.4
Desulph 2	29.5

Given these results, it was decided to solely focus on the Desulph 1 and Desulph 2 samples. Whilst there is potential for graphite recovery (in both the mass distribution and carbon content) in the Ladle Arc Cyclone collections, for purposes of time and efficiency, it was decided to neglect this sample (along with the other 4 samples) for the remainder of the project.

### **5.2.3 X-Ray Fluorescence (XRF) Analysis**

In order to better classify the samples, XRF analysis was also performed on the samples. It was also hoped that this, in conjunction with the loss on ignition analysis could provide a more accurate representation of the overall character of the samples (LOI analysis is based on the loss in mass – assumed in this project to be solely comprised of carbon). However, whilst the XRF spectrometer delivered a report detailing the elemental analysis of the number of powder, the spectrometer used

was unable to detect carbon as an element. Due to this, it was abandoned as a primary analytic tool, but could be utilised as an analysis of the waste streams and ash samples from the LOI tests.

As reflected in other literature, the two impurities present in both the Desulph 1 and 2 streams mainly consisted of calcium and iron with a varying degree of other elements (Magnesium, Sulphur, Silicon and Manganese for Desulph 1, Potassium, Magnesium, Sulphur, Sodium and Silicon for Desulph 2), with the remainder being composed of trace elements (less than 0.5% of the stream).

For a more in depth analysis of the XRF spectroscopy, please see the Appendix A.

#### **5.2.4 Magnetic Separation**

Wet High Intensity Magnetic Separation was applied to a number of the samples. The results were disappointing with very little concentration of graphite in the non-magnetic fractions. As already discussed, this lack of graphite separation is attributed to ferromagnetic material (notably the iron particles) 'carrying' the graphite flakes with it, either by being embedded in the flakes themselves, or simply mechanically. As such, any further testing with this method was abandoned.

### **5.3 Primary Experiments**

Focussing on the Desulph 1 and 2 powders, the next (and main) stage of the project was to develop a method in order to isolate and refine the graphite found in the kish to a purity of 95% C. This was done as part of a two stage process – physical beneficiation, and a likely chemical cleaning stage (Fig 5.10):

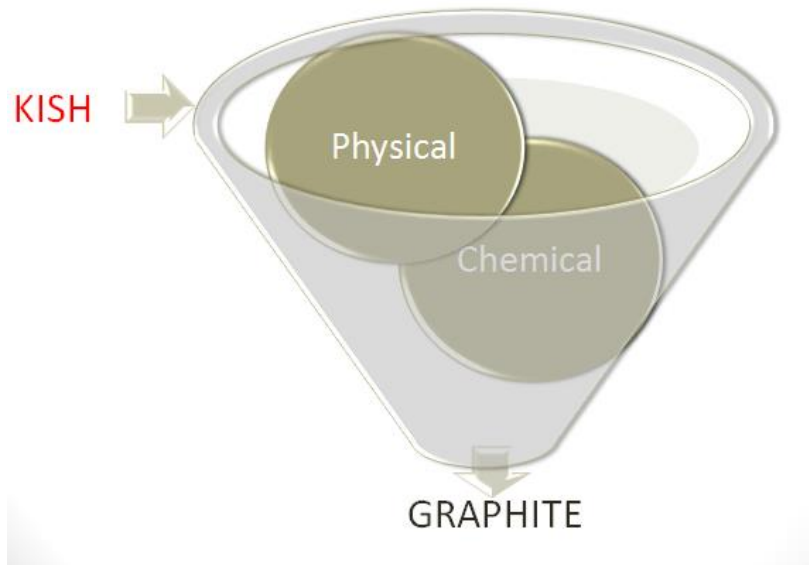


**Figure 5.10: A representation of the processes needed to refine the graphite**

### **5.3.1 Physical Separation through Mechanically Agitated Dry Sieving**

Whilst initial testwork showed that the dry sieving was extremely successful in liberating the larger particle size graphite flakes from the kish dust. However, upon additional analysis using LOI the purity of the flake samples was found to be lower than expected. Whilst the larger flake sizes appeared to be of high purity the discrepancy highlighted by the LOI test can be attributed to the presence of atypical impurities, such as pieces of grit, ceramic etc. which could wildly skew result depending on the composition of the sample. To this end, in the subsequent sieving stages (and as will be used when calculating the yields, purities etc.) an additional screen of 2.5mm was used to screen out the larger, non-standard impurities.

With regards to the methodology employed with the dry sieving, the process underwent several iterations before a standardised procedure was decided upon that appeared to fully separate all the relevant fractions. Initially the sieve tower was placed on the mechanical agitator and vibrated for 10 minutes per 250g at 20Hz, and then by a series of optimization tests a standard procedure was

adopted that fulfilled the objectives. This procedure was to sieve every 250g of material for 10 minutes at a frequency of 30Hz with the addition of agitation beads. Observational analysis showed that sieving for any longer than this did not appear to produce any significant change in the particle distributions. Whilst there may be more efficient ways to separate the particles, once this method was adopted there were no further attempts to optimise it.

Using this methodology, numerous fractions of the Desulph 1 and 2 dusts were produced, with the mass distributions as follows (Fig 5.11) (for a more in-depth analysis of particle size measurement, see Allen (1997)):

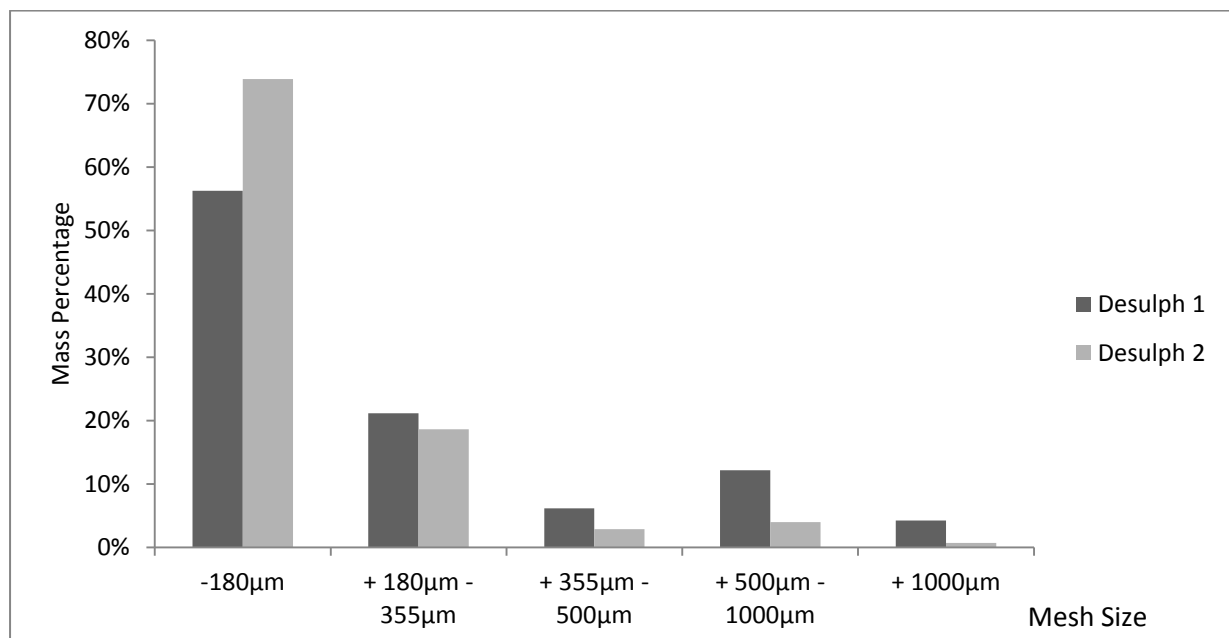


**Figure 5.11: A Graph Detailing the Particle Size distribution after Sieving of Desulph 1 and Desulph 2**

The results show that whilst the majority of the dust mass is found in the particles that pass through the 180µm screen, a significant amount of the mass is found in the larger size fractions (approximately 45% in the Desulph 1 sample). The waste fraction does contain graphite which could be further liberated, but due to the low amounts present, and the utility afforded from flakes of this size being lower than the other flakes (as detailed above), this fraction was treated as a discard at

the time of the experiments. Subsequently this fraction was investigated for its potential also (section 5.4).

For both of the samples, the majority of exploitable graphite was observed in the 500-1000 $\mu\text{m}$  and 180-355 $\mu\text{m}$  fractions (Table 3) – whilst the highest quality flakes are present in the largest fractions, the mass percentage is skewed due to the presence of non-standardised impurities which are unlike the kish dust. The purities of the fractions below 355 $\mu\text{m}$  tended to vary from between 40-60%, so it was clear that more refinement was definitely needed, with froth flotation undertaken on these fractions to raise the purity.

**Table 3: The carbon content of the different size fractions**

SIZE FRACTION	CARBON CONTENT (%)	
	DESULPH 1	DESULPH 2
1000 $\mu\text{m}$	82.5	86.7
500 $\mu\text{m}$	50.6	69.1
355 $\mu\text{m}$	49.6	48
180 $\mu\text{m}$	39.0	54.8
<180 $\mu\text{m}$	14.9	73.6

### 5.3.2 Physical Separation through Froth Flotation

#### 5.3.2.1 Desulph 1

The initial froth flotation tests were undertaken on the fractions from 180 $\mu\text{m}$  to 500 $\mu\text{m}$  as the majority of the mass was in these fractions, and it was clear that in order to produce a marketable

product, further beneficiation was required. The results for the individual fractions are as follows

(Fig 5.12):

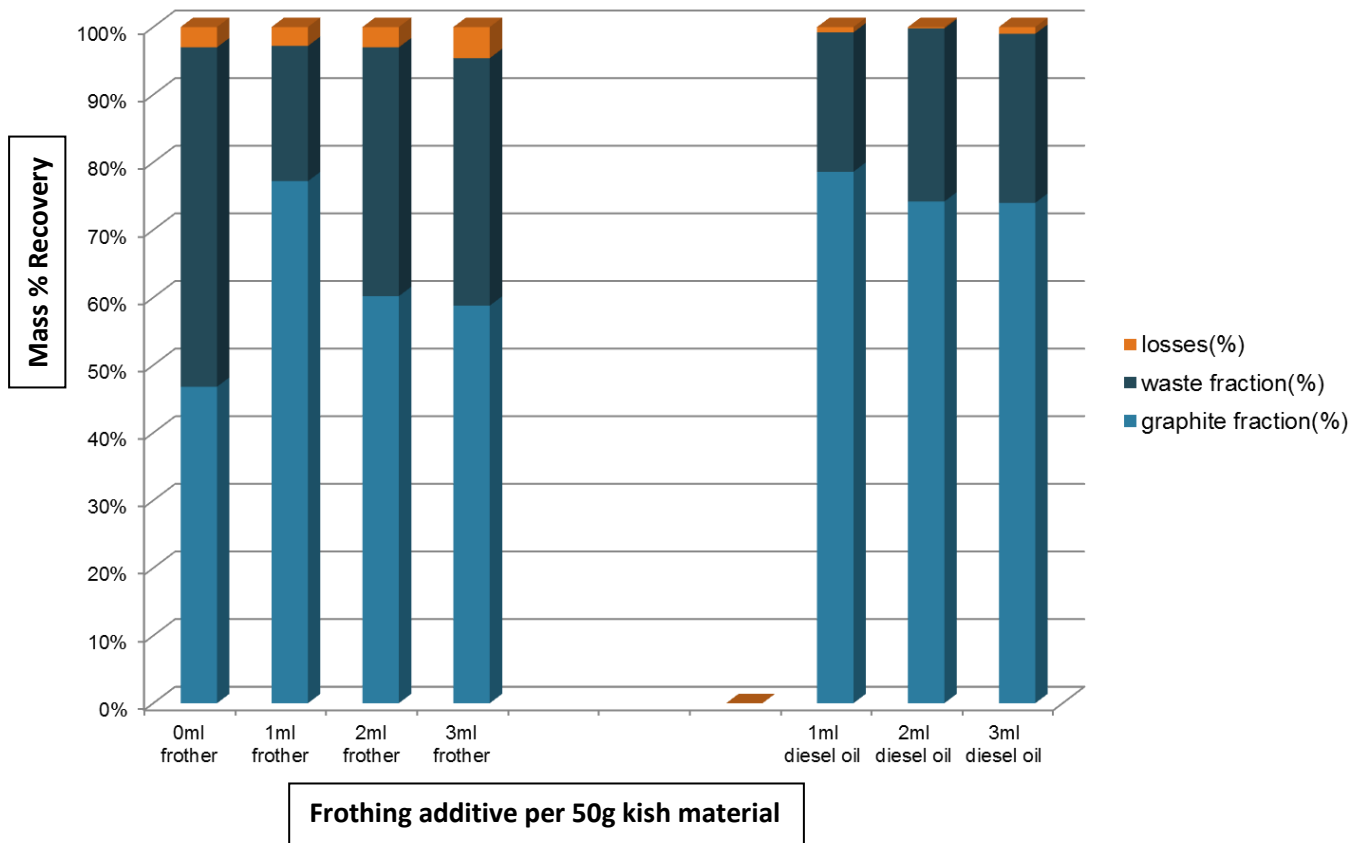


**Figure 5.12: A Graph Detailing the effect of varying frother additions on yield for the**

**+180µm, - 355µm Desulph 1 sample**

Whilst there is more of the mass present in the 180-355µm fraction, it is more comparable in size to the impurities so is harder to separate. As illustrated above (Fig 5.12), even without any additives the graphite separates effectively from the waste material – this is due to the extreme hydrophobic properties of the flakes, and their comparable size to the bubbles formed in the Denver cell. With the addition of the teefroth (the frothing agent), the mass floated was significantly increased (increasing from around 45% to 75%). However, with the teefroth dosage level being increased further (2ml, 3ml per 50g), this appeared to have a detrimental effect on the mass floated – this was

likely due to the additional teefroth being too effective, rendering the frothing process too violent. This results in the hydrophilic silicates and iron oxides being floated as well.

With the addition of the diesel oil (acting as a collector), there was no appreciable difference in the mass floated (all diesel oil additions were done with a base level of 1ml teefroth also): Varying the amount of diesel oil does not appear to have a pronounced effect on the mass floated, and since it is comparable to the mass obtained with no diesel oil additions it can be considered as superfluous to the optimisation of the process (at least for this size fraction).

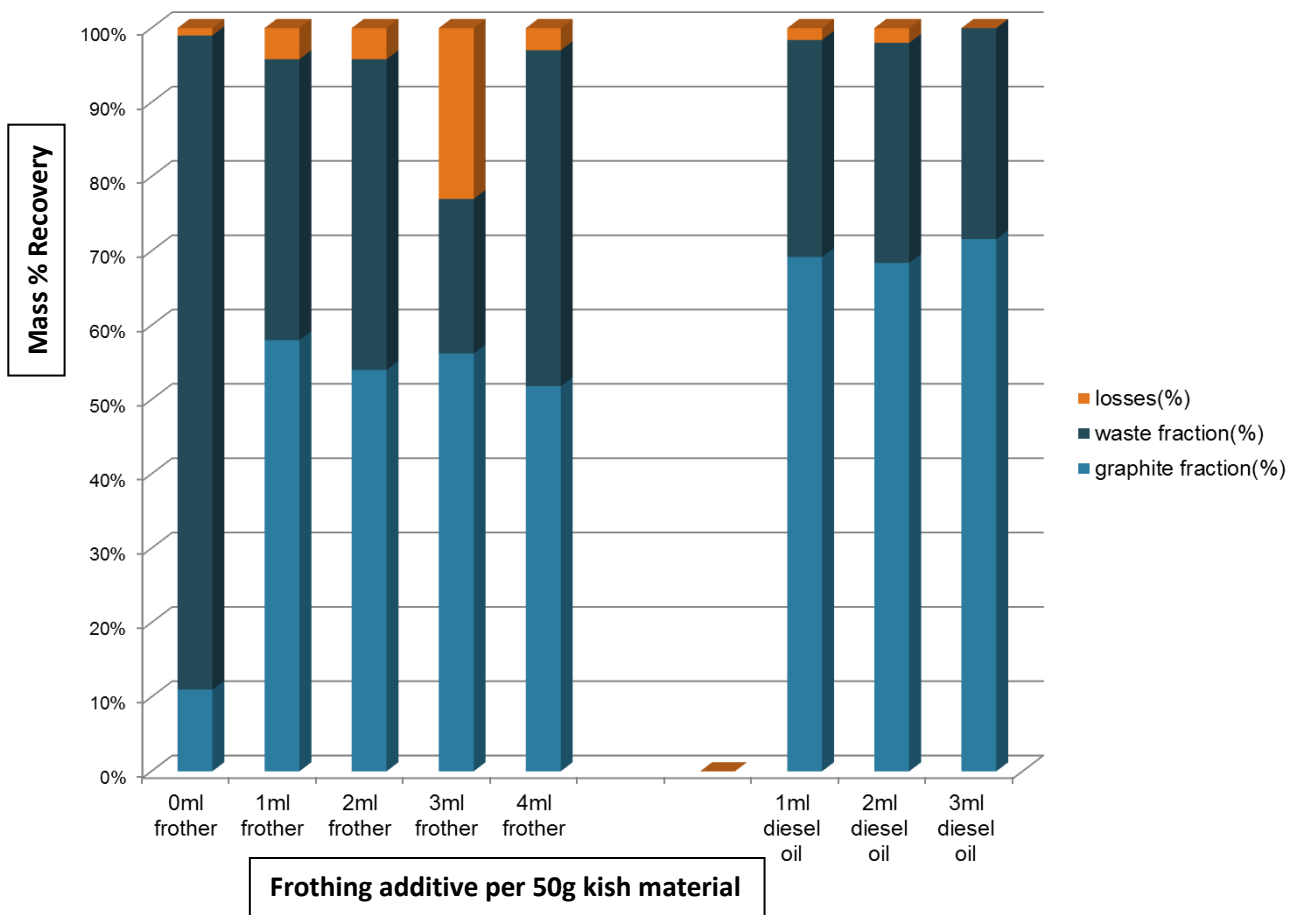


**Figure 5.13: A Graph Detailing the effect of varying frother additions on yield for the +355µm, - 500µm Desulph 1 sample**

Fig 5.13 (above) illustrates similar behaviour in the 355µm-500µm fraction. In general, the same pattern was observed: The addition of teefroth greatly increases the mass floated from the process,

but a detrimental effect can be observed if an over dosage occurs (resulting in the volume of bubbles mechanically entraining the hydrophilic iron oxides). With regards to the addition of diesel oil to act as a collector to enhance graphite flotation, there was a marginal increase in the mass floated obtained, but due to the relatively low proportion of particles in this size range, it is unlikely this improvement is significant enough to make the addition cost effective. Furthermore, whilst the addition of the diesel oil can result in an increase in the mass floated, there was a notable *decrease* in the carbon content when the samples underwent LOI testing (see Fig 5.14 and Fig 5.15). The reason for this is thought to be that the diesel oil in these instances is too effective, and caused unwanted particles to become entrained in the resultant foam (Note that typical error level for the LOI tests performed was +/-2%).

### LOI of Desulph 1 with varying frother additions

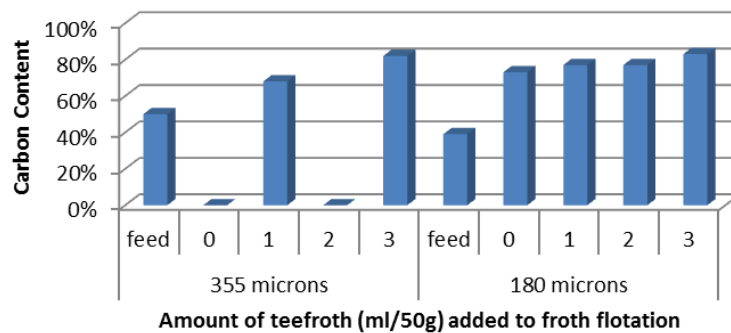


**Figure 5.14: A Graph Detailing the effect of varying frother additions to the Carbon Content for the 355µm and 180µm Desulph 1 sample**

## LOI on Desulph 1 with varying diesel oil additions

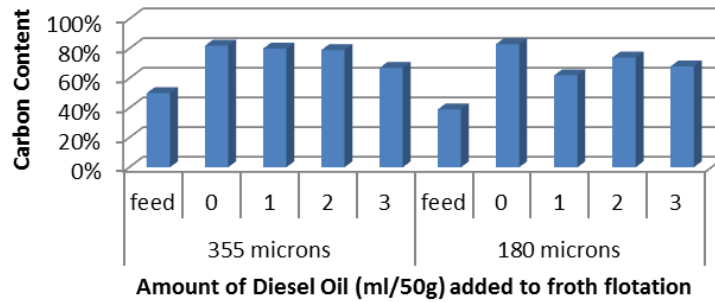


**Figure 5.15: A Graph Detailing the effect of varying diesel oil additions to the Carbon Content for the 355 $\mu$ m and 180 $\mu$ m Desulph 1 sample**

The above data shows the carbon content of the various flotations concentrates samples (note that in Fig 5.14 the results at 355 microns for 0 and 2 ml/50g of teefroth are missing due to lack of resources, and are not indicating 0% carbon content). In general, an increase in the carbon content is observed when any kind of froth flotation is performed. The variation of teefroth additive, whilst having a pronounced effect on the mass obtained, does not appear to have as pronounced an effect on the carbon content of the flotation concentrate. Whilst the carbon content is improved by a considerable degree (up to around 80%), it is still not reaching the purity required from the project (+95%), and as such further processing is likely to be needed. However, with regards the addition of diesel oil as a frothing aid, there was no increase in purity observed (and in some cases a sizeable decrease), so it was concluded that diesel oil was not needed in the froth flotation processing of the Desulph 1 sample.

### 5.3.2.2 Desulph 2

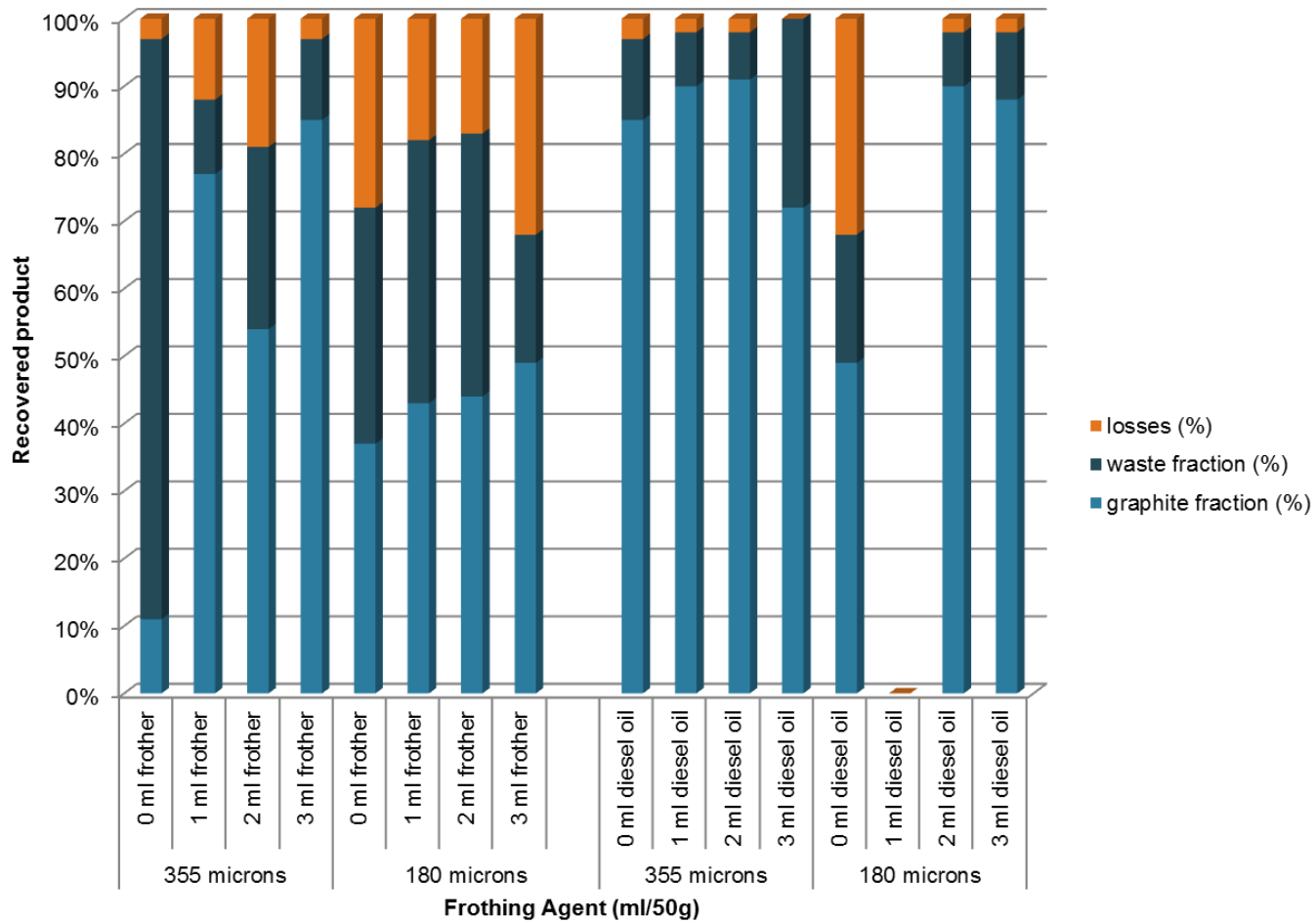


**Figure 5.16: A Graph Detailing the effect of varying frother additions on yield for the 355µm and 180µm Desulph 2 sample**

Fig 5.16 illustrates that similar results were found with the Desulph 1 sample. The addition of frother greatly improved the mass floated obtained, but in general increasing beyond 1ml per 50g of sample had a detrimental effect on the mass floated - although the 3ml per 50g of sample does appear to have increased the mass floated, it is not by a sizeable amount, and as such seems unlikely to be worth economically pursuing on mass recovery alone.

The addition of diesel oil appeared to not greatly increase the mass floated of the 355-500µm sample, but did appear to have increased the mass floated of the 180-355µm sample. However, it is

unclear as to why such a pronounced effect occurred for such a specific sample, and as such the results may have been anomalous and repeated to ascertain for certain.

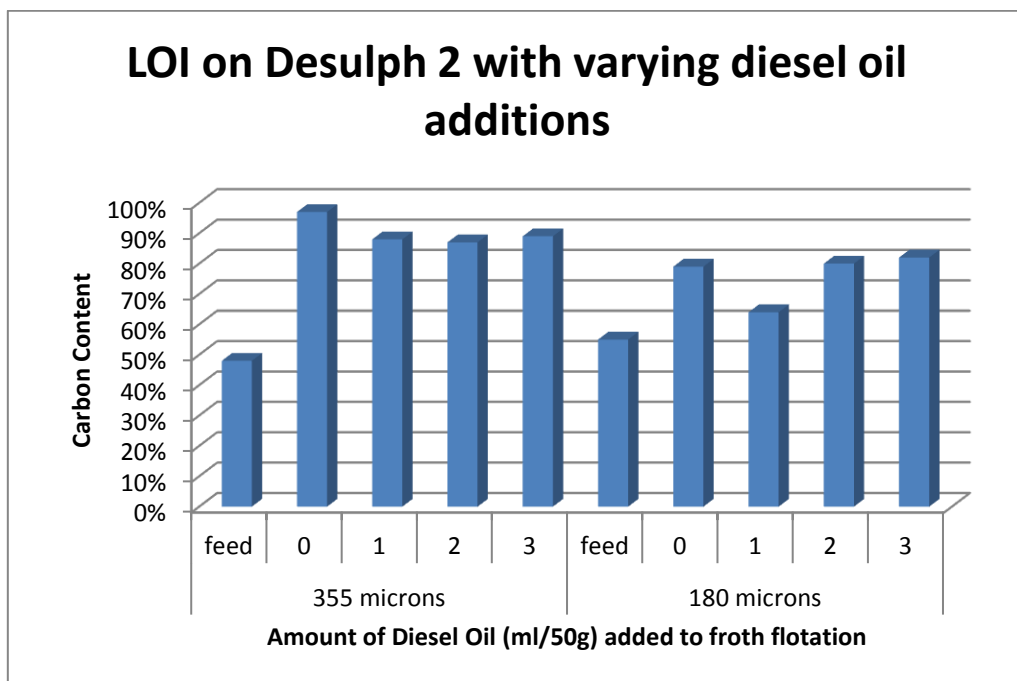
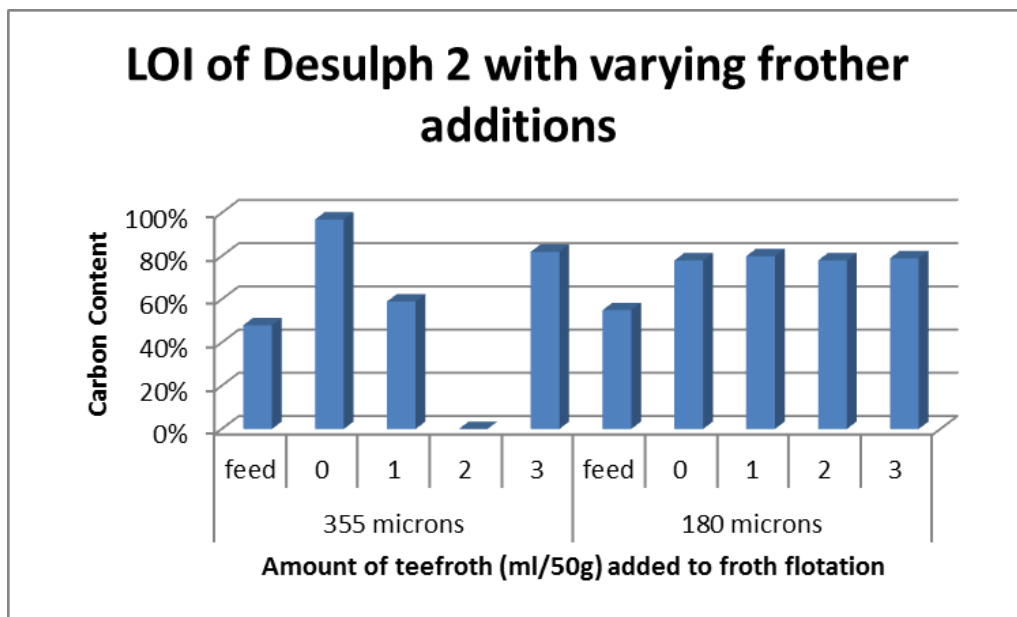


Figure 5.17 & 5.18: A Graph Detailing the effect of varying frother additions to the Carbon Content for the 355µm and 180µm Desulph 2 sample

From the above (Fig 5.17 and Fig 5.18), it can be seen that the froth flotation process has significantly improved the carbon content of the samples, and that again for the 180-355 $\mu$ m sample, the variance in teefroth does not have a pronounced effect on this carbon content. With regards the 355-500 $\mu$ m sample, whilst the diesel oil additions again show no positive net effect on the purities, the teefroth additions are less clear – due to the relatively low yields of the 355 $\mu$ m fraction, further tests would be recommended to verify this data.

### **5.3.3 Chemical Cleaning through Acid Leaching**

With one froth flotation stage being unable to raise the required purity of Desulph 1 and Desulph 2 to the >95% target, and the previous literature recommending the use of acid leaching as a final cleaning stage, a number of different cleaning methods were used (as detailed in the previous chapter). Taking a froth-floated sample of the 180 $\mu$ m and 355 $\mu$ m fraction, and a non-treated sample of the 500 $\mu$ m and 1000 $\mu$ m fractions (given their relatively high purity already, it was reasoned that chemical cleaning alone would raise it to the desired purity, eliminating the need for a costly additional step), three treatments were used, with the ultimate purities as follows (Table 4):

**Table 4: The different Carbon Contents of the samples after varying cleaning treatments**

Sample	Size fraction (microns)	Carbon Content (%)				
		Screened	Flotation Conc.	Acid bath	Water bath and ultrasound	Acid bath and ultrasound
Desulph 1	+1000	85	N/A	<b>95</b>	93	91
	-1000, +500	73	N/A	84	77	79
	-500, +355	50	82	<b>95</b>	-	-
	-355, +180	39	88	90	-	-
Desulph 2	+1000	83	N/A	<b>&gt;99</b>	<b>&gt;99</b>	87
	-1000, +500	87	N/A	<b>&gt;99</b>	94	<b>98</b>
	-500, +355	48	<b>97</b>	<b>&gt;99</b>	<b>97</b>	<b>96</b>
	-355, +180	55	78	<b>97</b>	79	<b>96</b>

As detailed above, three different methods of chemically cleaning the graphite flakes were attempted (acid bath and mixing, water bath and ultrasound, and acid bath and ultrasound). All three were successful in raising the purity of the graphite, to varying degrees (Table 4). Whilst there was a clear difference between the water and sulphuric acid cleaning (acid being far more effective), there is less variation between the sulphuric acid ultrasound and sulphuric acid-mixing variants. Given there is a slight increase to the purities when the mixed, and that the ultrasound would be more expensive, the simple acid mixing variant is the more preferable of the two (5% w/w H<sub>2</sub>SO<sub>4</sub>, 5ml/g ratio, ambient temperature).

However, given the unsuccessful purification of the Desulph 2 +500µm – 1000µm sample, and undesirable consequences of the impurities still present in the feed (see the tertiary experiments section below), it was decided that the best course of action would be to in fact froth float any

fractions above 500µm also. After this was performed on the Desulph 1 1000µm and 500µm samples, it appeared to remove all of the grit-like, heavy impurities – resulting in a more homogenous material – and raised the purities pre-acid leaching to 96% and 86% C respectively (Table 5):

**Table 5: The revised Carbon Content of the larger flake sizes of Desulph 1 after froth flotation**

Sample	Size fraction (microns)	Carbon Content (%)	
		As received	Post froth-flotation
Desulph 1	+1000	85	96
	-1000, +500	73	86

Given the already high purity, and the effectiveness of the water bath and ultrasound on the flakes of higher size, it could be possible to purify the +100µm and -1000µm +500µm flakes to a marketable grade without exposing them to potentially expensive acid leaching.

#### 5.3.4 Top-up Bags (Desulph 1β & 2β) and Additional Samples

As stocks ran low on the Desulph 1 and 2 dusts, replacement bags were delivered from the steel plant. Whilst ostensibly these were the same as the original Desulph 1 and 2 samples (and should consequently possess largely the same characteristics), it soon became apparent that there were a number of discrepancies: The new samples had a lower concentration of Carbon, different particle size distributions, and were more cohesive powders than their predecessors. In order to distinguish these from the original samples, they were denoted Desulph 1β and 2β.

Extensive testing on these powders was not performed (with the exception of the sub 180µm fraction of Desulph 2 β in the secondary experiment), but the mass distributions and relative purities were as follows (and comparing these results to the original samples) (Fig 5.19):

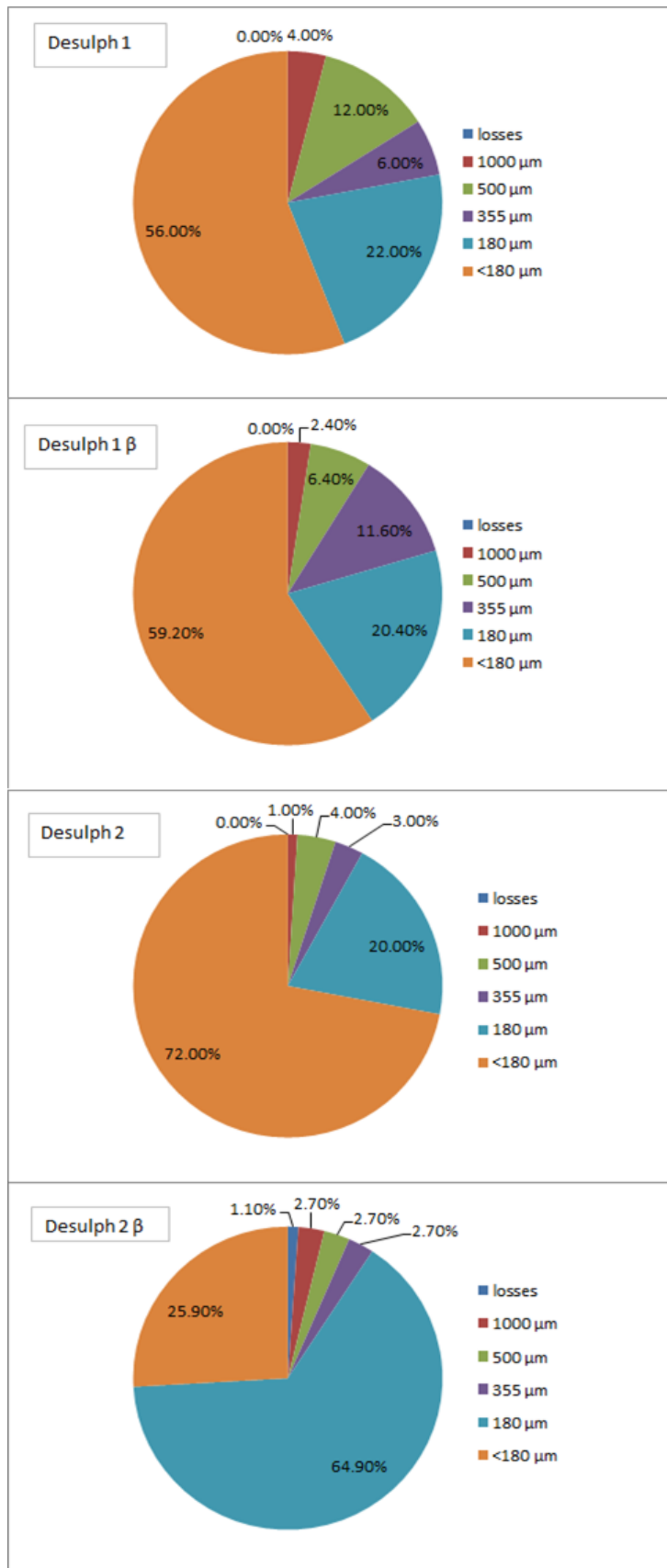


Figure 5.19: Comparison of particle size distribution for Desulph 1 & 1β, 2 & 2β.

There is clearly more than just a superficial difference: Whilst the Desulph 1 samples were largely consistent with regards the lower size fractions, there were considerable differences amongst the 355 $\mu\text{m}$  and above fractions. The Desulph 2/2 $\beta$  differences are more significant, most clearly with the 2 $\beta$  sample having a larger 180 $\mu\text{m}$  fraction, as this may indicate different plant operation conditions for the second samples or possibly a different sampling protocol by Tata Steel.

The loss on ignition data also showed some variation (Table 6):

**Table 6: The Loss on Ignition data comparison for Desulph 1 & 1 $\beta$ , 2 & 2 $\beta$**

FLAKE SIZE ( $\mu\text{m}$ )	CARBON CONTENT (%)			
	DESULPH 1	DESULPH 1 $\beta$	DESULPH 2	DESULPH 2 $\beta$
RAW (as received)	32	38	30	10
+1000,-2000	85	70	83	37
+500, -1000	73	95	87	14
+355, -500	50	53	48	35
+180, -355	39	54	55	11
-180	15	25	25	10

From Tale 6 the difference in the  $\beta$ -sample purities is interesting. Desulph 1 $\beta$  has in general a greater carbon content, but Desulph 2 $\beta$  has a significantly lower one. In order to obtain an accurate picture of a plant's potential ability to process graphite, a more comprehensive survey of the plant and materials over a period of time would be recommended.

In addition to the  $\beta$ -samples, a number of other samples from other potential sources were received (having undergone varying treatments), with their purities calculated as follows (Table 7):

**Table 7: The Loss on Ignition of Miscellaneous samples Supplied by Tata Steel**

Sample	Carbon Content (%)
Desulph dust Bulk Sample, bag 5 (1/5/2013)	14.7
Desulph dust Bulk Sample, bag 3 (1/5/2013)	8.3
Bulk Sample (1/5/2013), bags 1+3+5+7, +180 - 500 micron, acid washed	57.7
Desulph dust (March 2013), wet sieved	57.2
Bulk Sample (1/5/2013), bags 1+3+5+7, + 500 micron, acid washed	92.7
New Material 1	24.4
New Material 2	12.9

The analysis of the miscellaneous sample indicates that there are a number of other potential sources and sites for kish recovery on the Scunthorpe site, with varying degrees of success – in terms of the wider goals of the project, it shows that even simple processing of other sources can produce a high grade product (in particular the ‘New Material 1’ sample).

#### **5.4 Processing of minus 180 micron fraction**

In addition to the main experiment of processing the +180µm fractions of Desulph 1&2, a secondary experiment investigating the sub 180µm fraction of each was performed. Using the same methodology employed in the main experiment, the previously rejected material was initially sieved into fractions of 150µm, 120µm, 90µm and 60µm. Due to time constraints and considerations of feasibility, the 150µm and 120µm fractions were removed as the yield obtained from them was too low to be of any practical use. Any material less than 60µm was treated as discard, as the Loss on Ignition testing indicated the carbon content was approaching (or had already dropped below) the

10% Carbon mark, and the flake sizes were becoming comparable to low-grade graphite dust, rendering the potential monetary reward as less appealing. Froth flotation tests and acid ( $H_2SO_4$ ) leaching were then performed on these remaining fractions in order to obtain the highest purity product possible.

(Note: As has been mentioned previously, part-way through these experiments, the Desulph 2 deposits ran out. As such, the Desulph 2  $\beta$  sample was used in the latter stages, and consequently the final analysis.)

In general the results mirrored the results of the larger size fractions, but with a few key differences – the most prominent of these is that there appeared to be a different optimal amount of frother (namely around 2ml/50g) to attain both yield and purity. This is likely due to the larger surface area of graphite per gram of feed material in the minus 180 $\mu$ m fraction. Given this secondary experiment occurred later in the project's lifecycle, there was more of a time constraint associated with it, so further verification would be needed for this. Another possible reason for this result is that as the graphite flake sizes approach the actual size of the majority of the sample dust particles, it is harder for the graphite flakes to reach the froth without being impeded by the impurities (the lift resultant from the hydrophobicity of the graphite is not enough to migrate through the rest of the kish dust). With the additional frother, this creates a better mixing environment which enhances the probability of contact between an air bubble and a graphite flake, allowing the flakes that otherwise would not reach the froth to settle there.

As a consequence of the low purity of the product after the first froth flotation stage it was subjected to a second stage with the aim of improving the purity. The second stage of froth flotation successfully raised the purity which confirms the results obtained (section 3.4), as illustrated below (Table 8):

**Table 8: The Carbon Content of the non-treated sub-180 micron samples tested**

<b>KISH SAMPLE</b>	<b>CARBON CONTENT (%)</b>		
	<b>SIZE FRACTION (MICRONS)</b>		
	<b>-180, +90</b>	<b>-90, +63</b>	<b>-63</b>
<b>DESULPH 1</b>	80.6	63.0	38.1
<b>DESULPH 2<math>\beta</math></b>	69.5	31.8	10.4

Finally, in order to raise their purity to the highest possible level, a number of the floated samples underwent acid leaching (specifically the Desulph 1 -180 $\mu$ m +90 $\mu$ m and -90 $\mu$ m +63 $\mu$ m fractions, due to their already high purity). The highest purities obtained were 94.7% and 94.0% for the 90 $\mu$ m fraction and 63 $\mu$ m fraction, respectively (Table 9) (ff stands for 'froth flotation'):

**Table 9: The final Carbon Content achieved on some of the sub-180 micron samples tested**

<b>SAMPLE</b>	<b>TEEFROTH (ml)</b>	<b>CARBON CONTENT (%)</b>
Desulph 1 -180µm +90µm (ff)	1	78.0
Desulph 1 -180µm +90µm (ff)	2	85.2
Desulph 1 -90µm +63µm (ff)	1	93.0
Desulph 1 -90µm +63µm (ff)	2	91.0
Desulph 1 -90µm +63µm (ff)	3	93.1
Desulph 1 -90µm +63µm (re-ff)	1	92.7
Desulph 1 -63µm (ff)	1	88.2
Desulph 1 -63µm (ff)	2	89.7
Desulph 1 -63µm (ff)	3	91.9
Desulph 1 -63µm (re-ff)	1	94.0
Desulph 2 -180µm (ff)	1	77.8
Desulph 2β -180µm +90µm (re-ff)	1	94.7

Given these results, if the acid leaching (and previous processing) were to be optimised on the re-floated samples, it is not unreasonable that the target purity of 95% could be achieved. For a fuller breakdown of the results in the secondary experiments, please see the Appendix C.

### **5.5 Thermal and Electrical Conductivity (Morgan PLC)**

A number of samples were sent for testing (with one of the project's industrial partners) as part of their assessment for use in manufacturing graphite-based products. For the most part, this consisted of pressing the flakes (with a binder) to form a block, and testing the electrical conductivity

of the block (with the thermal conductivity being derived from this result). General findings were that whilst the kish flakes could be successfully used in these applications, the results were not as good as the standard material used (primary graphite) – as such, it was concluded that for the industrial partner’s needs, only the fraction above 500µm would be suitable. Using this fraction, it was found that whilst the sample was nominally >95% C, the impurities that were present would inhibit the creation of the block, rendering it difficult to fabricate. Due to this, even though a high purity could be obtained from the ‘dry’ dust, froth flotation was performed in order to remove the grit-like impurities (this was detailed earlier). It was concluded that the <500µm fraction would be best suited for other tasks (i.e. crucible manufacture etc.). For a more detailed breakdown of the results in the secondary experiments, please see the Appendix D.

## **5.6 Cost Analysis**

(The calculations performed in this section are covered in much greater detail in Appendix B).

Given the inherent limitations of the project (see section 6.3), the following cost analysis will be performed taking a relatively conservative estimate of the amount of >95% C graphite concentration and an estimate of the cost of setting up an adjoining plant for the processing. As such, due to the two Desulph 1 samples being fairly consistent with one another, but the Desulph 2β sample having much lower purities, the ‘final’ product was taken to be a conservative approximation of the average of purity and size distribution between the two (it should be clear that even though these calculations are intentionally approximated – yet conservative - the eventual analysis will show that it is a probable profitable venture, so any additional income will be considered a bonus). The cost of facilities and equipment etc. will be based on the higher end of comparable facilities.

The figure supplied by the project’s industrial partner for the amount of kish dust produced (from the desulphurisation plants) was 10,000 tonnes a year, which roughly works out at around 6 tonnes

per hour. Given 10,000 tonnes of Desulph dust a year, the amount of harvestable graphite from the findings of this project work out at around 1820 Kg per hour. This means 3033 tonnes a year, which at a value of \$900 per tonne delivers an income of \$2.7 million per year. Given the relatively simple equipment used in the purification, even the industrial sized versions top-end costs are of the order of around \$950,000. Coupling this with the operational, storage, handling and transportation costs, a typical plant designed for this application would be expected to generate an up-front cost of around \$3.5 million dollars. Factoring in these running costs, it would appear that on this fairly conservative view the income generated from the graphite would be sufficient to pay any large immediate outgoings off in around 18 months, and should generate a profit from there onwards. However, it should be taken into account that the graphite price used is subject to market variation (depending on supply and demand) but the TSB consortium that funded this thesis are sufficiently confident in the financial viability of the process as to look for investors for commercial development. This is however currently in hiatus due to the impending sale by TATA of the Scunthorpe site which the work is based on. The costings developed are based on IChemE guidelines and the payback period of 18 months is not unreasonable based on the simplicity of the plant proposed, high price of graphite per tonne and the fact that the plant would be based on site hence transport and waste disposal costs are minimalised. This is particularly apparent when considering this was only calculated with considerations of a conservative estimate of the Desulph dust with flake size fractions over 180 $\mu$ m; it should be apparent from the project outcomes that not only are there numerous other potential sources of graphite available, but there is great potential in the <180 $\mu$ m fraction also. Money is also being inherently saved by the recycling of previously-considered waste material, and reducing the costs associated with landfill sites.

## 5.7 Results Summary

To summarise, the results demonstrate that in a relatively non-invasive and simple manner it is possible to extract significant amounts of high-grade graphite from the kish dust found in steel-plants, and that the location of the kish dust which provides the most promise is in the desulphurisation plants: The aim of the project was to produce saleable grades of graphite (+95% C) and provide samples for application testing at Morgan Crucibles. Of the samples provided by Tata Steel two contained sufficient graphite to warrant investigation (Desulph 1 at 32.4% C and Desulph 2 at 29.5% C).

The first process applied to these samples was screening to provide a +500 micron and +1000 micron fraction. These fractions proved to be high in carbon content although the finer fractions required further processing in the form of froth flotation and H<sub>2</sub>SO<sub>4</sub> leaching. The testwork completed indicates that it is possible to produce +95% C concentrates from most size ranges of Desulph 1 and Desulph 2.

Product grades ranging from 95-99% C have been made in the laboratory and selected samples of these have been sent to Morgan Crucibles for appraisal and comparison with their current primary (mineral) graphite feedstocks. Their initial views are that the high aspect ratio of the kish graphite has not given any significant production advantages. Also, the impurities in the kish graphite structures can create fabrication issues, meaning a froth flotation stage is recommended for the +500 microns fraction of the kish graphite flakes.

Investigation into the finer fraction has indicated that all fractions above 63 micron can be processed into a saleable product (+95% C). However, it would appear that a double froth flotation stage and leaching may be required to reach this goal.

Cost analysis showed that whilst there are a number of factors to consider, given the right conditions the creation of a pilot plant to recover kish graphite in an up-scaled version of this project to an industrial level is a venture worthy of serious consideration.

## Chapter 6 – Future recommendations

### 6.1 Post-results Outline

Whilst the previous chapter has outlined the main findings of the project it is now worth evaluating the results as a whole and making recommendations for further research.

### 6.2 Meta-analysis of Results

For the purposes of processing, the findings from this project recommend that graphite wastes should be divided into 3 fractions: Large flakes, Medium flakes and Small flakes. The large flakes would correspond to those of a size 500 $\mu$ m and above, the medium flakes corresponding to the size range of 180 $\mu$ m-500 $\mu$ m and the small flakes corresponding to the size range of 63 $\mu$ m-180 $\mu$ m. Any flake sizes smaller than 63 $\mu$ m should be treated as discard due to low graphite concentrations.

Whilst this strategy does not map exactly to industry standards (generally flake sizes over 80 $\mu$ m are considered large) there is a clear distinction within these groups as to how a 95% C product can be obtained. As such, if the liberation of graphite from kish dust is taken to an industrial standard using the methods utilised in this project, it is recommended combining the screen sizes to only separate for these fractions. This would result in a screen tower consisting of a large mesh to remove any 'large' impurities (a 3mm aperture size was used in this project), followed by a screen of 500 $\mu$ m, 180 $\mu$ m and 60 $\mu$ m. Once the large impurities are removed, and the feed is divided into these fractions, from the results of the project it is recommended that the following treatments are used in order to obtain a 95% C product:

**Large flakes:** This is the simplest and least costly process. Since the separation from the sieves has already liberated the graphite to a high purity (82-85% C) the main concern is to eliminate the impurities that will prevent physical distortion of the flakes during fabrication. To this end, one froth flotation stage with the addition of teefroth (to the ratio of 1ml per 50g of feed) would remove these grit-like impurities leaving a product which should be in excess of 90% Carbon. Whilst 5% H<sub>2</sub>SO<sub>4</sub>

leaching would undoubtedly upgrade this product to >99% pure standard, it is proposed that exposure to ultrasonic waves in a water bath would be sufficient in raising the purity to over 95% (industry standard being 94%), without the potential damage to the flakes and specifically the flake edges that exposure to acid could cause.

**Medium flakes:** This is a slightly more involved process but again with a well-defined method in order to obtain a marketable product. Unlike the large flakes, the impurities are not an issue with regards the physical manipulation of the product, rather they are an issue due to them lowering the purity. Froth flotation is again recommended, with the additions of teefroth at the same dosage level. Once a single froth flotation has been performed, there are two options: Either the sample can undergo further froth flotation stages to raise the purity further, or it can undergo acid leaching to raise the purity. Since from this fraction the purity is unlikely to rise to >95% C with froth flotation alone, it will need to undergo an acid cleaning stage anyway, and as such (for considerations of cost and yield) it is recommended putting the product straight through a 5% H<sub>2</sub>SO<sub>4</sub> leaching phase once the first froth float is completed. If scaling-up to an industrial scale mirrors the results from this project, this should deliver a product of >95% C (whether or not this is the case will be discussed further below).

**Small flakes:** This process is not finalised but a potential method of refinement can be deduced from the laboratory results. Unlike the previous two methods, selection of the feeds may take a more important role in this process, as a number of the Desulph 2β fraction – even though they met the size specification – were judged to be too low in carbon content to undergo refinement. This may not actually be the case, and they may well have responded well to the treatments, but it is something that will need to be investigated further should it be scaled up. Regardless, the methodology here is very similar to the one recommended for the medium flakes, with the caveats that it would appear a higher dosage of teefroth would be needed in the froth flotation stages (around 3ml per 50g of feed), and it seems clear that multiple froth flotation stages would be

required before the product underwent acid leaching to raise the purity a final time. Whilst a marketable purity was only just (but not reliably) obtained in the project itself (the best result being 94.67%), it is likely that if the specified feed underwent the above process a >95% C product could be obtained at these flake sizes.

### **6.3 Scaling-up to industrial quantities**

The main criticisms with this project's commercial relevance are mainly concerned with the veracity with which it mirrors an industrial project: As encountered in the previous chapter, it soon became apparent that whilst there was great promise in the two original Desulph samples received, when a top-up batch of both was received, there were discrepancies between the two – most noticeably there was a severe drop in the carbon content of the Desulph 2 sample, which could potentially undermine the project's ultimate goals. Conversely, the second bag of Desulph 1 actually appeared to offer more promise (albeit marginally), but regardless of whether or not there is a greater or lesser potential for the recovery of graphite than this project has shown, it is clear that the dusts which were tested (supplied by Tata) for this project were not truly representative of the types found in bulk in industry. This is as much an issue with the quantities involved than anything – the amounts used in this project are in the order of kilograms whereas in industry it is of the order of thousands of tonnes. Given it is a real and dynamic material, a truly representative sample would have been hard and impractical to obtain. These sorts of issues are echoed elsewhere: When performing the acid leaching, given the small samples used, the waste product has essentially been calculated as negligible. This is clearly not the case, and when scaled up to the proportions required by industry will be fairly sizeable and unable to be ignored. Loss on Ignitions analysis also is inherently flawed, in that it does not take into account any potential materials that can gain mass as a result of being heated, and it cannot be guaranteed that all the combustible material has been burnt up, as carbon could be completely encased in other particles (it is also worth taking the

inherent error into account - as mentioned in section 5.2.2.1 - of +/- 2%. There could indeed be 'fringe' cases where this tips the balance on the grade of graphite obtained). Whilst it is a useful indicator of the purity, a more accurate method would be needed to ascertain these figures if scaled up. As such, with regards the final evaluations and cost analysis, these can only be viewed as preliminary. However, it still appears that the scaling-up of this project would be a profitable venture.

#### **6.4 Future Research and Conclusions**

So it is clear that there is great utility afforded from the harvesting of graphite outlined by the project's methods, but as mentioned earlier, there are still plenty of avenues of enquiry to pursue, and methodologies to refine. First and foremost amongst these is simply the scaling-up of the project to an industrial setting: A more representative classification of the materials available and a more thorough methodology will need to be developed in order to truly glean the value that harvesting graphite from steel wastage offers. However, what this project has conclusively shown is simply that it *is* possible to liberate a quality product, and using methods and processes that are simple and cost effective: For this reason, whilst there is potential in other methods (such as cyclone technology or electrostatic separation), there appears to be no need - at least from a practical point of view - to have any need to research this further (not to mention the danger with electrostatic separation that there could be an explosion in the separator during the processing of finely divided graphite). The use of screening and froth flotation are some of the most simple and cost-effective tools in industry; as such it seems counter-intuitive to complicate a process further when a high quality product is already achievable. However, these simple methods are not without their own problems, such as the difficulty of screening at fine sizes (due to the unit capacity declining rapidly with size), and the recovery, handling and disposal of the relatively large amounts of water and reagents needed for froth flotation, to name a few. Ultimately however, this project has shown that

with the price and demand of graphite ever on the increase, there exists potential in setting up such processes to harvest kish graphite. This, in turn, could indicate an exciting future for this new potential resource.

## **Bibliography**

### **References**

- 1) Abell, A., Willis, K., and Lange, D. (1999), 'Mercury Intrusion Porosimetry and Image Analysis of Cement-Based Materials', *Journal of Colloid and Interface Science* [Electronic], vol. 211, Issue 1, March, pp. 39-44, Available: <http://www.sciencedirect.com/science/article/pii/S0021979798959860> (11<sup>th</sup> December 2014)
- 2) Acheson, E. G. (1896), 'Manufacture of Graphite', U.S. Patent 568,323 [Electronic], September 29<sup>th</sup>, Available: <http://www.google.co.uk/patents/US568323#v=onepage&q&f=false> (11<sup>th</sup> December 2014)
- 3) Allen, T. (1997), 'Particle Size Measurement', *Chapman & Hall* [Electronic], 4th edition, Available: [http://download.springer.com/static/pdf/586/bfm%253A978-94-009-0417-0%252F1.pdf?auth66=1418314707\\_16e7769c8aa61b22a350976eb068080b&ext=.pdf](http://download.springer.com/static/pdf/586/bfm%253A978-94-009-0417-0%252F1.pdf?auth66=1418314707_16e7769c8aa61b22a350976eb068080b&ext=.pdf) (11<sup>th</sup> December 2014)
- 4) Bellis, M., 'Edward Goodrich Acheson – Carborundum', [Online], Available: <http://inventors.about.com/library/inventors/blacheson.htm> (11<sup>th</sup> December 2014)
- 5) Bennett *et al.* (1997), 'Beneficiation of kish graphite', US Patent 5,672,327 [Electronic], September 30<sup>th</sup>, Available: <http://www.google.co.uk/patents/US5672327> (11<sup>th</sup> December 2014)
- 6) Brown, T *et al.* (2011), 'World Mineral Production 2005-09', *British Geological Survey* [Electronic], Available (as download): <https://www.bgs.ac.uk/downloads/start.cfm?id=1987> (11<sup>th</sup> December 2014)
- 7) Buhrke, V. E., Jenkins, R., Smith, D. K., (1998), 'A Practical Guide for the Preparation of Specimens for XRF and XRD Analysis', *Wiley*, [ISBN 0-471-19458-1](https://doi.org/10.1002/9780471194581), February
- 8) Canada Carbon, 'What is Graphite?', [Online], Available: <http://www.canadacarbon.com/what-is-graphite> (11<sup>th</sup> December 2014)
- 9) Carolina Biological Supply Company (2011), 'CARBORUNDUM – Material Safety Data Sheet', [Online], Available: <https://intranet.ssp.ulaval.ca/cgpc/fsss/fichiers/carborundum.pdf> (11<sup>th</sup> December 2014)

- 10) Cho, Y.S. and Laslowski, J.S., (2002), 'Effect of flotation frothers on bubble size and foam stability', *International Journal of Mineral Processing* [Electronic], vol. 64, Issues 2-3, March, pp 69-80, Available: <http://www.sciencedirect.com/science/article/pii/S0301751601000643> (11<sup>th</sup> December 2014)
- 11) Deprez, N.; McLachan, D. S. (1988). 'The analysis of the electrical conductivity of graphite conductivity of graphite powders during compaction', *Journal of Physics D: Applied Physics*, vol. 21, Issue 1, Available: <http://iopscience.iop.org/0022-3727/21/1/015> (11<sup>th</sup> December 2014)
- 12) Dictionary.com, 'Kish', [Online], Available: <http://dictionary.reference.com/browse/kish> (11<sup>th</sup> December 2014)
- 13) Dresselhaus, M.S., Dresselhaus, G., Sugihara, K., Spain, I.L., and Goldberg, H.A. (1988), 'Graphite Fibers and Filaments', *Springer-Verlag*, vol. 5
- 14) European Commission (2010), 'Critical raw materials for the EU', [Online], Available: [http://ec.europa.eu/enterprise/policies/raw-materials/files/docs/report-b\\_en.pdf](http://ec.europa.eu/enterprise/policies/raw-materials/files/docs/report-b_en.pdf) (11<sup>th</sup> December 2014)
- 15) Feiyu, K *et al.* (August 2002), "Effect of preparation conditions on the characteristics of exfoliated graphite", *Carbon* [Electronic], vol. 40, Issue 9, pp. 1575-1581, Available: <http://www.sciencedirect.com/science/article/pii/S0008622302000234> (11<sup>th</sup> December 2014)
- 16) Focus Graphite, 'The Carbon Age...', [Online], Available: <http://www.focusgraphite.com/technology/graphite/> (11<sup>th</sup> December 2014)
- 17) Giesche, H. (2006), 'Mercury Porosimetry: A General (Practical) Overview', *Particle and Particle System Characterization* [Electronic], vol. 23, Issue 1, June, pp. 9-19, Available: <http://onlinelibrary.wiley.com/doi/10.1002/ppsc.200601009/abstract> (11<sup>th</sup> December 2014)
- 18) Industrial Minerals (2010), 'Concern over Battery grade Graphite supplies', [Online], Available: <http://www.northerngraphite.com/wp-content/uploads/2010/08/Concern-over-battery-grade-graphite-supplies.pdf> (11<sup>th</sup> December 2014)
- 19) Kazmi *et al.* (2008), 'Kish Beneficiation by Flotation', *Journal of The Chemical Society of Pakistan* [Electronic], Available: <http://jcsp.org.pk/ArticleUpload/676-2931-1-CE.pdf> (11<sup>th</sup> December 2014)

- 20) Kroto, H. W.; Heath, J. R.; O'Brien, S. C.; Curl, R. F.; Smalley, R. E. (1985). 'C<sub>60</sub> – The Third Man', *Nature* [Electronic], vol. 318, pp. 162–163, Available:  
<http://www.garfield.library.upenn.edu/classics1993/A1993LT56400001.pdf> (11<sup>th</sup> December 2014)
- 21) Kuvardina, E. V., Novokshonova, L.A., Lomakin, S. M., Timan, S. A. and Tchmutin, I. A., (2012), 'Effect of the graphite nanoplatelet size on the mechanical, thermal, and electrical properties of polypropylene/exfoliated graphite nanocomposites', *Journal of Applied Polymer Science* [Electronic], vol. 128, Issue 3, 5<sup>th</sup> May, pp: 1417-1424, Available: <http://onlinelibrary.wiley.com/doi/10.1002/app.38237/abstract> (11<sup>th</sup> December 2014)
- 22) Lavery, P. D.; Nicks, L. J.; Walters, L.A. (1994), 'Recovery of Flake Graphite From Steelmaking Kish', *Report of Investigations 9512 – United States Department of the Interior - Bureau of Mines* [Electronic], Available (as download):  
[http://stacks.cdc.gov/view/cdc/10221/cdc\\_10221\\_DS1.pdf&sa=U&ei=mWJZU\\_TcJtK98QGktoDwCw&ved=0CD\\_oQFiAG&usg=AFQjCNEbZX7axkQo314G4P\\_ivHH9Y9LhTg](http://stacks.cdc.gov/view/cdc/10221/cdc_10221_DS1.pdf&sa=U&ei=mWJZU_TcJtK98QGktoDwCw&ved=0CD_oQFiAG&usg=AFQjCNEbZX7axkQo314G4P_ivHH9Y9LhTg) (11<sup>th</sup> December 2014)
- 23) Lavrakas, V. (1957), 'Textbook errors: Guest column. XII: The lubricating properties of graphite', *Journal of Chemical Education* [Electronic], vol. 34, Issue 5, May, p. 240, Available:  
<http://pubs.acs.org/doi/abs/10.1021/ed034p240> (11<sup>th</sup> December 2014)
- 24) Ledbetter, H. and Datta, S. (1989), 'Effect of Graphite Aspect Ratio on Cast-Iron Elastic Constants', *Nondestructive Characterization of Materials* [Electronic], pp. 361-367, Available:  
[http://link.springer.com/chapter/10.1007%2F978-3-642-84003-6\\_42](http://link.springer.com/chapter/10.1007%2F978-3-642-84003-6_42) (11<sup>th</sup> December 2014)
- 25) Lipson, H., Stokes, A. R., (1942), 'A New Structure of Carbon', *Nature* [Electronic], vol. 149, 21<sup>st</sup> March, p. 328, Available: <http://www.nature.com/nature/journal/v149/n3777/abs/149328a0.html> (11<sup>th</sup> December 2014)
- 26) Liu, S., Loper Jr., C. R., (1991), 'Kish a source of crystalline graphite' *Carbon* [Electronic], vol. 29, Issue 8, pp. 1119-1124, Available: <http://www.sciencedirect.com/science/article/pii/0008622391900291> (11<sup>th</sup> December 2014)
- 27) Mersen, 'Manufacturing Artificial Graphite', [Online], Available:  
<http://www.mersen.com/en/focus/article/manufacturing-artificial-graphite.html> (11<sup>th</sup> December 2014)

- 28) Mining Turkey (2012), 'Graphite: A Critical Raw Material and Turkey', [Online], 1<sup>st</sup> September, Available: <http://www.slideshare.net/saituysal/graphite-a-critical-raw-material-and-turkey> (11<sup>th</sup> December 2014)
- 29) Mitchell, C. J. (1993), "Industrial Minerals Laboratory Manual: Flake graphite", *British Geological Survey, Technical Report WG/92/30* [Electronic], Available: [http://www.bgs.ac.uk/research/international/dfid-kar/wg92030\\_col.pdf](http://www.bgs.ac.uk/research/international/dfid-kar/wg92030_col.pdf) (11<sup>th</sup> December 2014)
- 30) Nishi, Y., Iwashita, N and Inagaki, M. (2002), 'Evaluation of Pore Structure of Exfoliated Graphite by Mercury Porosimeter', *Tanso* [Electronic], vol. 2002, no. 201, pp. 31-34. Available: [https://www.istage.jst.go.jp/article/tanso1949/2002/201/2002\\_201\\_31/\\_article](https://www.istage.jst.go.jp/article/tanso1949/2002/201/2002_201_31/_article) (11<sup>th</sup> December 2014)
- 31) Olson, D. (2004), 'Graphite', *US Geological Survey Minerals Yearbook – 2004* [Electronic], pp. 33.1 – 33.9, Available: <http://minerals.usgs.gov/minerals/pubs/commodity/graphite/graphmyb04.pdf> (11<sup>th</sup> December 2014)
- 32) Schoolderman, H. and Mathlener, R. (2011), 'Minerals and metals scarcity in manufacturing: the ticking timebomb', *PWC* [Online], December, Available: <http://www.pwc.com/resourcescarcity> (11<sup>th</sup> December 2014)
- 33) Schubert, H. and Bischofberger, C. (1978), 'On the hydrodynamics of flotation machines', *International Journal of Mineral Processing* [Electronic], vol. 5, Issue 2, July, pp. 131-142, Available: <http://www.sciencedirect.com/science/article/pii/0301751678900108> (11<sup>th</sup> December 2014)
- 34) Sung-Su, D. (2003), 'Hydrodynamic characterisation of a Denver laboratory flotation cell', [Online], Available: [http://digitool.library.mcgill.ca/dtl\\_publish/6/80007.html](http://digitool.library.mcgill.ca/dtl_publish/6/80007.html) (11<sup>th</sup> December 2014)

## Images

(The images pertaining to the below links were all found using the Google image search engine and were accessed in June 2014/December 2014. If an image does not have a reference associated with it, then it was included as part of the project.)

- 1) Figure 1.2: <http://batteryblog.ca/> (11<sup>th</sup> December 2014)

- 2) Figure 1.3: <http://www.canadacarbon.com/rs/what-is-graphite/>. (11<sup>th</sup> December 2014)
- 3) Figure 1.4: <http://smokechemicals.com/shop/images/Graphite%20Flake%20+80%20Mesh.jpg> (11<sup>th</sup> December 2014)
- 4) Figure 1.6: <http://image.made-in-china.com/2f0j00FeyaEKjRlkhN/Carbon-Flake-Graphite-300-Mesh.jpg> (11<sup>th</sup> December 2014)
- 5) Figure 1.7: [http://grupolandfer.com/es/wp-content/uploads/2012/01/Amorphous\\_Graphite.jpg](http://grupolandfer.com/es/wp-content/uploads/2012/01/Amorphous_Graphite.jpg) (11<sup>th</sup> December 2014)
- 6) Figure 1.8: [http://www.saintjeancarbon.com/files/cache/da8b75ecd67053a60df9b7c07ec3ca24\\_f212.jpg](http://www.saintjeancarbon.com/files/cache/da8b75ecd67053a60df9b7c07ec3ca24_f212.jpg) (11<sup>th</sup> December 2014)
- 7) Figure 1.12: [http://en.wikipedia.org/wiki/Pencil#mediaviewer/File:Pencils\\_hb.jpg](http://en.wikipedia.org/wiki/Pencil#mediaviewer/File:Pencils_hb.jpg) (11<sup>th</sup> December 2014)
- 8) Figure 1.13: <http://www.robotroom.com/Rust-Removal-5.html> (11<sup>th</sup> December 2014)
- 9) Figure 1.14: [http://en.wikipedia.org/wiki/Altos\\_Hornos\\_de\\_Vizcaya#mediaviewer/File:Alto\\_horno\\_antiguo\\_Sestao.jpg](http://en.wikipedia.org/wiki/Altos_Hornos_de_Vizcaya#mediaviewer/File:Alto_horno_antiguo_Sestao.jpg) (11<sup>th</sup> December 2014)
- 10) Figure 2.1: <http://www.graphiteproduct.in/graphite-powder.html> (11<sup>th</sup> December 2014)
- 11) Figure 2.2: [http://upload.wikimedia.org/wikipedia/commons/e/e5/BLW\\_Carborundum\\_crystals.jpg](http://upload.wikimedia.org/wikipedia/commons/e/e5/BLW_Carborundum_crystals.jpg) (11<sup>th</sup> December 2014)
- 12) Figure 4.9: [http://serc.carleton.edu/research\\_education/geochemsheets/techniques/XRF.html](http://serc.carleton.edu/research_education/geochemsheets/techniques/XRF.html) (11<sup>th</sup> December 2014)
- 13) Figure 4.10: <http://upload.wikimedia.org/wikipedia/commons/thumb/2/28/XRFScan.jpg/300px-XRFScan.jpg> (11<sup>th</sup> December 2014)

**Word Count**

**Word Count**

Approximately 16,320 words.

## **Appendix A: XRF Analysis**

Below is a brief aside on the mechanism behind XRF spectrometry, followed by the (limited) raw XRF data obtained as part of the project. For reasons outlined in the main text, this was not pursued further (I am particularly grateful to Zubera Iqbal for her assistance in the performing of XRF analysis on the samples).

### **An aside: How XRF spectrometry works**

Essentially, XRF analysis is the process where a sample is bombarded with high-energy X-rays. These X-rays are in turn absorbed by the particles present in the sample, exciting the electrons in the orbitals of the atoms. Once these electrons have been excited, they in turn emit a characteristic secondary X-ray (of unique frequency and amplitude) of its own which is picked up by a detector. These specific X-ray ‘fingerprints’ are well documented, so the XRF spectrometer can detect them, analyse the data, and report to a high degree of accuracy the chemical composition of the sample, and in what proportions these elements are to each other.

More specifically, the radiation emitted from the XRF spectrometer hits the atoms in the sample causing an electron in one of the inner orbitals to be removed from the atom. In order to achieve a lower energy state, an electron from an outer orbital lowers to replace it – the moving from one orbital to another constitutes a change in energy level. This change in energy is facilitated by the release of a photon (the fluorescent effect) with a unique wavelength due to the specific structure of the element. The wavelength,  $\lambda$  is equal to  $h.c/E$  (Planck’s law). Since each atom has its own characteristic wavelength peaks for a given energy, XRF analysis can determine which elements are in a sample. XRF analysis can determine the relative proportion of the elements in question by comparing the amplitudes of these peaks (Figs 4.9 & 4.10).

Raw Data 1:

DESULP2RAW												
Formula	Z	Concentration	Status	Line 1	Net int.	Used intensity	Calc. concentration	Stat. error	LLD	Analyzed layer	Line 2	Net int.
orig-g		0.51	Input									
added-g		0.1	Input									
Ca	20	45.94%	XRF 1	Ca KA1-HR-Tr	66.72	1464	45.9	0.69%	113.2 PPM	19.1 um	Ca KB1-HR-Tr	7.433
Fe	26	37.51%	XRF 1	Fe KA1-HR-Tr	114.3	2491	37.51	0.53%	71.2 PPM	25.5 um	Fe KB1-HR-Tr	20.22
K	19	2.71%	XRF 1	K KA1-HR-Tr	4.645	100.2	2.71	2.65%	80.2 PPM	16.1 um	K KB1-HR-Tr	0.5213
Mg	12	1.74%	XRF 1	Mg KA1-HR-Tr	1.242	31.93	1.74	5.17%	160.8 PPM	1.38 um		
S	16	1.27%	XRF 1	S KA1-HR-Tr	2.185	65.72	1.27	3.87%	56.3 PPM	6.3 um		
Na	11	1.10%	XRF 1	Na KA1-HR-Tr	0.1941	6.934	1.1	12.80%		0.88 um		
Si	14	0.69%	XRF 1	Si KA1-HR-Tr	0.4767	13.44	0.69	8.19%		3.1 um	Si KB1-HR-Tr/EI	0.031
Mn	25	0.26%	XRF 1	Mn KA1-HR-Tr	0.5983	13.02	0.26	8.07%	85.9 PPM	20.5 um	Mn KB1-HR-Tr	0.2525
Al	13	0.17%	XRF 1	Al KA1-HR-Tr	0.09439	2.653	0.17	18.40%		2.05 um	Al KB1-HR-Tr/EI	0.00413
La	57	0.15%	XRF 1	La LA1-HR-Tr	0.04175	0.9332	0.15	27.70%		11.0 um	La LB1-HR-Tr	0.04402
Ti	22	0.10%	XRF 1	Ti KA1-HR-Tr	0.09963	2.224	0.1	17.90%		10.2 um	Ti KB1-HR-Tr	0.04941
P	15	0.08%	XRF 1	P KA1-HR-Tr	0.07354	2.212	0.076	20.90%		4.4 um		
Sr	38	0.06%	XRF 1	Sr KA1-HR-Tr	1.133	20.88	0.064	7.00%	30.7 PPM	111 um	Sr KB1-HR-Tr	0.305
		91.78%										

Used intensity	Calc. concentration	Stat. error	LLD	Analyzed layer	Line 3	Net int.	Used intensity	Calc. concentration	Stat. error	LLD	Analyzed layer	XRF %
163.1	43.4	2.08%	790.9 PPM	24.0 um								45.9
440.6	36.6	1.26%	398.4 PPM	33 um	Fe LA1-HR	0.01994			40.10%		0.74 um	37.51
11.25	2.8	8.38%	720.3 PPM	20.0 um								2.71
												1.74
												1.27
												1.1
0.8743	1.7	80.30%		3.5 um								0.69
-0.2419	-0.026	36.10%	714.2 PPM	26.4 um	Mn LA1-HR	0.00097			454%		0.60 um	0.26
0.1159	0.79	220%		2.30 um								0.17
0.9841	0.22	27.00%		13.6 um	La KA1-HR-Tr	-0.00936	-0.1102	-0.004		603.3 PPM	1.35 mm	0.15
0.9915	0.31	63.60%		12.8 um								0.1
												0.076
5.01	0.061	22.60%	147.0 PPM	152 um	Sr LA1-HR	0.00821	0.2163	0.033	156%		3.4 um	0.064

DESULP2POSTDS												
Formula	Z	Concentration	Status	Line 1	Net int.	Used intensity	Calc. concentration	Stat. error	LLD	Analyzed layer	Line 2	Net int.
orig-g		0.51	Input									
added-g		0.1	Input									
Ca	20	45.39%	XRF 1	Ca KA1-HR-Tr	66.06	1449	45.4	0.70%	116.3 PPM	19.1 um	Ca KB1-HR-Tr	8.253
Fe	26	37.96%	XRF 1	Fe KA1-HR-Tr	116.2	2534	37.96	0.53%	66.9 PPM	25.6 um	Fe KB1-HR-Tr	20.32
K	19	2.65%	XRF 1	K KA1-HR-Tr	4.547	98.14	2.65	2.65%		15.9 um	K KB1-HR-Tr	0.5333
Mg	12	1.72%	XRF 1	Mg KA1-HR-Tr	1.223	31.44	1.72	5.20%	154.8 PPM	1.37 um		
S	16	1.19%	XRF 1	S KA1-HR-Tr	2.052	61.74	1.19	3.95%		6.3 um		
Na	11	1.07%	XRF 1	Na KA1-HR-Tr	0.1886	6.74	1.1	13.00%		0.88 um		
Si	14	0.51%	XRF 1	Si KA1-HR-Tr	0.3502	9.877	0.51	9.56%		3.1 um	Si KB1-HR-Tr/EI	0.01391
Mn	25	0.27%	XRF 1	Mn KA1-HR-Tr	0.631	13.73	0.27	7.69%	76.6 PPM	20.5 um	Mn KB1-HR-Tr	0.2987
Cl	17	0.24%	XRF 1	Cl KA1-HR-Tr	0.2366	7.117	0.24	13.60%	117.8 PPM	8.6 um		
La	57	0.12%	XRF 1	La LA1-HR-Tr	0.03388	0.7573	0.12	30.70%		11.0 um	La LB1-HR-Tr	0.04229
Ti	22	0.08%	XRF 1	Ti KA1-HR-Tr	0.08166	1.825	0.085	19.80%		10.2 um	Ti KB1-HR-Tr	0.08004
Sr	38	0.06%	XRF 1	Sr KA1-HR-Tr	1.102	20.3	0.063	7.29%	32.2 PPM	110 um	Sr KB1-HR-Tr	0.2437
V	23	0.05%	XRF 1	V KA1-HR-Tr	0.06044	1.331	0.046	23.00%		13.0 um		
		91.31%										

Used intensity	Calc. concentration	Stat. error	LLD	Analyzed layer	Line 3	Net int.	Used intensity	Calc. concentration	Stat. error	LLD	Analyzed layer	XRF %
181.1	48.1	1.97%		23.9 um								45.4
442.9	36.6	1.26%	414.8 PPM	33 um	Fe LA1-HR	0.01746			107%		0.74 um	37.96
11.51	2.8	8.38%	793.4 PPM	19.8 um								2.65
												1.72
												1.19
												1.1
0.3922	0.76	120%		3.5 um								0.51
0.6445	0.069	12.70%	691.7 PPM	26.5 um	Mn LA1-HR	0.00099			449%		0.60 um	0.27
												0.24
0.9445	0.21	68.80%		13.6 um	La KA1-HR-Tr	0.326	2.981	0.11	79.80%	545.2 PPM	1.33 mm	0.12
1.56	0.48	50.00%		12.8 um								0.085
4.185	0.051	26.20%	132.3 PPM	151 um	Sr LA1-HR	0.04043	1.129	0.18	70.30%		3.4 um	0.063
												0.046

Graph	Formula	Z	Concentration	Status	Line 1	Net int.	Used intensity	Calc. concentration	Stat. error	LLD	Analyzed layer	Line 2	Net int.
orig-g			0.5	Input									
added-g			0.1	Input									
Fe	26	33.67%	XRF 1	Fe KA1-HR-Tr	114.2	2489	33.67	0.53%	62.1 PPM	32 um	Fe KB1-HR-Tr	21	
Ca	20	33.27%	XRF 1	Ca KA1-HR-Tr	49.13	1078	33.3	0.81%	92.6 PPM	21.4 um	Ca KB1-HR-Tr	5.868	
K	19	2.34%	XRF 1	K KA1-HR-Tr	3.964	85.55	2.34	2.86%	53.1 PPM	18.0 um	K KB1-HR-Tr	0.4098	
Mg	12	1.31%	XRF 1	Mg KA1-HR-Tr	1.04	26.72	1.31	5.66%	137.1 PPM	1.57 um			
Na	11	0.99%	XRF 1	Na KA1-HR-Tr	0.1992	7.116	0.99	12.70%		1.00 um			
S	16	0.91%	XRF 1	S KA1-HR-Tr	1.521	45.75	0.914	4.74%	64.1 PPM	7.2 um			
Si	14	0.59%	XRF 1	Si KA1-HR-Tr	0.4231	11.93	0.59	8.70%		3.5 um	Si KB1-HR-Tr/EI	0.05905	
Cl	17	0.41%	XRF 1	Cl KA1-HR-Tr	0.3916	11.78	0.41	10.40%	118.0 PPM	9.8 um			
Mn	25	0.23%	XRF 1	Mn KA1-HR-Tr	0.5881	12.8	0.23	8.26%	70.8 PPM	25.5 um	Mn KB1-HR-Tr	0.2759	
Al	13	0.17%	XRF 1	Al KA1-HR-Tr	0.1065	2.994	0.17	17.30%		2.33 um	Al KB1-HR-Tr/EI	0.003	
Ti	22	0.08%	XRF 1	Ti KA1-HR-Tr	0.08906	1.991	0.081	24.40%	106.0 PPM	12.6 um	Ti KB1-HR-Tr	0.02529	
Sr	38	0.06%	XRF 1	Sr KA1-HR-Tr	1.151	21.21	0.06	7.78%	32.5 PPM	126 um	Sr KB1-HR-Tr	0.1232	
As	33	0.03%	XRF 1	As KA1-HR-Tr	0.257	5.388	0.028	20.60%	42.3 PPM	56 um	As KB1-HR-Tr	-0.02785	
		74.06%											

Used intensity	Calc. concentration	Stat. error	LLD	Analyzed layer	Line 3	Net int.	Used intensity	Calc. concentration	Stat. error	LLD	Analyzed layer	XRF %
457.7	34	1.24%	364.1 PPM	41 um	Fe LA1-HR	0.01578				113%	0.92 um	33.67
128.7	33.6	2.35%	660.7 PPM	26.8 um								33.3
8.845	2.2	9.72%	636.1 PPM	22.3 um								2.34
												1.31
												0.99
												0.914
1.665	3.1	23.30%		4.0 um								0.59
												0.41
-0.629	-0.06	35.60%	614.1 PPM	33 um	Mn LA1-HR	0.00149				367%	0.74 um	0.23
0.08434	0.53	258%		2.62 um								0.17
0.5652	0.15	197%	901.6 PPM	15.9 um								0.081
2.115	0.024	158%	144.1 PPM	173 um	Sr LA1-HR	0.0223	0.6133	0.099	94.70%		3.8 um	0.06
-0.5838	-0.015		243.9 PPM	75 um	As LA1-HR	0.1231	-0.7453	-0.19	48.10%	943.3 PPM	1.66 um	0.028

### Normalised 1:

Raw	Formula	Z	Concentration	Status	Line 1	Net int.	Used intensity	Calc. concentration	Stat. error	LLD	Analyzed layer	Line 2	Net int.
orig-g			0.51	Input									
added-g			0.1	Input									
Ca	20	49.34%	XRF 1	Ca KA1-HR-Tr	66.72	1593	49.3	0.69%	125.7 PPM	17.4 um	Ca KB1-HR-Tr	7.433	
Fe	26	41.34%	XRF 1	Fe KA1-HR-Tr	114.3	2710	41.34	0.53%	78.6 PPM	23.5 um	Fe KB1-HR-Tr	20.22	
K	19	2.89%	XRF 1	K KA1-HR-Tr	4.645	109.1	2.89	2.65%	89.1 PPM	14.6 um	K KB1-HR-Tr	0.5213	
Mg	12	2.00%	XRF 1	Mg KA1-HR-Tr	1.242	34.74	2	5.17%	179.2 PPM	1.26 um			
S	16	1.36%	XRF 1	S KA1-HR-Tr	2.185	71.51	1.36	3.87%	62.8 PPM	5.7 um			
Na	11	1.28%	XRF 1	Na KA1-HR-Tr	0.1941	7.544	1.3	12.80%		0.80 um			
Si	14	0.77%	XRF 1	Si KA1-HR-Tr	0.4767	14.63	0.77	8.19%		2.78 um	Si KB1-HR-Tr/EI	0.031	
Mn	25	0.29%	XRF 1	Mn KA1-HR-Tr	0.5983	14.17	0.29	8.07%	94.7 PPM	18.8 um	Mn KB1-HR-Tr	0.2525	
Al	13	0.19%	XRF 1	Al KA1-HR-Tr	0.09439	2.887	0.19	18.40%		1.86 um	Al KB1-HR-Tr/EI	0.00413	
La	57	0.16%	XRF 1	La LA1-HR-Tr	0.04175	1.015	0.16	27.70%		10.1 um	La LB1-HR-Tr	0.04402	
Ti	22	0.12%	XRF 1	Ti KA1-HR-Tr	0.09963	2.42	0.12	17.90%		9.4 um	Ti KB1-HR-Tr	0.04941	
P	15	0.08%	XRF 1	P KA1-HR-Tr	0.07354	2.407	0.083	20.90%		4.0 um			
Sr	38	0.07%	XRF 1	Sr KA1-HR-Tr	1.133	22.72	0.072	7.00%	34.2 PPM	101 um	Sr KB1-HR-Tr	0.305	

Used intensity	Calc. concentration	Stat. error	LLD	Analyzed layer	Line 3	Net int.	Used intensity	Calc. concentration	Stat. error	LLD	Analyzed layer	XRF %
177.4	47.5	2.08%	875.2 PPM	21.8 um								49.3
479.5	40.9	1.26%	439.9 PPM	30 um	Fe LA1-HR	0.01994				40.10%	0.68 um	41.34
12.24	3	8.38%	800.3 PPM	18.1 um								2.89
												2
												1.36
												1.3
0.9513	1.9	80.30%		3.2 um								0.77
-0.3388	-0.037	36.10%	799.1 PPM	24.3 um	Mn LA1-HR	0.00097				454%	0.55 um	0.29
0.1262	0.9	220%		2.09 um								0.19
1.071	0.24	27.00%		12.5 um	La KA1-HR-Tr	-0.00936	-0.1189	-0.005		670.2 PPM	1.22 mm	0.16
1.082	0.35	63.60%		11.8 um								0.12
												0.083
5.46	0.07	22.60%	163.3 PPM	139 um	Sr LA1-HR	0.00821	0.2351	0.036	156%		3.1 um	0.072

Post DS	Formula	Z	Concentration	Status	Line 1	Net int.	Used intensity	Calc. concentration	Stat. error	LLD	Analyzed layer	Line 2	Net int.
	orig-g			0.51	Input								
	added-g			0.1	Input								
	Ca	20	49.10%	XRF 1	Ca KA1-HR-Tr	66.06	1551	49.1	0.70%	126.5 PPM	17.3 um	Ca KB1-HR-Tr	8.253
	Fe	26	41.91%	XRF 1	Fe KA1-HR-Tr	116.2	2711	41.91	0.53%	72.5 PPM	23.4 um	Fe KB1-HR-Tr	20.32
	K	19	2.86%	XRF 1	K KA1-HR-Tr	4.547	105	2.86	2.65%		14.4 um	K KB1-HR-Tr	0.5333
	Mg	12	1.96%	XRF 1	Mg KA1-HR-Tr	1.223	33.65	1.96	5.20%	168.9 PPM	1.24 um		
	S	16	1.28%	XRF 1	S KA1-HR-Tr	2.052	66.08	1.28	3.95%		5.7 um		
	Na	11	1.23%	XRF 1	Na KA1-HR-Tr	0.1886	7.214	1.2	13.00%		0.79 um		
	Si	14	0.56%	XRF 1	Si KA1-HR-Tr	0.3502	10.57	0.56	9.56%		2.76 um	Si KB1-HR-Tr/EI	0.01391
	Mn	25	0.30%	XRF 1	Mn KA1-HR-Tr	0.631	14.69	0.3	7.69%	82.9 PPM	18.8 um	Mn KB1-HR-Tr	0.2987
	Cl	17	0.25%	XRF 1	Cl KA1-HR-Tr	0.2366	7.616	0.25	13.60%	128.5 PPM	7.8 um		
	La	57	0.13%	XRF 1	La LA1-HR-Tr	0.03388	0.8105	0.13	30.70%		10.1 um	La LB1-HR-Tr	0.04229
	Ti	22	0.09%	XRF 1	Ti KA1-HR-Tr	0.08166	1.954	0.094	19.80%		9.3 um	Ti KB1-HR-Tr	0.08004
	Sr	38	0.07%	XRF 1	Sr KA1-HR-Tr	1.102	21.73	0.07	7.29%	35.1 PPM	100 um	Sr KB1-HR-Tr	0.2437
	V	23	0.05%	XRF 1	V KA1-HR-Tr	0.06044	1.424	0.051	23.00%		11.9 um		

Used intensity	Calc. concentration	Stat. error	LLD	Analyzed layer	Line 3	Net int.	Used intensity	Calc. concentration	Stat. error	LLD	Analyzed layer	XRF %
193.8	51.8	1.97%		21.7 um								49.1
474	40.3	1.26%	449.4 PPM	30 um	Fe LA1-HR	0.01746			107%		0.68 um	41.91
12.32	3	8.38%	863.8 PPM	17.9 um								2.86
												1.96
												1.28
												1.2
0.4198	0.84	120%		3.2 um								0.56
0.589	0.065	12.70%	757.7 PPM	24.3 um	Mn LA1-HR	0.00099			449%		0.55 um	0.3
												0.25
1.011	0.22	68.80%		12.4 um	La KA1-HR-Tr	0.326	3.19	0.13	79.80%	594.3 PPM	1.21 mm	0.13
1.665	0.53	50.00%		11.7 um								0.094
4.479	0.057	26.20%	144.2 PPM	137 um	Sr LA1-HR	0.04043	1.208	0.19	70.30%		3.0 um	0.07
												0.051

Graph	Formula	Z	Concentration	Status	Line 1	Net int.	Used intensity	Calc. concentration	Stat. error	LLD	Analyzed layer	Line 2	Net int.
	orig-g			0.5	Input								
	added-g			0.1	Input								
	Fe	26	46.73%	XRF 1	Fe KA1-HR-Tr	114.2	3111	46.73	0.53%	81.1 PPM	23.7 um	Fe KB1-HR-Tr	21
	Ca	20	43.27%	XRF 1	Ca KA1-HR-Tr	49.13	1347	43.3	0.81%	122.7 PPM	15.5 um	Ca KB1-HR-Tr	5.868
	K	19	3.02%	XRF 1	K KA1-HR-Tr	3.964	106.9	3.02	2.86%	70.6 PPM	12.9 um	K KB1-HR-Tr	0.4098
	Mg	12	2.01%	XRF 1	Mg KA1-HR-Tr	1.04	33.4	2.01	5.66%	184.1 PPM	1.13 um		
	Na	11	1.56%	XRF 1	Na KA1-HR-Tr	0.1992	8.894	1.6	12.70%		0.73 um		
	S	16	1.17%	XRF 1	S KA1-HR-Tr	1.521	57.19	1.17	4.74%	86.0 PPM	5.1 um		
	Si	14	0.83%	XRF 1	Si KA1-HR-Tr	0.4231	14.92	0.83	8.70%		2.50 um	Si KB1-HR-Tr/EI	0.05905
	Cl	17	0.51%	XRF 1	Cl KA1-HR-Tr	0.3916	14.73	0.51	10.40%	157.9 PPM	7.0 um		
	Mn	25	0.32%	XRF 1	Mn KA1-HR-Tr	0.5881	16	0.32	8.26%	92.2 PPM	19.0 um	Mn KB1-HR-Tr	0.2759
	Al	13	0.26%	XRF 1	Al KA1-HR-Tr	0.1065	3.742	0.26	17.30%		1.67 um	Al KB1-HR-Tr/EI	0.003
	Ti	22	0.11%	XRF 1	Ti KA1-HR-Tr	0.08906	2.489	0.11	24.40%	137.1 PPM	9.4 um	Ti KB1-HR-Tr	0.02529
	Sr	38	0.09%	XRF 1	Sr KA1-HR-Tr	1.151	26.51	0.089	7.78%	43.3 PPM	91 um	Sr KB1-HR-Tr	0.1232
	As	33	0.04%	XRF 1	As KA1-HR-Tr	0.257	6.735	0.04	20.60%	56.4 PPM	40 um	As KB1-HR-Tr	-0.02785

Used intensity	Calc. concentration	Stat. error	LLD	Analyzed layer	Line 3	Net int.	Used intensity	Calc. concentration	Stat. error	LLD	Analyzed layer	XRF %
572.1	47	1.24%	476.1 PPM	31 um	Fe LA1-HR	0.01578			113%		0.69 um	46.73
160.9	42.9	2.35%	868.3 PPM	19.4 um								43.3
11.06	2.8	9.72%	844.6 PPM	16.1 um								3.02
												2.01
												1.6
												1.17
2.082	4.3	23.30%		2.87 um								0.83
												0.51
-1.196	-0.13	35.60%	830.8 PPM	24.5 um	Mn LA1-HR	0.00149			367%		0.55 um	0.32
0.1054	0.78	258%		1.88 um								0.26
0.7065	0.21	197%	0.12%	11.8 um								0.11
2.644	0.035	158%	192.0 PPM	125 um	Sr LA1-HR	0.0223	0.7659	0.12	94.70%		2.76 um	0.089
-0.7298	-0.022		324.9 PPM	54 um	As LA1-HR	0.1231	-1.565	-0.43	48.10%	0.13%	1.20 um	0.04

Raw Data 2 – Sheet 1

Desulpdust2ndbestpdsppfw												
Formula	Z	Concentra	Status	Line 1	Net int.	Used inten	Calc. conc	Stat. error	LLD	Analyzed	Line 2	Net int.
orig-g		0.5	Input									
added-g		0.1	Input									
Fe	26	47.41%	XRF 1	Fe KA1-Hf	149.3	3255	47.41	0.27%	37.6 PPM	24.1 um	Fe KB1-Hf	26.12
Ca	20	42.53%	XRF 1	Ca KA1-Hf	65.71	1442	42.53	0.40%	54.8 PPM	17.4 um	Ca KB1-Hf	7.751
Mg	12	2.56%	XRF 1	Mg KA1-H	1.693	43.51	2.56	2.53%	81.8 PPM	1.11 um		
Si	14	0.84%	XRF 1	Si KA1-HR	0.543	15.31	0.842	4.43%		2.44 um	Si KB1-HR	0.00079
S	16	0.31%	XRF 1	S KA1-HF	0.5014	15.07	0.306	4.76%	28.2 PPM	5.0 um		
Mn	25	0.30%	XRF 1	Mn KA1-H	0.7373	16.03	0.305	4.06%	43.0 PPM	19.3 um	Mn KB1-H	0.3834
K	19	0.21%	XRF 1	K KA1-HF	0.3542	7.645	0.206	5.80%	34.8 PPM	13.1 um	K KB1-HF	0.05897
Al	13	0.13%	XRF 1	Al KA1-HR	0.0683	1.919	0.13	14.70%	92.3 PPM	1.63 um	Al KB1-HR	0.00361
P	15	0.08%	XRF 1	P KA1-HF	0.07136	2.146	0.079	14.60%	50.8 PPM	3.5 um		
Pb	82	0.07%	XRF 1	Pb LB1-HF	0.2187	4.586	0.067	13.20%	67.1 PPM	64 um	Pb LA1-HF	0.2797
Sr	38	0.06%	XRF 1	Sr KA1-HF	1.028	18.95	0.0634	4.16%	17.9 PPM	88 um	Sr KB1-HF	0.3274
Zn	30	0.05%	XRF 1	Zn KA1-HF	0.2492	5.368	0.051	9.05%	32.2 PPM	22.8 um	Zn KB1-HF	0.01174
Cr	24	0.04%	XRF 1	Cr KA1-HF	0.07045	1.533	0.037	17.50%	44.1 PPM	15.4 um	Cr KB1-HF	0.00839
As	33	51 PPM	XRF 1	As KA1-Hf	0.2797	0.8606	0.005	9.10%	30.0 PPM	39 um	As KB1-Hf	-0.01348
Zr	40	51 PPM	XRF 1	Zr KA1-HR	0.3274	1.853	0.005	11.10%	19.1 PPM	119 um	Zr KB1-HR	0.04144
100%												

Used inten	Calc. conc	Stat. error	LLD	Analyzed	Line 3	Net int.	Used inten	Calc. conc	Stat. error	LLD	Analyzed	XRF %
569.2	46	0.64%	217.1 PPM	31 um	Fe LA1-HF	0.01468			67.40%		0.70 um	47.41
170	42.5	1.18%	377.1 PPM	21.8 um								42.53
												2.56
0.01122	0.023	1415%	0.23%	2.80 um								0.842
												0.306
0.9351	0.096	15.40%	393.7 PPM	25.0 um	Mn LA1-Hf	0.00627			41.30%		0.57 um	0.305
1.273	0.31	48.80%	397.9 PPM	16.2 um								0.206
0.1014	0.75	328%	0.80%	1.83 um								0.13
												0.079
5.178	0.09	9.10%	66.5 PPM	39 um	Pb MA1-H	0.00681	0.2049	0.025	239%	138.7 PPM	5.2 um	0.067
4.435	0.059	11.10%	87.2 PPM	121 um	Sr LA1-HR	0.01128	0.3011	0.049	117%	148.5 PPM	2.69 um	0.0634
0.2528	0.014	382%	206.9 PPM	30 um	Zn LA1-HR	0.00971	0.2587	0.092	82.90%		0.66 um	0.051
0.05414	0.007	329%	309.0 PPM	19.7 um	Cr LA1-HR	-0.00019					0.45 um	0.037
-0.2826	-0.008		137.7 PPM	52 um	As LA1-HF	0.2496	0.6155	0.17	17.30%	651.3 PPM	1.17 um	0.005
0.7115	0.011	230%	107.8 PPM	164 um	Zr LA1-HR	-0.00734	-0.2208	-0.026		145.5 PPM	3.6 um	0.005

Formula	Z	Concentra	Status	Line 1	Net int.	Used inten	Calc. conc	Stat. error	LLD	Analyzed	Line 2	Net int.
orig-g		0.5	Input									
added-g		0.1	Input									
Fe	26	50.37%	XRF 1	Fe KA1-Hf	149.3	3434	50.37	0.27%	40.0 PPM	22.9 um	Fe KB1-Hf	26.12
Ca	20	44.40%	XRF 1	Ca KA1-Hf	65.71	1521	44.4	0.40%	58.5 PPM	16.3 um	Ca KB1-Hf	7.751
Mg	12	2.79%	XRF 1	Mg KA1-H	1.693	45.9	2.79	2.53%	87.6 PPM	1.04 um		
Si	14	0.90%	XRF 1	Si KA1-HR	0.543	16.16	0.902	4.43%		2.29 um	Si KB1-HR	0.00079
Mn	25	0.32%	XRF 1	Mn KA1-H	0.7373	16.91	0.324	4.06%	45.7 PPM	18.3 um	Mn KB1-H	0.3834
S	16	0.32%	XRF 1	S KA1-HF	0.5014	15.9	0.32	4.76%	30.2 PPM	4.7 um		
K	19	0.22%	XRF 1	K KA1-HF	0.3542	8.066	0.216	5.80%	37.3 PPM	12.3 um	K KB1-HF	0.05897
Al	13	0.14%	XRF 1	Al KA1-HR	0.0683	2.025	0.14	14.70%	98.9 PPM	1.53 um	Al KB1-HR	0.00361
P	15	0.08%	XRF 1	P KA1-HF	0.07136	2.265	0.084	14.60%	54.4 PPM	3.3 um		
Pb	82	0.07%	XRF 1	Pb LB1-HF	0.2187	4.838	0.07	13.20%	71.8 PPM	60 um	Pb LA1-HF	0.2797
Sr	38	0.07%	XRF 1	Sr KA1-HF	1.028	19.99	0.0681	4.16%	19.1 PPM	83 um	Sr KB1-HF	0.3274
Zn	30	0.05%	XRF 1	Zn KA1-HF	0.2492	5.664	0.055	9.05%	34.5 PPM	21.5 um	Zn KB1-HF	0.01174
Cr	24	0.04%	XRF 1	Cr KA1-HF	0.07045	1.617	0.039	17.50%	46.8 PPM	14.6 um	Cr KB1-HF	0.00839
As	33	59 PPM	XRF 1	As KA1-Hf	0.2797	0.9654	0.006	9.10%	32.2 PPM	37 um	As KB1-Hf	-0.01348
Zr	40	53 PPM	XRF 1	Zr KA1-HR	0.3274	1.893	0.005	11.10%	20.5 PPM	112 um	Zr KB1-HR	0.04144

Used inten	Calc. conc	Stat. error	LLD	Analyzed	Line 3	Net int.	Used inten	Calc. conc	Stat. error	LLD	Analyzed	XRF %
600.5	49.3	0.64%	231.0 PPM	29.5 um	Fe LA1-HF	0.01468				67.40%	0.66 um	50.37
179.4	44.9	1.18%	402.2 PPM	20.5 um								44.4
												2.79
0.01201	0.025	1415%	0.25%	2.63 um								0.902
0.9328	0.097	15.40%	422.9 PPM	23.7 um	Mn LA1-HF	0.00627				41.30%	0.54 um	0.324
												0.32
1.343	0.33	48.80%	425.5 PPM	15.3 um								0.216
0.1069	0.81	328%	0.86%	1.72 um								0.14
												0.084
5.406	0.094	9.10%	71.5 PPM	37 um	Pb MA1-H	0.00681	0.2162	0.026	239%	148.6 PPM	4.9 um	0.07
4.703	0.064	11.10%	93.4 PPM	114 um	Sr LA1-HR	0.01128	0.3175	0.052	117%	159.4 PPM	2.53 um	0.0681
0.2668	0.015	382%	221.2 PPM	28.4 um	Zn LA1-HR	0.00971	0.2694	0.099	82.90%		0.62 um	0.055
0.05603	0.007	329%	328.4 PPM	18.7 um	Cr LA1-HR	-0.00019					0.42 um	0.039
-0.2982	-0.009		147.3 PPM	49 um	As LA1-HF	0.2496	0.4601	0.13	17.30%	709.8 PPM	1.10 um	0.006
0.7507	0.012	230%	115.3 PPM	155 um	Zr LA1-HR	-0.00734	-0.233	-0.027		155.9 PPM	3.4 um	0.005

## Raw Data 2 – Sheet 2

Desulp(2nd)pdspffgraph												
Formula	Z	Concentra	Status	Line 1	Net int.	Used inten	Calc. conc	Stat. error	LLD	Analyzed	Line 2	Net int.
orig-g		0.5	Input									
added-g		0.1	Input									
Fe	26	29.50%	XRF 1	Fe KA1-HF	134.4	2928	29.5	0.28%	22.9 PPM	51 um	Fe KB1-HF	23.84
Ca	20	13.98%	XRF 1	Ca KA1-HF	22.89	502.2	14	0.68%	20.2 PPM	25.8 um	Ca KB1-HF	2.775
Mg	12	0.88%	XRF 1	Mg KA1-H	0.8237	21.16	0.88	3.71%	62.6 PPM	1.76 um		
Si	14	0.84%	XRF 1	Si KA1-HR	0.6411	18.08	0.844	4.18%	42.7 PPM	3.9 um	Si KB1-HR	-0.00455
Cl	17	0.53%	XRF 1	Cl KA1-HR	0.4772	14.35	0.53	5.08%	37.3 PPM	10.9 um		
Mn	25	0.40%	XRF 1	Mn KA1-H	1.396	30.38	0.399	2.94%	24.4 PPM	41 um	Mn KB1-H	0.5041
Na	11	0.39%	XRF 1	Na KA1-HI	0.1003	3.45	0.39	11.10%	132.2 PPM	1.12 um		
K	19	0.36%	XRF 1	K KA1-HF	0.6222	13.43	0.362	4.25%	16.8 PPM	19.8 um	K KB1-HF	0.08301
Al	13	0.27%	XRF 1	Al KA1-HR	0.1841	5.173	0.27	8.09%	47.0 PPM	2.60 um	Al KB1-HR	0.0041
S	16	0.20%	XRF 1	S KA1-HF	0.3149	9.474	0.2	6.38%	21.4 PPM	7.8 um		
Ti	22	0.15%	XRF 1	Ti KA1-HR	0.2134	4.77	0.15	8.62%	40.2 PPM	20.1 um	Ti KB1-HR	0.05276
Zn	30	0.06%	XRF 1	Zn KA1-HF	0.4075	8.777	0.062	7.49%	24.7 PPM	37 um	Zn KB1-HF	0.04759
V	23	0.06%	XRF 1	V KA1-HF	0.112	2.411	0.056	15.80%	41.1 PPM	25.6 um		
Sr	38	0.03%	XRF 1	Sr KA1-HF	0.6425	11.84	0.028	8.09%	15.9 PPM	141 um	Sr KB1-HF	0.5039
Cu	29	0.02%	XRF 1	Cu KA1-HI	0.1263	2.722	0.024	18.00%	27.0 PPM	30 um	Cu KB1-HF	0.00339
As	33	0.02%	XRF 1	As KA1-HI	0.2349	4.925	0.022	14.20%	20.0 PPM	63 um	As KB1-HI	-0.02283
Zr	40	0.01%	XRF 1	Zr KA1-HR	0.5039	5.573	0.011	11.00%	15.5 PPM	190 um	Zr KB1-HR	0.2785
100%												

Used inten	Calc. conc	Stat. error	LLD	Analyzed	Line 3	Net int.	Used inten	Calc. conc	Stat. error	LLD	Analyzed	XRF %
519.7	28.4	0.67%	140.3 PPM	64 um	Fe LA1-HF	0.01122				77.10%	1.47 um	29.5
60.88	14	1.97%	151.7 PPM	32 um								14
												0.88
-0.1282	-0.23		0.16%	4.4 um								0.844
												0.53
0.7197	0.05	14.20%	226.6 PPM	53 um	Mn LA1-HF	0.00269				157%	1.21 um	0.399
												0.39
1.792	0.44	34.20%	162.0 PPM	24.5 um								0.362
0.1152	0.65	311%	0.47%	2.92 um								0.27
												0.2
0.4506	0.091	74.90%	394.2 PPM	25.3 um								0.15
1.025	0.041	139%	160.3 PPM	48 um	Zn LA1-HR	0.01492	0.1981	0.052	66.90%		1.05 um	0.062
												0.056
4.093	0.038	11.00%	77.2 PPM	192 um	Sr LA1-HR	0.00417	0.08573	0.015	149%	118.6 PPM	4.3 um	0.028
0.07299	0.003	1732%	172.0 PPM	40 um	Cu LA1-HF	0.00438	0.1565	0.08	123%		0.89 um	0.024
-0.4786	-0.01		114.1 PPM	84 um	As LA1-HF	0.09781	-1.151	-0.27	33.20%	404.6 PPM	1.86 um	0.022
4.782	0.049	22.30%	92.3 PPM	262 um	Zr LA1-HR	0.00151	0.0454	0.006	992%	81.8 PPM	5.7 um	0.011

Formula	Z	Concentra	Status	Line 1	Net int.	Used inter	Calc. conc	Stat. error	LLD	Analyzed	Line 2	Net int.
orig-g		0.5	Input									
added-g		0.1	Input									
Fe	26	64.99%	XRF 1	Fe KA1-Hf	134.4	5051	64.99	0.28%	46.4 PPM	25.1 um	Fe KB1-Hf	23.84
Ca	20	25.27%	XRF 1	Ca KA1-Hf	22.89	866.3	25.3	0.68%	42.4 PPM	11.6 um	Ca KB1-Hf	2.775
Mg	12	2.43%	XRF 1	Mg KA1-H	0.8237	36.49	2.43	3.71%	136.2 PPM	0.79 um		
Si	14	1.92%	XRF 1	Si KA1-HR	0.6411	31.19	1.92	4.18%	92.4 PPM	1.73 um	Si KB1-HR	-0.00455
Na	11	1.16%	XRF 1	Na KA1-Hf	0.1003	5.909	1.2	11.10%	294.8 PPM	0.51 um		
Cl	17	0.92%	XRF 1	Cl KA1-HR	0.4772	24.76	0.923	5.08%	80.5 PPM	4.9 um		
Mn	25	0.85%	XRF 1	Mn KA1-H	1.396	52.41	0.849	2.94%	48.8 PPM	20.0 um	Mn KB1-H	0.5041
Al	13	0.68%	XRF 1	Al KA1-HR	0.1841	8.923	0.68	8.09%	101.8 PPM	1.17 um	Al KB1-HR	0.0041
K	19	0.66%	XRF 1	K KA1-Hf	0.6222	23.16	0.663	4.25%	35.7 PPM	8.9 um	K KB1-Hf	0.08301
S	16	0.37%	XRF 1	S KA1-Hf	0.3149	16.34	0.37	6.38%	46.4 PPM	3.5 um		
Ti	22	0.28%	XRF 1	Ti KA1-HR	0.2134	8.229	0.28	8.62%	78.6 PPM	9.9 um	Ti KB1-HR	0.05276
Zn	30	0.16%	XRF 1	Zn KA1-Hf	0.4075	15.14	0.16	7.49%	52.6 PPM	16.7 um	Zn KB1-Hf	0.04759
V	23	0.11%	XRF 1	V KA1-Hf	0.112	4.16	0.11	15.80%	81.4 PPM	12.6 um		
Sr	38	0.08%	XRF 1	Sr KA1-Hf	0.6425	20.43	0.075	8.09%	34.0 PPM	64 um	Sr KB1-Hf	0.5039
Cu	29	0.06%	XRF 1	Cu KA1-Hf	0.1263	4.695	0.061	18.00%	57.6 PPM	13.9 um	Cu KB1-Hf	0.00339
As	33	0.06%	XRF 1	As KA1-Hf	0.2349	8.496	0.056	14.20%	42.6 PPM	28.4 um	As KB1-Hf	-0.02283
Zr	40	0.03%	XRF 1	Zr KA1-HR	0.5039	8.261	0.025	11.00%	34.5 PPM	86 um	Zr KB1-HR	0.2785

Used inter	Calc. conc	Stat. error	LLD	Analyzed	Line 3	Net int.	Used inter	Calc. conc	Stat. error	LLD	Analyzed	XRF %
896.4	65.6	0.67%	285.3 PPM	32 um	Fe LA1-Hf	0.01122				77.10%	0.73 um	64.99
105	25.8	1.97%	317.5 PPM	14.6 um								25.3
												2.43
-0.2212	-0.51		0.34%	1.99 um								1.92
												1.2
												0.923
-0.3777	-0.033	14.20%	504.0 PPM	26.0 um	Mn LA1-Hf	0.00269				157%	0.61 um	0.849
0.1988	1.6	311%	1.01%	1.31 um								0.68
3.09	0.8	34.20%	342.6 PPM	11.0 um								0.663
												0.37
0.813	0.18	74.90%	797.1 PPM	12.5 um								0.28
1.768	0.11	139%	342.1 PPM	21.9 um	Zn LA1-HR	0.01492	0.1084	0.043	66.90%		0.48 um	0.16
												0.11
6.371	0.094	11.00%	171.2 PPM	87 um	Sr LA1-HR	0.00417	0.1449	0.026	149%	261.3 PPM	1.91 um	0.075
0.1259	0.009	1732%	366.7 PPM	18.1 um	Cu LA1-Hf	0.00438	0.2699	0.21	123%		0.40 um	0.061
-0.8256	-0.027		243.6 PPM	38 um	As LA1-Hf	0.09781	-3.847	-1.2	33.20%	998.0 PPM	0.84 um	0.056
8.248	0.14	22.30%	197.4 PPM	119 um	Zr LA1-HR	0.00151	0.07831	0.01	992%	177.5 PPM	2.53 um	0.025

Raw Data 2 – Sheet 3

Desulpbest.raw												
Formula	Z	Concentration	Status	Line 1	Net int.	Used inten	Calc. conc	Stat. error	LLD	Analyzed	Line 2	Net int.
orig-g		0.5	Input									
added-g		0.1	Input									
Ca	20	30.95%	XRF 1	Ca KA1-HI	47.9	1051	30.95	0.47%	35.8 PPM	25.3 um	Ca KB1-HI	5.787
Fe	26	30.07%	XRF 1	Fe KA1-HI	106.1	2312	30.07	0.32%	29.7 PPM	35 um	Fe KB1-HI	19.51
Mg	12	1.48%	XRF 1	Mg KA1-H	1.252	32.19	1.48	2.98%	73.4 PPM	1.73 um		
S	16	1.22%	XRF 1	S KA1-HF	2.008	60.42	1.22	2.35%	29.5 PPM	7.7 um		
Si	14	0.88%	XRF 1	Si KA1-HR	0.648	18.27	0.876	4.06%		3.8 um	Si KB1-HR	0.01712
Mn	25	0.75%	XRF 1	Mn KA1-H	2.018	43.92	0.752	2.36%	32.7 PPM	27.9 um	Mn KB1-H	0.613
Cl	17	0.41%	XRF 1	Cl KA1-HR	0.3878	11.67	0.413	5.81%	53.2 PPM	10.4 um		
Al	13	0.32%	XRF 1	Al KA1-HR	0.2072	5.822	0.32	7.70%	68.0 PPM	2.55 um	Al KB1-HR	0.02315
Na	11	0.31%	XRF 1	Na KA1-HI	0.06961	2.407	0.31	12.40%		1.10 um		
Ti	22	0.26%	XRF 1	Ti KA1-HR	0.2977	6.655	0.26	6.50%	52.0 PPM	13.9 um	Ti KB1-HR	0.04862
K	19	0.16%	XRF 1	K KA1-HF	0.2657	5.734	0.16	6.71%	22.5 PPM	19.0 um	K KB1-HF	0.03373
Zn	30	0.05%	XRF 1	Zn KA1-HF	0.2949	6.353	0.05	8.71%	26.2 PPM	35 um	Zn KB1-HF	0.01103
P	15	0.04%	XRF 1	P KA1-HF	0.03471	1.044	0.035	24.20%	35.9 PPM	5.4 um		
Sr	38	0.03%	XRF 1	Sr KA1-HF	0.6512	12	0.032	6.38%	14.4 PPM	138 um	Sr KB1-HF	0.3153
Zr	40	58 PPM	XRF 1	Zr KA1-HR	0.3153	2.613	0.006	12.80%	14.4 PPM	187 um	Zr KB1-HR	0.06836
100%												

Used inten	Calc. conc	Stat. error	LLD	Analyzed	Line 3	Net int.	Used inten	Calc. conc	Stat. error	LLD	Analyzed	XRF %
126.9	31.4	1.36%	253.0 PPM	32 um								30.95
425.3	30.6	0.74%	182.6 PPM	44 um	Fe LA1-HF	0.01569			26.10%		1.00 um	30.07
												1.48
												1.22
0.4827	0.88	92.20%	0.16%	4.4 um								0.876
6.768	0.623	4.73%	301.5 PPM	36 um	Mn LA1-HF	0.00292			151%		0.82 um	0.752
												0.413
0.6507	3.9	21.50%		2.87 um								0.32
												0.31
1.087	0.29	69.80%	524.8 PPM	17.5 um								0.26
0.728	0.18	72.40%	267.8 PPM	23.7 um								0.16
0.2375	0.011	462%	160.9 PPM	47 um	Zn LA1-HR	0.01748	0.4123	0.12	61.70%		1.02 um	0.05
												0.035
3.491	0.037	12.80%	68.8 PPM	189 um	Sr LA1-HR	0.00917	0.2328	0.038	144%	110.1 PPM	4.2 um	0.032
1.174	0.014	158%	82.3 PPM	257 um	Zr LA1-HR	-0.00062	-0.01857	-0.002		101.9 PPM	5.6 um	0.006

Formula	Z	Concentration	Status	Line 1	Net int.	Used inten	Calc. conc	Stat. error	LLD	Analyzed	Line 2	Net int.
orig-g		0.5	Input									
added-g		0.1	Input									
Fe	26	46.81%	XRF 1	Fe KA1-HF	106.1	3157	46.81	0.32%	43.1 PPM	23.5 um	Fe KB1-HF	19.51
Ca	20	43.78%	XRF 1	Ca KA1-HI	47.9	1435	43.78	0.47%	52.9 PPM	16.3 um	Ca KB1-HI	5.787
Mg	12	2.63%	XRF 1	Mg KA1-H	1.252	43.96	2.63	2.98%	110.0 PPM	1.11 um		
S	16	1.70%	XRF 1	S KA1-HF	2.008	82.52	1.7	2.35%	44.5 PPM	4.9 um		
Si	14	1.39%	XRF 1	Si KA1-HR	0.648	24.96	1.39	4.06%		2.43 um	Si KB1-HR	0.01712
Mn	25	1.17%	XRF 1	Mn KA1-H	2.018	59.98	1.17	2.36%	47.3 PPM	18.8 um	Mn KB1-H	0.613
Na	11	0.58%	XRF 1	Na KA1-HI	0.06961	3.276	0.58	12.40%		0.71 um		
Cl	17	0.56%	XRF 1	Cl KA1-HR	0.3878	15.93	0.561	5.81%	79.9 PPM	6.6 um		
Al	13	0.55%	XRF 1	Al KA1-HR	0.2072	7.952	0.55	7.70%	102.5 PPM	1.63 um	Al KB1-HR	0.02315
Ti	22	0.40%	XRF 1	Ti KA1-HR	0.2977	9.089	0.4	6.50%	74.4 PPM	9.3 um	Ti KB1-HR	0.04862
K	19	0.22%	XRF 1	K KA1-HF	0.2657	7.831	0.22	6.71%	33.6 PPM	12.2 um	K KB1-HF	0.03373
Zn	30	0.08%	XRF 1	Zn KA1-HF	0.2949	8.676	0.083	8.71%	39.1 PPM	22.9 um	Zn KB1-HF	0.01103
Sr	38	0.05%	XRF 1	Sr KA1-HF	0.6512	16.39	0.055	6.38%	21.5 PPM	89 um	Sr KB1-HF	0.3153
P	15	0.05%	XRF 1	P KA1-HF	0.03471	1.426	0.053	24.20%	54.2 PPM	3.4 um		
Zr	40	85 PPM	XRF 1	Zr KA1-HR	0.3153	3.092	0.009	12.80%	22.1 PPM	120 um	Zr KB1-HR	0.06836

Used inten	Calc. conc	Stat. error	LLD	Analyzed	Line 3	Net int.	Used inten	Calc. conc	Stat. error	LLD	Analyzed	XRF %
580.8	48	0.74%	265.8 PPM	29.7 um	Fe LA1-HF	0.01569				26.10%	0.67 um	46.81
173.4	44.4	1.36%	372.0 PPM	20.4 um								43.78
												2.63
												1.7
0.6592	1.4	92.20%	0.24%	2.79 um								1.39
8.652	0.905	4.73%	461.8 PPM	24.3 um	Mn LA1-HF	0.00292			151%		0.55 um	1.17
												0.58
												0.561
0.8887	6.6	21.50%		1.83 um								0.55
1.484	0.44	69.80%	750.8 PPM	11.7 um								0.4
0.9942	0.25	72.40%	398.5 PPM	15.2 um								0.22
0.3244	0.018	462%	240.3 PPM	30 um	Zn LA1-HR	0.01748	0.4959	0.18	61.70%		0.66 um	0.083
4.817	0.064	12.80%	104.4 PPM	122 um	Sr LA1-HR	0.00917	0.3162	0.051	144%	168.0 PPM	2.67 um	0.055
												0.053
1.603	0.024	158%	123.1 PPM	166 um	Zr LA1-HR	-0.00062	-0.02536	-0.003		153.8 PPM	3.6 um	0.009

## Raw Data 2 – Sheet 4

Desulpfallout(best)pds500ym												
Formula	Z	Concentra	Status	Line 1	Net int.	Used inten	Calc. conc	Stat. error	LLD	Analyzed	Line 2	Net int.
orig-g		0.5	Input									
added-g		0.1	Input									
Fe	26	37.36%	XRF 1	Fe KA1-HF	178.3	3887	37.36	0.25%	24.0 PPM	50 um	Fe KB1-HF	31.55
Ca	20	10.14%	XRF 1	Ca KA1-HF	16.82	369.1	10.1	0.80%	19.2 PPM	21.0 um	Ca KB1-HF	2.12
Mn	25	0.67%	XRF 1	Mn KA1-H	2.52	54.81	0.669	2.15%	26.0 PPM	40 um	Mn KB1-H	0.7929
Mg	12	0.51%	XRF 1	Mg KA1-H	0.4385	11.27	0.511	5.05%	43.0 PPM	1.34 um		
Si	14	0.43%	XRF 1	Si KA1-HF	0.3117	8.792	0.43	6.15%	48.4 PPM	3.00 um	Si KB1-HR	0.00438
S	16	0.37%	XRF 1	S KA1-HF	0.5726	17.22	0.372	4.64%	27.9 PPM	6.2 um		
Cl	17	0.33%	XRF 1	Cl KA1-HR	0.2908	8.748	0.33	17.40%	47.1 PPM	8.5 um		
Ti	22	0.23%	XRF 1	Ti KA1-HR	0.3662	8.185	0.23	6.06%	33.5 PPM	19.9 um	Ti KB1-HR	0.06466
Na	11	0.16%	XRF 1	Na KA1-HI	0.03795	1.314	0.16	16.80%		0.85 um		
Al	13	0.11%	XRF 1	Al KA1-HR	0.0717	2.015	0.11	14.70%	62.1 PPM	2.01 um	Al KB1-HR	0.01244
P	15	0.05%	XRF 1	P KA1-HF	0.04508	1.355	0.048	20.10%	32.2 PPM	4.3 um		
Cr	24	0.02%	XRF 1	Cr KA1-HF	0.09128	1.519	0.024	18.80%	27.2 PPM	32 um	Cr KB1-HF	0.0231
Zn	30	0.02%	XRF 1	Zn KA1-HF	0.1395	3.004	0.023	17.30%	26.4 PPM	28.0 um	Zn KB1-HF	0.01334
Zr	40	0.01%	XRF 1	Zr KA1-HR	0.4694	6.69	0.015	9.26%	13.1 PPM	144 um	Zr KB1-HR	0.1602
Sr	38	0.01%	XRF 1	Sr KA1-HF	0.293	5.4	0.014	12.80%	13.5 PPM	107 um	Sr KB1-HF	0.2813
100%												

Used inten	Calc. conc	Stat. error	LLD	Analyzed	Line 3	Net int.	Used inten	Calc. conc	Stat. error	LLD	Analyzed	XRF %
687.7	36.57	0.59%	150.4 PPM	63 um	Fe LA1-HF	0.00656				101%	1.44 um	37.36
46.52	10.5	2.26%	146.6 PPM	26.3 um								10.1
4.009	0.26	10.80%	235.1 PPM	52 um	Mn LA1-HF	0.00169				198%	1.23 um	0.669
												0.511
0.1235	0.23	354%	0.18%	3.4 um								0.43
												0.372
												0.33
0.9698	0.18	62.60%	336.4 PPM	25.1 um								0.23
												0.16
0.3495	2.1	73.20%		2.26 um								0.11
												0.048
-0.1803	-0.015	70.90%	165.7 PPM	41 um	Cr LA1-HR	0.00173				196%	0.98 um	0.024
0.2874	0.013	171%	163.0 PPM	37 um	Zn LA1-HR	0.00782	0.1569	0.045	92.30%		0.80 um	0.023
2.751	0.032	29.30%	80.2 PPM	199 um	Zr LA1-HR	-0.00288	-0.08677	-0.012		90.5 PPM	4.5 um	0.015
-0.5303	-0.006	36.60%	69.1 PPM	146 um	Sr LA1-HR	0.00179	0.03536	0.006	828%	130.1 PPM	3.3 um	0.014

Formula	Z	Concentra	Status	Line 1	Net int.	Used inten	Calc. conc	Stat. error	LLD	Analyzed	Line 2	Net int.
orig-g		0.5	Input									
added-g		0.1	Input									
Fe	26	76.95%	XRF 1	Fe KA1-Hf	178.3	6369	76.95	0.25%	46.1 PPM	26.4 um	Fe KB1-Hf	31.55
Ca	20	16.86%	XRF 1	Ca KA1-Hf	16.82	604.7	16.9	0.80%	37.8 PPM	10.1 um	Ca KB1-Hf	2.12
Mg	12	1.32%	XRF 1	Mg KA1-H	0.4385	18.47	1.32	5.05%	86.9 PPM	0.65 um		
Mn	25	1.32%	XRF 1	Mn KA1-H	2.52	89.81	1.32	2.15%	49.6 PPM	21.1 um	Mn KB1-H	0.7929
Si	14	0.93%	XRF 1	Si KA1-HR	0.3117	14.41	0.93	6.15%	98.3 PPM	1.44 um	Si KB1-HR	0.00438
S	16	0.65%	XRF 1	S KA1-Hf	0.5726	28.22	0.652	4.64%	56.7 PPM	2.96 um		
Cl	17	0.55%	XRF 1	Cl KA1-HR	0.2908	14.33	0.55	17.40%	95.3 PPM	4.1 um		
Na	11	0.45%	XRF 1	Na KA1-Hf	0.03795	2.142	0.45	16.80%		0.41 um		
Ti	22	0.39%	XRF 1	Ti KA1-HR	0.3662	13.41	0.39	6.06%	62.1 PPM	10.4 um	Ti KB1-HR	0.06466
Al	13	0.27%	XRF 1	Al KA1-HR	0.0717	3.302	0.27	14.70%	125.9 PPM	0.97 um	Al KB1-HR	0.01244
P	15	0.09%	XRF 1	P KA1-Hf	0.04508	2.22	0.094	20.10%	65.6 PPM	2.07 um		
Zn	30	0.06%	XRF 1	Zn KA1-Hf	0.1395	4.922	0.055	17.30%	53.3 PPM	13.6 um	Zn KB1-Hf	0.01334
Cr	24	0.04%	XRF 1	Cr KA1-Hf	0.09128	2.544	0.04	18.80%	51.3 PPM	16.8 um	Cr KB1-Hf	0.0231
Sr	38	0.04%	XRF 1	Sr KA1-Hf	0.293	8.849	0.035	12.80%	27.3 PPM	52 um	Sr KB1-Hf	0.2813
Zr	40	0.03%	XRF 1	Zr KA1-HR	0.4694	10.48	0.035	9.26%	27.3 PPM	70 um	Zr KB1-HR	0.1602

Used inten	Calc. conc	Stat. error	LLD	Analyzed	Line 3	Net int.	Used inten	Calc. conc	Stat. error	LLD	Analyzed	XRF %
1127	78.95	0.59%	290.6 PPM	33 um	Fe LA1-Hf	0.00656				101%	0.76 um	76.95
76.22	17.8	2.26%	287.3 PPM	12.7 um								16.9
												1.32
4.978	0.4	10.80%	491.8 PPM	27.4 um	Mn LA1-Hf	0.00169				198%	0.65 um	1.32
0.2024	0.49	354%	0.36%	1.65 um								0.93
												0.652
												0.55
												0.45
1.648	0.32	62.60%	637.4 PPM	13.2 um								0.39
0.5727	5	73.20%		1.09 um								0.27
												0.094
0.4709	0.03	171%	328.5 PPM	17.8 um	Zn LA1-HR	0.00782	0.1807	0.078	92.30%		0.39 um	0.055
-0.3408	-0.03	70.90%	315.7 PPM	21.6 um	Cr LA1-HR	0.00173			196%		0.52 um	0.04
-2.371	-0.038	36.60%	147.2 PPM	71 um	Sr LA1-HR	0.00179	0.05617	0.01	828%	267.1 PPM	1.59 um	0.035
4.507	0.081	29.30%	161.8 PPM	96 um	Zr LA1-HR	-0.00288	-0.1422	-0.019		183.8 PPM	2.14 um	0.035

## Raw Data 2 – Sheet 5

Desulpfallout.bets.ps.1000ym -Errors (thus will repeat)												
Formula	Z	Concentra	Status	Line 1	Net int.	Used inten	Calc. conc	Stat. error	LLD	Analyzed	Line 2	Net int.
orig-g		0.5	Input									
added-g		0.1	Input									
Fe	26	14.46%	XRF 1	Fe KA1-Hf	92.86	2024		0.34%		106 um	Fe KB1-Hf	17.5
Ca	20	5.94%	XRF 1	Ca KA1-Hf	9.199	201.8		1.08%		51 um	Ca KB1-Hf	1.174
Mn	25	0.66%	XRF 1	Mn KA1-H	3.179	69.17		1.91%		85 um	Mn KB1-H	0.8099
Cl	17	0.47%	XRF 1	Cl KA1-HR	0.4161	12.52		14.10%		21.6 um		
Si	14	0.30%	XRF 1	Si KA1-HR	0.2632	7.422		6.75%		7.7 um	Si KB1-HR	0.00397
Ti	22	0.25%	XRF 1	Ti KA1-HR	0.3874	8.659		6.27%		43 um	Ti KB1-HR	0.1689
S	16	0.23%	XRF 1	S KA1-Hf	0.3648	10.98		5.95%		15.7 um		
Mg	12	0.21%	XRF 1	Mg KA1-H	0.2709	6.964		6.73%		3.5 um		
Al	13	0.12%	XRF 1	Al KA1-HR	0.1038	2.918		11.50%		5.2 um	Al KB1-HR	0.0016
P	15	0.03%	XRF 1	P KA1-Hf	0.03617	1.088		23.10%		11.0 um		
Zn	30	0.02%	XRF 1	Zn KA1-Hf	0.186	4.006		16.90%		72 um	Zn KB1-Hf	0.01967
Sr	38	0.02%	XRF 1	Sr KA1-Hf	0.276	5.087		18.90%		276 um	Sr KB1-Hf	0.1174
100%												

Used inten	Calc. conc	Stat. error	LLD	Analyzed	Line 3	Net int.	Used inten	Calc. conc	Stat. error	LLD	Analyzed	XRF %
		0.79%		127 um	Fe LA1-HF	0.00231			170%		2.93 um	
		3.06%		64 um								
		4.49%		110 um	Mn LA1-HF	0.00443			123%		2.56 um	
		390%		8.9 um								
		13.40%		54 um								
		719%		5.9 um								
		413%		95 um	Zn LA1-HR	0.00485			117%		2.06 um	
		118%		0.38 mm	Sr LA1-HR	0.00284			535%		8.5 um	

Formula	Z	Concentra	Status	Line 1	Net int.	Used inten	Calc. conc	Stat. error	LLD	Analyzed	Line 2	Net int.
orig-g		0.5	Input									
added-g		0.1	Input									
Fe	26	72.82%	XRF 1	Fe KA1-Hf	92.86	6035	72.82	0.34%	55.4 PPM	26.5 um	Fe KB1-HF	17.5
Ca	20	17.00%	XRF 1	Ca KA1-Hf	9.199	601.8	17	1.08%	35.4 PPM	10.2 um	Ca KB1-Hf	1.174
Mn	25	3.07%	XRF 1	Mn KA1-H	3.179	206.3	3.07	1.91%	56.3 PPM	21.1 um	Mn KB1-H	0.8099
Mg	12	1.46%	XRF 1	Mg KA1-H	0.2709	20.77	1.5	6.73%	120.1 PPM	0.68 um		
Cl	17	1.43%	XRF 1	Cl KA1-HR	0.4161	37.33	1.4	14.10%	97.2 PPM	4.2 um		
Si	14	1.41%	XRF 1	Si KA1-HR	0.2632	22.13	1.4	6.75%	97.4 PPM	1.50 um	Si KB1-HR	0.00397
Ti	22	0.75%	XRF 1	Ti KA1-HR	0.3874	25.82	0.75	6.27%	84.0 PPM	10.5 um	Ti KB1-HR	0.1689
S	16	0.75%	XRF 1	S KA1-HF	0.3648	32.73	0.75	5.95%	52.8 PPM	3.0 um		
Al	13	0.69%	XRF 1	Al KA1-HR	0.1038	8.702	0.69	11.50%	119.9 PPM	1.01 um	Al KB1-HR	0.0016
P	15	0.14%	XRF 1	P KA1-HF	0.03617	3.245	0.14	23.10%	62.3 PPM	2.13 um		
Zn	30	0.13%	XRF 1	Zn KA1-HF	0.186	11.95	0.13	16.90%	70.6 PPM	14.2 um	Zn KB1-HF	0.01967
Sr	38	0.06%	XRF 1	Sr KA1-HF	0.276	15.17	0.059	18.90%	39.9 PPM	54 um	Sr KB1-HF	0.1174

Used inten	Calc. conc	Stat. error	LLD	Analyzed	Line 3	Net int.	Used inten	Calc. conc	Stat. error	LLD	Analyzed	XRF %	
	1138	82.1	0.79%	375.3 PPM	31 um	Fe LA1-HF			170%		0.72 um	72.82	
	76.78	18.2	3.06%	294.3 PPM	12.7 um							17	
	12.65	1.04	4.49%	621.9 PPM	27.5 um	Mn LA1-Hf	0.00443		123%		0.65 um	3.07	
												1.5	
												1.4	
	0.3335	0.8	390%	0.36%	1.72 um							1.4	
	11.26	2.2	13.40%	761.5 PPM	13.3 um							0.75	
												0.75	
	0.1344	1.2	719%	1.01%	1.13 um							0.69	
												0.14	
	1.264	0.08	413%	461.8 PPM	18.6 um	Zn LA1-HR	0.00485	0.1848	0.078	117%	0.40 um	0.13	
	6.011	0.095	118%	171.6 PPM	74 um	Sr LA1-HR	0.00284	0.1704	0.031	535%	275.2 PPM	1.65 um	0.059

Repeated run on same sample												
Formula	Z	Concentra	Status	Line 1	Net int.	Used inten	Calc. conc	Stat. error	LLD	Analyzed	Line 2	Net int.
orig-g		0.5	Input									
added-g		0.1	Input									
Fe	26	14.64%	XRF 1	Fe KA1-HF	93.23	2032		0.34%		105 um	Fe KB1-HF	17.22
Ca	20	6.07%	XRF 1	Ca KA1-Hf	9.391	206		1.07%		50 um	Ca KB1-Hf	1.153
Mn	25	0.64%	XRF 1	Mn KA1-H	3.093	67.3		1.93%		84 um	Mn KB1-H	0.7712
Cl	17	0.56%	XRF 1	Cl KA1-HR	0.4957	14.91		5.10%		21.4 um		
Si	14	0.34%	XRF 1	Si KA1-HR	0.2953	8.328		6.33%		7.7 um	Si KB1-HR	0.00167
S	16	0.25%	XRF 1	S KA1-HF	0.401	12.06		5.68%		15.7 um		
Mg	12	0.23%	XRF 1	Mg KA1-H	0.2997	7.704		6.25%		3.4 um		
Ti	22	0.20%	XRF 1	Ti KA1-HR	0.3182	7.112		7.30%		42 um	Ti KB1-HR	0.1501
Al	13	0.11%	XRF 1	Al KA1-HR	0.09566	2.689		11.80%		5.2 um	Al KB1-HR	0.00324
Zn	30	0.03%	XRF 1	Zn KA1-HF	0.2304	4.963		14.10%		71 um	Zn KB1-HF	0.04533
	100%											

Used inten	Calc. conc	Stat. error	LLD	Analyzed	Line 3	Net int.	Used inten	Calc. conc	Stat. error	LLD	Analyzed	XRF %
		0.80%		126 um	Fe LA1-HF	0.00516			114%		2.90 um	
		3.09%		63 um								
		4.62%		109 um	Mn LA1-HF	0.00216			176%		2.53 um	
			355%	8.8 um								
		15.10%		53 um								
		368%		5.8 um								
		74.30%		94 um	Zn LA1-HR	0.00744			94.60%		2.04 um	

Formula	Z	Concentra	Status	Line 1	Net int.	Used inten	Calc. conc	Stat. error	LLD	Analyzed	Line 2	Net int.
orig-g		0.5	Input									
added-g		0.1	Input									
Fe	26	72.44%	XRF 1	Fe KA1-Hf	93.23	5999	72.44	0.34%	54.6 PPM	26.5 um	Fe KB1-HF	17.22
Ca	20	17.25%	XRF 1	Ca KA1-Hf	9.391	608.2	17.3	1.07%	36.4 PPM	10.2 um	Ca KB1-Hf	1.153
Mn	25	2.96%	XRF 1	Mn KA1-H	3.093	198.7	2.96	1.93%	53.7 PPM	21.2 um	Mn KB1-H	0.7712
Cl	17	1.69%	XRF 1	Cl KA1-HR	0.4957	44.02	1.69	5.10%	100.4 PPM	4.2 um		
Mg	12	1.59%	XRF 1	Mg KA1-H	0.2997	22.74	1.6	6.25%	102.1 PPM	0.68 um		
Si	14	1.56%	XRF 1	Si KA1-HR	0.2953	24.59	1.6	6.33%	96.4 PPM	1.51 um	Si KB1-HR	0.00167
S	16	0.82%	XRF 1	S KA1-HF	0.401	35.61	0.816	5.68%	55.0 PPM	3.1 um		
Al	13	0.63%	XRF 1	Al KA1-HR	0.09566	7.937	0.63	11.80%	105.0 PPM	1.02 um	Al KB1-HR	0.00324
Ti	22	0.62%	XRF 1	Ti KA1-HR	0.3182	21	0.62	7.30%	90.0 PPM	10.5 um	Ti KB1-HR	0.1501
Zn	30	0.16%	XRF 1	Zn KA1-HF	0.2304	14.65	0.16	14.10%	71.3 PPM	14.3 um	Zn KB1-HF	0.04533

Used inten	Calc. conc	Stat. error	LLD	Analyzed	Line 3	Net int.	Used inten	Calc. conc	Stat. error	LLD	Analyzed	XRF %
1108	79.9	0.80%	382.0 PPM	31 um	Fe LA1-HF	0.00516			114%		0.73 um	72.44
74.68	17.8	3.09%	300.6 PPM	12.8 um								17.3
10.28	0.844	4.62%	617.1 PPM	27.5 um	Mn LA1-Hf	0.00216			176%		0.65 um	2.96
												1.69
												1.6
0.1391	0.33	355%	0.36%	1.73 um								1.6
												0.816
0.2688	2.3	368%	1.00%	1.14 um								0.63
9.907	2	15.10%	794.7 PPM	13.3 um								0.62
2.883	0.18	74.30%	471.1 PPM	18.8 um	Zn LA1-HR	0.00744	0.4629	0.19	94.60%		0.41 um	0.16

## Raw Data 2 – Sheet 6

Formula	Z	Concentra	Status	Line 1	Net int.	Used inten	Calc. conc	Stat. error	LLD	Analyzed	Line 2	Net int.
Desulpfallout(best)pds355ym												
orig-g		0.5	Input									
added-g		0.1	Input									
Fe	26	32.54%	XRF 1	Fe KA1-Hf	160.9	3507	32.54	0.26%	21.5 PPM	55 um	Fe KB1-HF	28.77
Ca	20	9.98%	XRF 1	Ca KA1-Hf	16.72	366.7	9.98	0.80%	17.4 PPM	23.7 um	Ca KB1-Hf	2.084
Mn	25	0.76%	XRF 1	Mn KA1-H	2.937	63.9	0.763	1.97%	22.9 PPM	44 um	Mn KB1-H	0.8308
Mg	12	0.50%	XRF 1	Mg KA1-H	0.4552	11.7	0.498	4.99%	45.6 PPM	1.54 um		
Si	14	0.44%	XRF 1	Si KA1-HR	0.3322	9.37	0.44	5.93%	42.9 PPM	3.4 um	Si KB1-HR	0.0093
S	16	0.40%	XRF 1	S KA1-HF	0.6268	18.86	0.403	4.36%	22.6 PPM	7.0 um		
Cl	17	0.38%	XRF 1	Cl KA1-HR	0.341	10.26	0.38	15.60%	40.4 PPM	9.7 um		
Ti	22	0.23%	XRF 1	Ti KA1-HR	0.3742	8.366	0.23	6.04%	33.2 PPM	21.6 um	Ti KB1-HR	0.06321
Al	13	0.16%	XRF 1	Al KA1-HR	0.1092	3.069	0.16	9.88%		2.30 um	Al KB1-HR	0.00239
Na	11	0.14%	XRF 1	Na KA1-Hf	0.04335	1.262	0.14	15.70%		0.98 um		
Zn	30	0.14%	XRF 1	Zn KA1-HF	0.9135	19.68	0.144	4.05%	22.4 PPM	32 um	Zn KB1-HF	0.138
V	23	0.05%	XRF 1	V KA1-HF	0.1152	2.396	0.05	15.50%	34.4 PPM	27.6 um		
P	15	0.04%	XRF 1	P KA1-HF	0.04296	1.292	0.044	20.80%	28.5 PPM	4.9 um		
K	19	0.04%	XRF 1	K KA1-HF	0.07453	1.609	0.043	14.30%	16.0 PPM	17.7 um	K KB1-HF	0.02662
Sr	38	0.01%	XRF 1	Sr KA1-HF	0.2514	4.634	0.011	14.90%	12.3 PPM	123 um	Sr KB1-HF	0.125
100%												

Used inten	Calc. conc	Stat. error	LLD	Analyzed	Line 3	Net int.	Used inten	Calc. conc	Stat. error	LLD	Analyzed	XRF %
626.9	32.1	0.61%	136.2 PPM	67 um	Fe LA1-HF	0.00919			85.20%		1.55 um	32.54
45.72	10.2	2.28%	133.7 PPM	29.7 um								9.98
5.567	0.347	4.15%	212.6 PPM	57 um	Mn LA1-HF	0.00163			202%		1.33 um	0.763
												0.498
0.2623	0.48	71.70%	0.16%	3.9 um								0.44
												0.403
												0.38
0.6214	0.11	63.70%	325.5 PPM	27.3 um								0.23
0.0672	0.39	446%	0.40%	2.59 um								0.16
												0.14
2.974	0.12	18.70%	147.2 PPM	42 um	Zn LA1-HR	0.00874	0.1903	0.051	87.40%		0.92 um	0.144
												0.05
												0.044
0.5746	0.14	30.90%	152.7 PPM	22.0 um								0.043
2.146	0.02	78.80%	53.4 PPM	167 um	Sr LA1-HR	-0.0041	-0.132	-0.023		116.6 PPM	3.8 um	0.011

Formula	Z	Concentra	Status	Line 1	Net int.	Used inten	Calc. conc	Stat. error	LLD	Analyzed	Line 2	Net int.
orig-g		0.5	Input									
added-g		0.1	Input									
Fe	26	74.45%	XRF 1	Fe KA1-HF	160.9	6114	74.45	0.26%	45.4 PPM	26.2 um	Fe KB1-HF	28.77
Ca	20	17.98%	XRF 1	Ca KA1-HF	16.72	639.2	18	0.80%	37.7 PPM	10.3 um	Ca KB1-HF	2.084
Mn	25	1.66%	XRF 1	Mn KA1-H	2.937	111.4	1.66	1.97%	47.7 PPM	20.9 um	Mn KB1-H	0.8308
Mg	12	1.44%	XRF 1	Mg KA1-H	0.4552	20.4	1.44	4.99%	102.1 PPM	0.67 um		
Si	14	1.05%	XRF 1	Si KA1-HR	0.3322	16.33	1	5.93%	96.4 PPM	1.48 um	Si KB1-HR	0.0093
S	16	0.76%	XRF 1	S KA1-HF	0.6268	32.87	0.755	4.36%	50.7 PPM	3.0 um		
Cl	17	0.69%	XRF 1	Cl KA1-HR	0.341	17.88	0.69	15.60%	90.5 PPM	4.2 um		
Na	11	0.44%	XRF 1	Na KA1-HF	0.04335	2.106	0.44	15.70%		0.43 um		
Ti	22	0.43%	XRF 1	Ti KA1-HR	0.3742	14.58	0.43	6.04%	67.3 PPM	10.3 um	Ti KB1-HR	0.06321
Al	13	0.43%	XRF 1	Al KA1-HR	0.1092	5.351	0.43	9.88%		0.99 um	Al KB1-HR	0.00239
Zn	30	0.38%	XRF 1	Zn KA1-HF	0.9135	34.3	0.379	4.05%	49.9 PPM	14.0 um	Zn KB1-HF	0.138
P	15	0.10%	XRF 1	P KA1-HF	0.04296	2.253	0.095	20.80%	64.1 PPM	2.12 um		
V	23	0.09%	XRF 1	V KA1-HF	0.1152	4.2	0.092	15.50%	70.6 PPM	13.2 um		
K	19	0.08%	XRF 1	K KA1-HF	0.07453	2.804	0.08	14.30%	35.2 PPM	7.7 um	K KB1-HF	0.02662
Sr	38	0.03%	XRF 1	Sr KA1-HF	0.2514	8.079	0.032	14.90%	27.3 PPM	53 um	Sr KB1-HF	0.125

Used inten	Calc. conc	Stat. error	LLD	Analyzed	Line 3	Net int.	Used inten	Calc. conc	Stat. error	LLD	Analyzed	XRF %
1093	77.5	0.61%	288.8 PPM	32 um	Fe LA1-HF	0.00919			85.20%		0.75 um	74.45
79.7	18.8	2.28%	288.1 PPM	12.9 um								18
7.778	0.638	4.15%	494.1 PPM	27.1 um	Mn LA1-HF	0.00163			202%		0.64 um	1.66
												1.44
0.4572	1.1	71.70%	0.36%	1.70 um								1
												0.755
												0.69
												0.44
1.189	0.23	63.70%	679.6 PPM	13.1 um								0.43
0.1172	1	446%	0.91%	1.12 um								0.43
5.184	0.33	18.70%	328.0 PPM	18.4 um	Zn LA1-HR	0.00874	0.254	0.11	87.40%		0.40 um	0.379
												0.095
												0.092
1.002	0.26	30.90%	334.9 PPM	9.6 um								0.08
3.74	0.059	78.80%	119.2 PPM	73 um	Sr LA1-HR	-0.0041	-0.2315	-0.043		265.5 PPM	1.63 um	0.032

Raw Data 2 – Sheet 7

Desulph fallout(best)pds 180ym												
Formula	Z	Concentration	Status	Line 1	Net int.	Used inten	Calc. conc	Stat. error	LLD	Analyzed	Line 2	Net int.
orig-g		0.5	Input									
added-g		0.1	Input									
Fe	26	28.65%	XRF 1	Fe KA1-HF	139.1	3031	28.65	0.28%	21.3 PPM	55 um	Fe KB1-HF	25.97
Ca	20	11.70%	XRF 1	Ca KA1-HF	19.69	431.9	11.7	0.74%	16.9 PPM	26.9 um	Ca KB1-HF	2.333
Mn	25	0.80%	XRF 1	Mn KA1-H	2.979	64.82	0.8	1.95%	22.7 PPM	44 um	Mn KB1-H	0.8869
Cl	17	0.50%	XRF 1	Cl KA1-HF	0.4506	13.55	0.502	5.32%	38.2 PPM	11.1 um		
S	16	0.49%	XRF 1	S KA1-HF	0.7698	23.16	0.488	3.90%	21.1 PPM	8.1 um		
Si	14	0.40%	XRF 1	Si KA1-HR	0.3066	8.646	0.4	6.20%	39.9 PPM	4.0 um	Si KB1-HR	0.00262
Mg	12	0.37%	XRF 1	Mg KA1-H	0.3556	9.141	0.371	5.67%	39.8 PPM	1.76 um		
Na	11	0.35%	XRF 1	Na KA1-HF	0.09215	3.211	0.35	10.80%		1.13 um		
Ti	22	0.27%	XRF 1	Ti KA1-HR	0.4202	9.393	0.271	5.63%	35.0 PPM	22.0 um	Ti KB1-HR	0.1002
Al	13	0.13%	XRF 1	Al KA1-HF	0.09547	2.683	0.13	11.80%	44.1 PPM	2.65 um	Al KB1-HF	0.00113
K	19	0.07%	XRF 1	K KA1-HF	0.1301	2.807	0.075	10.10%	15.3 PPM	20.2 um	K KB1-HF	0.03894
Zn	30	0.04%	XRF 1	Zn KA1-HF	0.2526	5.441	0.038	10.30%	21.4 PPM	37 um	Zn KB1-HF	0.01643
Sr	38	0.02%	XRF 1	Sr KA1-HF	0.3606	6.646	0.015	10.70%	11.2 PPM	141 um	Sr KB1-HF	0.1692
100%												

Used inten	Calc. conc	Stat. error	LLD	Analyzed	Line 3	Net int.	Used inten	Calc. conc	Stat. error	LLD	Analyzed	XRF %
566	29.4	0.65%	136.3 PPM	68 um	Fe LA1-HF	0.00574				108%	1.56 um	28.65
51.17	11.3	2.15%	132.4 PPM	34 um								11.7
8.266	0.533	3.98%	210.2 PPM	57 um	Mn LA1-HF	0.00096				263%	1.33 um	0.8
												0.502
												0.488
0.07391	0.13	576%	0.15%	4.5 um								0.4
												0.371
												0.35
2.241	0.43	43.60%	308.7 PPM	27.7 um								0.271
0.03171	0.18	874%	0.36%	2.98 um								0.13
0.8404	0.2	57.30%	144.4 PPM	25.1 um								0.075
0.354	0.014	348%	134.3 PPM	49 um	Zn LA1-HR	0.01096	0.07456	0.019	78.00%		1.05 um	0.038
2.906	0.026	22.80%	47.3 PPM	193 um	Sr LA1-HR	0.00153	0.0273	0.005	973%	108.3 PPM	4.4 um	0.015

Formula	Z	Concentration	Status	Line 1	Net int.	Used inten	Calc. conc	Stat. error	LLD	Analyzed	Line 2	Net int.
orig-g		0.5	Input									
added-g		0.1	Input									
Fe	26	69.42%	XRF 1	Fe KA1-HF	139.1	5496	69.42	0.28%	46.8 PPM	25.2 um	Fe KB1-HF	25.97
Ca	20	22.35%	XRF 1	Ca KA1-HF	19.69	783.3	22.4	0.74%	38.4 PPM	11.1 um	Ca KB1-HF	2.333
Mn	25	1.85%	XRF 1	Mn KA1-H	2.979	117.6	1.85	1.95%	49.2 PPM	20.2 um	Mn KB1-H	0.8869
Na	11	1.17%	XRF 1	Na KA1-HF	0.09215	5.793	1.2	10.80%		0.46 um		
Mg	12	1.14%	XRF 1	Mg KA1-H	0.3556	16.58	1.14	5.67%	93.7 PPM	0.72 um		
Si	14	0.98%	XRF 1	Si KA1-HR	0.3066	15.68	0.98	6.20%	94.4 PPM	1.61 um	Si KB1-HR	0.00262
S	16	0.94%	XRF 1	S KA1-HF	0.7698	42	0.94	3.90%	49.9 PPM	3.3 um		
Cl	17	0.92%	XRF 1	Cl KA1-HF	0.4506	24.58	0.923	5.32%	89.6 PPM	4.5 um		
Ti	22	0.54%	XRF 1	Ti KA1-HR	0.4202	17.03	0.544	5.63%	73.7 PPM	10.0 um	Ti KB1-HR	0.1002
Al	13	0.38%	XRF 1	Al KA1-HF	0.09547	4.866	0.38	11.80%	104.3 PPM	1.08 um	Al KB1-HF	0.00113
K	19	0.15%	XRF 1	K KA1-HF	0.1301	5.092	0.15	10.10%	35.2 PPM	8.3 um	K KB1-HF	0.03894
Zn	30	0.11%	XRF 1	Zn KA1-HF	0.2526	9.868	0.11	10.30%	49.9 PPM	15.2 um	Zn KB1-HF	0.01643
Sr	38	0.05%	XRF 1	Sr KA1-HF	0.3606	12.05	0.046	10.70%	26.3 PPM	58 um	Sr KB1-HF	0.1692

Used inten	Calc. conc	Stat. error	LLD	Analyzed	Line 3	Net int.	Used inten	Calc. conc	Stat. error	LLD	Analyzed	XRF %
1027	75.3	0.65%	301.7 PPM	31 um	Fe LA1-HF	0.00574				108%	0.71 um	69.42
92.8	22.3	2.15%	297.7 PPM	13.9 um								22.4
12.89	1.11	3.98%	512.8 PPM	26.1 um	Mn LA1-HF	0.00096				263%	0.61 um	1.85
												1.2
												1.14
0.134	0.31	576%	0.35%	1.85 um								0.98
												0.94
												0.923
4.064	0.87	43.60%	650.4 PPM	12.6 um								0.544
0.05751	0.49	874%	0.84%	1.21 um								0.38
1.524	0.39	57.30%	331.3 PPM	10.3 um								0.15
0.6419	0.04	348%	314.2 PPM	20.0 um	Zn LA1-HR	0.01096	-0.1207	-0.05	78.00%		0.43 um	0.11
5.269	0.081	22.80%	111.0 PPM	79 um	Sr LA1-HR	0.00153	0.04825	0.009	973%	259.3 PPM	1.77 um	0.046

Raw Data 2 – Sheet 8

Desulpfallout(best)pds <180ym												
Formula	Z	Concentrat	Status	Line 1	Net int.	Used inten	Calc. conc	Stat. error	LLD	Analyzed	Line 2	Net int.
orig-g		0.5	Input									
added-g		0.1	Input									
Ca	20	39.80%	XRF 1	Ca KA1-HI	60.25	1322	39.8	0.42%	49.4 PPM	22.1 um	Ca KB1-HF	7.322
Fe	26	33.91%	XRF 1	Fe KA1-Hf	110.1	2400	33.91	0.31%	36.4 PPM	29.0 um	Fe KB1-HF	19.61
Mg	12	2.60%	XRF 1	Mg KA1-H	2.007	51.58	2.6	2.35%	108.1 PPM	1.53 um		
S	16	1.79%	XRF 1	S KA1-HF	2.96	89.03	1.79	1.91%	28.8 PPM	6.7 um		
Si	14	1.46%	XRF 1	Si KA1-HR	1.025	28.92	1.46	3.28%	65.9 PPM	3.3 um	Si KB1-HR	0.00696
Mn	25	0.81%	XRF 1	Mn KA1-H	1.985	43.2	0.807	2.39%	42.3 PPM	23.3 um	Mn KB1-H	0.581
Al	13	0.50%	XRF 1	Al KA1-HR	0.2957	8.312	0.5	6.25%	71.9 PPM	2.23 um	Al KB1-HR	0.0018
Ti	22	0.23%	XRF 1	Ti KA1-HR	0.242	5.41	0.23	7.07%	51.1 PPM	11.6 um	Ti KB1-HR	0.06678
Na	11	0.17%	XRF 1	Na KA1-HI	0.03495	1.175	0.17	21.00%	187.0 PPM	0.97 um		
Cl	17	0.13%	XRF 1	Cl KA1-HR	0.1275	3.836	0.13	10.90%	51.4 PPM	8.9 um		
K	19	0.10%	XRF 1	K KA1-HF	0.1716	3.703	0.1	8.60%	27.4 PPM	16.5 um	K KB1-HF	0.01472
Zn	30	0.05%	XRF 1	Zn KA1-HF	0.3016	6.498	0.054	8.07%	27.5 PPM	31 um	Zn KB1-HF	0.05211
P	15	0.04%	XRF 1	P KA1-HF	0.03528	1.061	0.037	24.20%	44.8 PPM	4.7 um		
Sr	38	0.04%	XRF 1	Sr KA1-HF	0.682	12.57	0.0367	5.87%	15.6 PPM	122 um	Sr KB1-HF	0.2938
V	23	0.04%	XRF 1	V KA1-HF	0.05228	1.103	0.036	19.10%	46.5 PPM	14.7 um		
As	33	0.02%	XRF 1	As KA1-HI	0.165	3.458	0.018	14.50%	20.3 PPM	54 um	As KB1-Hf	0.08018
Zr	40	57 PPM	XRF 1	Zr KA1-HR	0.2938	2.356	0.006	13.00%	16.0 PPM	165 um	Zr KB1-HR	0.07519
100%												

Used inten	Calc. conc	Stat. error	LLD	Analyzed	Line 3	Net int.	Used inten	Calc. conc	Stat. error	LLD	Analyzed	XRF %
160.6	41	1.21%	323.7 PPM	27.7 um								39.8
427.3	33.5	0.74%	215.0 PPM	37 um	Fe LA1-HF	0.01226				73.70%	0.83 um	33.91
												2.6
												1.79
0.1964	0.37	231%	0.24%	3.8 um								1.46
6.642	0.669	4.88%	365.4 PPM	30 um	Mn LA1-Hf	0.00193				186%	0.68 um	0.807
0.05048	0.33	749%	0.79%	2.51 um								0.5
1.287	0.37	16.00%	431.1 PPM	14.5 um								0.23
												0.17
												0.13
0.3177	0.08	160%	359.6 PPM	20.5 um								0.1
1.122	0.054	37.70%	172.3 PPM	41 um	Zn LA1-HR	0.01031	0.2701	0.084	80.40%		0.90 um	0.054
												0.037
3.452	0.04	13.00%	76.0 PPM	167 um	Sr LA1-HR	0.01922	0.5064	0.081	38.70%	182.5 PPM	3.7 um	0.0367
												0.036
1.681	0.044	31.30%	118.8 PPM	72 um	As LA1-HF	0.2722	-0.3029	-0.075	17.90%	754.0 PPM	1.62 um	0.018
1.291	0.017	136%	91.5 PPM	228 um	Zr LA1-HR	-0.00232	-0.06981	-0.009		126.2 PPM	4.8 um	0.006

Formula	Z	Concentra	Status	Line 1	Net int.	Used inten	Calc. conc	Stat. error	LLD	Analyzed	Line 2	Net int.
orig-g		0.5	Input									
added-g		0.1	Input									
Ca	20	47.46%	XRF 1	Ca KA1-HI	60.25	1542	47.46	0.42%	59.8 PPM	17.6 um	Ca KB1-HI	7.322
Fe	26	42.39%	XRF 1	Fe KA1-HI	110.1	2799	42.39	0.31%	43.6 PPM	23.8 um	Fe KB1-HI	19.61
Mg	12	3.48%	XRF 1	Mg KA1-HI	2.007	60.16	3.48	2.35%	131.8 PPM	1.23 um		
S	16	2.12%	XRF 1	S KA1-HI	2.96	103.8	2.12	1.91%	35.2 PPM	5.3 um		
Si	14	1.85%	XRF 1	Si KA1-HR	1.025	33.73	1.85	3.28%	80.5 PPM	2.65 um	Si KB1-HR	0.00696
Mn	25	1.01%	XRF 1	Mn KA1-HI	1.985	50.38	1.01	2.39%	50.6 PPM	19.0 um	Mn KB1-HI	0.581
Al	13	0.65%	XRF 1	Al KA1-HR	0.2957	9.695	0.65	6.25%	87.8 PPM	1.78 um	Al KB1-HR	0.0018
Ti	22	0.29%	XRF 1	Ti KA1-HR	0.242	6.31	0.29	7.07%	60.8 PPM	9.5 um	Ti KB1-HR	0.06678
Na	11	0.23%	XRF 1	Na KA1-HI	0.03495	1.366	0.23	21.00%	229.3 PPM	0.78 um		
Cl	17	0.16%	XRF 1	Cl KA1-HR	0.1275	4.474	0.16	10.90%	62.7 PPM	7.1 um		
K	19	0.12%	XRF 1	K KA1-HI	0.1716	4.319	0.12	8.60%	33.3 PPM	13.2 um	K KB1-HI	0.01472
Zn	30	0.07%	XRF 1	Zn KA1-HI	0.3016	7.579	0.07	8.07%	33.4 PPM	25.2 um	Zn KB1-HI	0.05211
Sr	38	0.05%	XRF 1	Sr KA1-HI	0.682	14.66	0.0474	5.87%	19.0 PPM	98 um	Sr KB1-HI	0.2938
P	15	0.05%	XRF 1	P KA1-HI	0.03528	1.237	0.046	24.20%	54.8 PPM	3.7 um		
V	23	0.04%	XRF 1	V KA1-HI	0.05228	1.284	0.045	19.10%	55.7 PPM	12.0 um		
As	33	0.02%	XRF 1	As KA1-HI	0.165	4.034	0.023	14.50%	24.6 PPM	43 um	As KB1-HI	0.08018
Zr	40	69 PPM	XRF 1	Zr KA1-HR	0.2938	2.588	0.007	13.00%	19.7 PPM	133 um	Zr KB1-HR	0.07519

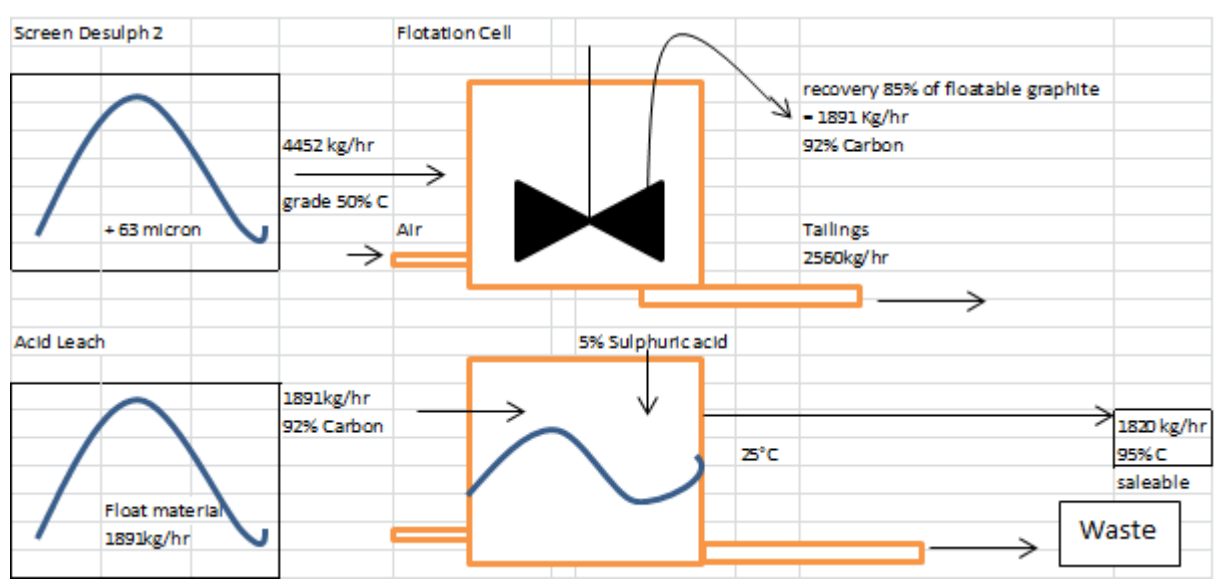
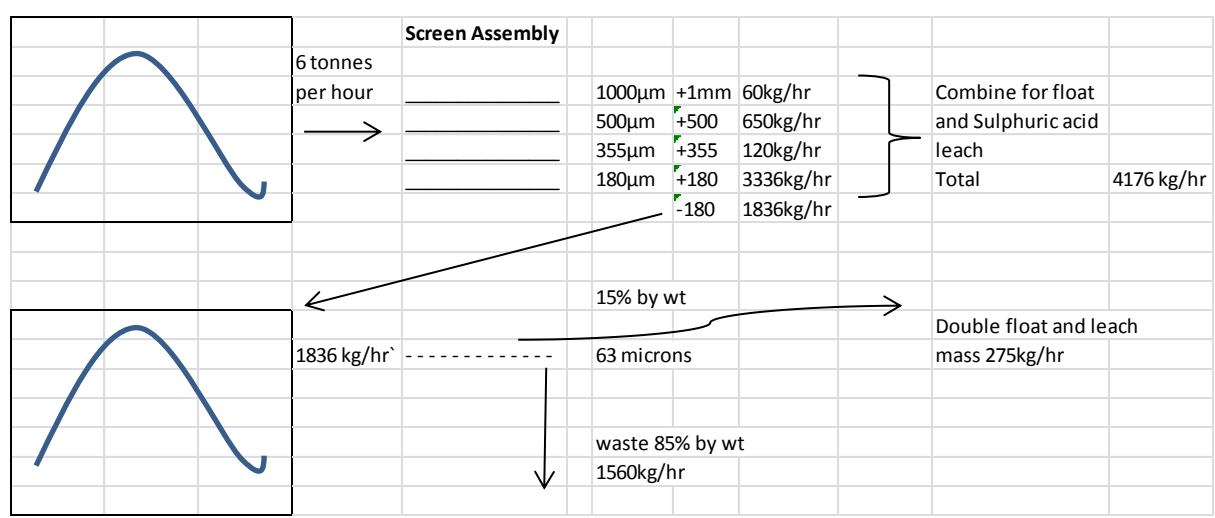
Used inten	Calc. conc	Stat. error	LLD	Analyzed	Line 3	Net int.	Used inten	Calc. conc	Stat. error	LLD	Analyzed	XRF %
187.4	48.4	1.21%	390.7 PPM	22.1 um								47.46
498.4	41.7	0.74%	258.0 PPM	30 um	Fe LA1-HI	0.01226			73.70%		0.68 um	42.39
												3.48
												2.12
0.2291	0.47	231%	0.29%	3.0 um								1.85
7.504	0.804	4.88%	449.1 PPM	24.6 um	Mn LA1-HI	0.00193			186%		0.56 um	1.01
0.05888	0.43	749%	0.97%	2.00 um								0.65
1.493	0.46	16.00%	519.5 PPM	11.9 um								0.29
												0.23
												0.16
0.3705	0.094	160%	436.8 PPM	16.4 um								0.12
1.309	0.069	37.70%	209.3 PPM	33 um	Zn LA1-HR	0.01031	0.3023	0.11	80.40%		0.73 um	0.07
4.038	0.052	13.00%	93.0 PPM	134 um	Sr LA1-HR	0.01922	0.5894	0.093	38.70%	224.0 PPM	2.92 um	0.0474
												0.046
												0.045
1.961	0.056	31.30%	144.4 PPM	58 um	As LA1-HI	0.2722	-1.11	-0.3	17.90%	956.3 PPM	1.30 um	0.023
1.506	0.022	136%	111.2 PPM	183 um	Zr LA1-HR	-0.00232	-0.08142	-0.009		154.3 PPM	3.9 um	0.007

**Appendix B: Cost-analysis**

Below is a more in-depth analysis in the cost-assessment of building a pilot plant at the Scunthorpe site than presented in the main text, complete with the sorts of processing the Desulph samples would undergo (I am particularly grateful to my supervisor Neil Rowson for his input on these calculations).

**Plant Costings**

Desulph 2: 10,000 tonnes per year (260 days, 29.5% Carbon) equates to 6 tonnes per hour of graphite feed.



**Income:**

Prices accessed: 01/10/2013

Industrial Minerals

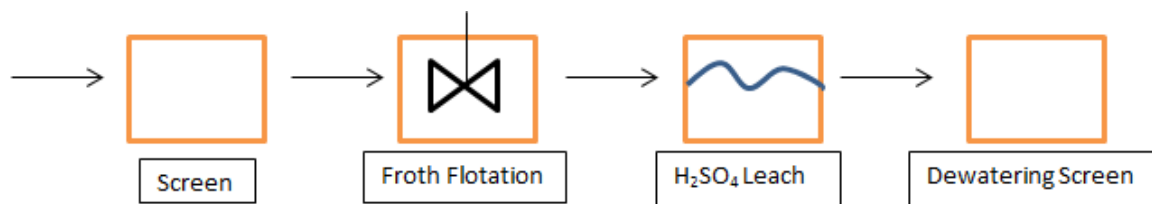
Graphite Flake 94-97% C

-100 mesh CIF (Europe) - \$900 per tonne

Saleable graphite 1820 Kg/hr

3033 Tonnes per year = \$ 2.7 million per year.

**Cost of Plant:**



Equipment Costs from Matche.com:

Four Deck Screen	\$22,000
Storage Bins x5	\$2,300 each
Centrifugal Pump	\$4,500
Dewater Screen	\$17,500
Reactor (glass lined) 400 gallon	\$26,000
Froth Flotation Tank	\$13,500
<b>Total (x10)</b>	<b>\$950,000</b>

**Total Capital Investment:**

(Based on Plant Design Economics, I Chem E Handbook, Solid/Fluid Processing Plant)

DIRECT COSTS:

Purchased Equipment	\$950,000
Purchased Equipment Installation (39%)	\$370,000
Control + Instruments (13%)	\$123,500
Piping (31%)	\$294,500
Electricals (10%)	\$95,000
Buildings (29%)	\$275,500
<b>Total Plant Direct Cost</b>	<b>\$2,108,500</b>

INDIRECT COSTS:

Engineering + Supervision (32%)	\$304,000
Construction Expenses (54%)	\$323,000
<b>Total Indirect Cost</b>	<b>\$627,000</b>

Contingency (10% of direct + indirect)	\$273,550
--	-----------

Total Erected Cost \$3,009,050

Working capital of cost (15%) \$451,357

**TOTAL CAPITAL INVESTMENT \$3,460,407**

**Conclusion:**

Plant Build 2 months

Land and waste disposal Free (carried out at Scunthorpe)

Payback Time ≈ 18 months

**PROJECT: Worthy of serious consideration**

### **Appendix C: Sub-180 micron Raw Results**

Below is a selection of the raw results pertaining to the investigation of the sub-180 micron Desulph material. As with Appendix A, whilst not exhaustive, it should give the reader a better idea of the real numbers obtained in this stage of the experiment (I am particularly grateful to Rajesh Gurung for his help in obtaining this data).

#### **Sieving Sizes**

<b>SEIVING DONE FOR DESULPH1, DESULPH2 &amp; DESULPH2 (BETA)</b>				
<i>from 06/05/2013 till 03/07/2013</i>				
<b>Sieving done for Desulph 2 (Beta)</b>				
			<b>Total Mass In (g):</b>	1200
<b>SN</b>	<b>Mesh Size (µm)</b>	<b>Bag Size(g)</b>	<b>Product + Bag (g)</b>	<b>Product (g)</b>
1	1000	3.6	27.6	24
2	500	3.6	22	18.4
3	355	3.6	25.4	21.8
4	180	3.6	150.7	147.1
5	90	3.6	215.2	211.6
6	63	3.6	282	278.4
7	< 63	3.6	500.2	496.6
<b>Total Mass Collected:</b>			1223.1	1197.9
<b>Mass Lost: (g)</b>		2.1		

Sieving done for Desulph 1				
			<b>Total Mass In (g):</b>	1000
<b>SN</b>	<b>Mesh Size (µm)</b>	<b>Bag Size(g)</b>	<b>Product + Bag (g)</b>	<b>Product (g)</b>
1	1000	3.8	29.4	25.6
2	500	3.8	75.4	71.6
3	355	3.8	62.4	58.6
4	180	3.8	181.6	177.8
5	90	3.8	167.6	163.8
6	63	3.8	85.2	81.4
7	< 63	3.8	422	418.2
<b>Total Mass Collected:</b>			1023.6	997
<b>Mass Lost: (g)</b>		3		

Sieving done for Desulph 1				
			<b>Total Mass In (g):</b>	500
<b>SN</b>	<b>Mesh Size (µm)</b>	<b>Bag Size(g)</b>	<b>Product + Bag (g)</b>	<b>Product (g)</b>
1	1000	0.7	11	10.3
2	500	0.7	15.1	14.4
3	355	0.7	15.3	14.6
4	180	3.7	97.4	93.7
5	< 180	3.7	368.6	364.9
<b>Total Mass Collected:</b>			507.4	497.9
<b>Mass Lost: (g)</b>		2.1		

Sieving done for Desulph 1				
			<b>Total Mass In (g):</b>	150
SN	Mesh Size (µm)	Bag Size(g)	Product + Bag (g)	Product (g)
1	150	0.8	5.3	4.5
2	125	0.8	8.2	7.4
3	90	0.8	19.4	18.6
4	72	0	0	0
5	63	0.8	16.3	15.5
6	< 63	3.7	107	103.3
	<b>Total Mass Collected:</b>		156.2	149.3
	<b>Mass Lost: (g)</b>	0.7		

Mass Balance

MASS BALANCE FOR DESULPH1, DESULPH2 & DESULPH2 (BETA)																																			
<i>from 06/05/2013 till 03/07/2013</i>																																			
<b>MASS BALANCE DATA 1 [13/06/2013]</b>																																			
<table border="1"> <thead> <tr> <th colspan="2">Raw product</th> </tr> <tr> <th>Product</th> <th>Mass(g) + Bag</th> </tr> </thead> <tbody> <tr> <td>DeSulph 1 [&lt;180 µm]</td> <td>50</td> </tr> <tr> <td>DeSulph 2 [&lt;180 µm]</td> <td>50</td> </tr> </tbody> </table>			Raw product		Product	Mass(g) + Bag	DeSulph 1 [<180 µm]	50	DeSulph 2 [<180 µm]	50	<table border="1"> <tbody> <tr> <td>Tee-froth Used:</td> <td>1 ml</td> </tr> <tr> <td>Small Bag (g):</td> <td>0.9 g</td> </tr> <tr> <td>Big Bag (g):</td> <td>3.6 g</td> </tr> </tbody> </table>			Tee-froth Used:	1 ml	Small Bag (g):	0.9 g	Big Bag (g):	3.6 g																
Raw product																																			
Product	Mass(g) + Bag																																		
DeSulph 1 [<180 µm]	50																																		
DeSulph 2 [<180 µm]	50																																		
Tee-froth Used:	1 ml																																		
Small Bag (g):	0.9 g																																		
Big Bag (g):	3.6 g																																		
<table border="1"> <thead> <tr> <th colspan="3">After Froth-Flotation</th> </tr> <tr> <th>Product</th> <th>Mass(g) + Bag</th> <th>Mass (g)</th> </tr> </thead> <tbody> <tr> <td>DeSulph 1 [Froth]</td> <td>22.9</td> <td>19.3</td> </tr> <tr> <td>DeSulph 1 [Waste]</td> <td>26.2</td> <td>25.3</td> </tr> <tr> <td><b>TOTAL</b></td> <td><b>49.1</b></td> <td><b>44.6</b></td> </tr> </tbody> </table>			After Froth-Flotation			Product	Mass(g) + Bag	Mass (g)	DeSulph 1 [Froth]	22.9	19.3	DeSulph 1 [Waste]	26.2	25.3	<b>TOTAL</b>	<b>49.1</b>	<b>44.6</b>	<table border="1"> <thead> <tr> <th colspan="3">After Froth-Flotation</th> </tr> <tr> <th>Product</th> <th>Mass(g) + Bag</th> <th>Mass (g)</th> </tr> </thead> <tbody> <tr> <td>DeSulph 2 [Froth]</td> <td>10</td> <td>9.1</td> </tr> <tr> <td>DeSulph 2 [Waste]</td> <td>32.3</td> <td>31.4</td> </tr> <tr> <td><b>TOTAL</b></td> <td><b>42.3</b></td> <td><b>40.5</b></td> </tr> </tbody> </table>			After Froth-Flotation			Product	Mass(g) + Bag	Mass (g)	DeSulph 2 [Froth]	10	9.1	DeSulph 2 [Waste]	32.3	31.4	<b>TOTAL</b>	<b>42.3</b>	<b>40.5</b>
After Froth-Flotation																																			
Product	Mass(g) + Bag	Mass (g)																																	
DeSulph 1 [Froth]	22.9	19.3																																	
DeSulph 1 [Waste]	26.2	25.3																																	
<b>TOTAL</b>	<b>49.1</b>	<b>44.6</b>																																	
After Froth-Flotation																																			
Product	Mass(g) + Bag	Mass (g)																																	
DeSulph 2 [Froth]	10	9.1																																	
DeSulph 2 [Waste]	32.3	31.4																																	
<b>TOTAL</b>	<b>42.3</b>	<b>40.5</b>																																	
<b>MASS BALANCE DATA 2 [15/06/2013]</b>																																			
<table border="1"> <thead> <tr> <th colspan="2">Raw product</th> </tr> <tr> <th>Product</th> <th>Mass(g) + Bag</th> </tr> </thead> <tbody> <tr> <td>DeSulph 1 [&lt;180 µm]</td> <td>50</td> </tr> <tr> <td>DeSulph 2 [&lt;180 µm]</td> <td>50</td> </tr> </tbody> </table>			Raw product		Product	Mass(g) + Bag	DeSulph 1 [<180 µm]	50	DeSulph 2 [<180 µm]	50	<table border="1"> <tbody> <tr> <td>Tee-froth Used:</td> <td>1 ml</td> </tr> <tr> <td>Small Bag (g):</td> <td>n/a</td> </tr> <tr> <td>Big Bag (g):</td> <td>3.6</td> </tr> </tbody> </table>			Tee-froth Used:	1 ml	Small Bag (g):	n/a	Big Bag (g):	3.6																
Raw product																																			
Product	Mass(g) + Bag																																		
DeSulph 1 [<180 µm]	50																																		
DeSulph 2 [<180 µm]	50																																		
Tee-froth Used:	1 ml																																		
Small Bag (g):	n/a																																		
Big Bag (g):	3.6																																		
<table border="1"> <thead> <tr> <th colspan="3">After Froth-Flotation</th> </tr> <tr> <th>Product</th> <th>Mass(g) + Bag</th> <th>Mass (g)</th> </tr> </thead> <tbody> <tr> <td>DeSulph 1 [Froth]</td> <td>14.6</td> <td>11</td> </tr> <tr> <td>DeSulph 1 [Waste]</td> <td>36.2</td> <td>36.2</td> </tr> <tr> <td><b>TOTAL</b></td> <td><b>50.8</b></td> <td><b>47.2</b></td> </tr> </tbody> </table>			After Froth-Flotation			Product	Mass(g) + Bag	Mass (g)	DeSulph 1 [Froth]	14.6	11	DeSulph 1 [Waste]	36.2	36.2	<b>TOTAL</b>	<b>50.8</b>	<b>47.2</b>	<table border="1"> <thead> <tr> <th colspan="3">After Froth-Flotation</th> </tr> <tr> <th>Product</th> <th>Mass(g) + Bag</th> <th>Mass (g)</th> </tr> </thead> <tbody> <tr> <td>DeSulph 2 [Froth]</td> <td>10</td> <td>6.4</td> </tr> <tr> <td>DeSulph 2 [Waste]</td> <td>32.3</td> <td>28.7</td> </tr> <tr> <td><b>TOTAL</b></td> <td><b>42.3</b></td> <td><b>35.1</b></td> </tr> </tbody> </table>			After Froth-Flotation			Product	Mass(g) + Bag	Mass (g)	DeSulph 2 [Froth]	10	6.4	DeSulph 2 [Waste]	32.3	28.7	<b>TOTAL</b>	<b>42.3</b>	<b>35.1</b>
After Froth-Flotation																																			
Product	Mass(g) + Bag	Mass (g)																																	
DeSulph 1 [Froth]	14.6	11																																	
DeSulph 1 [Waste]	36.2	36.2																																	
<b>TOTAL</b>	<b>50.8</b>	<b>47.2</b>																																	
After Froth-Flotation																																			
Product	Mass(g) + Bag	Mass (g)																																	
DeSulph 2 [Froth]	10	6.4																																	
DeSulph 2 [Waste]	32.3	28.7																																	
<b>TOTAL</b>	<b>42.3</b>	<b>35.1</b>																																	

**MASS BALANCE DATA 3 [18/06/2013]**

Raw product	
Product	Mass(g) + Bag
DeSulph 1 [<180 µm]	50
DeSulph 2 [<180 µm]	50

Tee-froth Used:	2 ml
Small Bag (g):	0.7
Big Bag (g):	n/a

After Froth-Flotation		
Product	Mass(g) + Bag	Mass (g)
DeSulph 1 [Froth]	20	19.3
DeSulph 1 [Waste]	26.1	25.4
<b>TOTAL</b>	<b>46.1</b>	<b>44.7</b>

After Froth-Flotation		
Product	Mass(g) + Bag	Mass (g)
DeSulph 2 [Froth]	11.2	10.5
DeSulph 2 [Waste]	32.8	32.1
<b>TOTAL</b>	<b>44</b>	<b>42.6</b>

**MASS BALANCE DATA 6 [18/06/2013]**

Raw product		
Product	Mass(g) + Bag	Tee-froth Used (ml)
DeSulph 1 [90 µm]	50	1
DeSulph 1 [63 µm]	25	0.5
DeSulph 1 [<63 µm]	50	1

Small Bag (g):	0.7
Big Bag (g):	n/a

After Froth-Flotation		
Product	Mass(g) + Bag	Mass (g)
DeSulph 1 [90 µm]	30.8	30.1
DeSulph 1 [63 µm]	9.8	9.1
DeSulph 1 [<63 µm]	18.4	17.7
<b>TOTAL</b>	<b>59</b>	<b>56.9</b>

After Froth-Flotation		
Product	Mass(g) + Bag	Mass (g)
DeSulph 1 [90 µm]	18.8	18.1
DeSulph 1 [63 µm]	14.5	13.8
DeSulph 1 [<63 µm]	26.5	25.8
<b>TOTAL</b>	<b>59.8</b>	<b>57.7</b>

**MASS BALANCE DATA 8 @ <63  $\mu\text{m}$  [25/06/2013]**

Product @ <63 $\mu\text{m}$		
Product	Mass(g) + Bag	Tee-froth Used (ml)
Sample A	50	1
Sample B	50	2
Sample C	50	3
Sample D	50	1

Small Bag (g):	n/a
Big Bag (g):	0.8

Froth after Froth-Flotation		
Product	Mass(g) + Bag	Mass (g)
Sample A	6.9	6.1
Sample B	7.4	6.6
Sample C	7.9	7.1
Sample D	2.9	2.1
<b>TOTAL</b>	<b>25.1</b>	<b>21.9</b>

Waste after Froth-Flotation		
Product	Mass(g) + Bag	Mass (g)
Sample A	39.9	39.1
Sample B	38.6	37.8
Sample C	39.4	38.6
Sample D (Waste 1)	37	36.2
Sample D (Waste 2)	4.9	4.1
<b>TOTAL</b>	<b>119.9</b>	<b>116.7</b>

**MASS BALANCE DATA 9 @ 63  $\mu\text{m}$  [25/06/2013]**

Product @ 63 $\mu\text{m}$		
Product	Mass(g) + Bag	Tee-froth Used (ml)
Sample A	50	1
Sample B	50	2
Sample C	50	3
Sample D	50	1

Small Bag (g):	n/a
Big Bag (g):	0.8

Froth after Froth-Flotation		
Product	Mass(g) + Bag	Mass (g)
Sample A	2.9	2.1
Sample B	2.5	1.7
Sample C	2.6	1.8
Sample D	1.8	1
<b>TOTAL</b>	<b>9.8</b>	<b>6.6</b>

Waste after Froth-Flotation		
Product	Mass(g) + Bag	Mass (g)
Sample A	41.5	40.7
Sample B	43.4	42.6
Sample C	43.2	42.4
Sample D (Waste 1)	42.2	41.4
Sample D (Waste 2)	2.6	1.8
<b>TOTAL</b>	<b>172.9</b>	<b>128.2</b>

**MASS BALANCE DATA 10 @ 90  $\mu\text{m}$  [25/06/2013]**

Product @ <63 $\mu\text{m}$		
Product	Mass(g) + Bag	Tee-froth Used (ml)
Sample A	50	1
Sample B	50	2
Sample C	50	3
Sample D	50	1

Small Bag (g):	n/a
Big Bag (g):	0.8

Froth after Froth-Flotation			Waste after Froth-Flotation		
Product	Mass(g) + Bag	Mass (g)	Product	Mass(g) + Bag	Mass (g)
Sample A	6.9	6.1	Sample A	39.9	39.1
Sample B	7.4	6.6	Sample B	38.6	37.8
Sample C	7.9	7.1	Sample C	39.4	38.6
Sample D	2.9	2.1	Sample D (Waste 1)	37	36.2
<b>TOTAL</b>	<b>25.1</b>	<b>21.9</b>	Sample D (Waste 2)	4.9	4.1
			<b>TOTAL</b>	<b>119.9</b>	<b>116.7</b>

LOSS AND EMISSION DATA FOR DESULPH1, DESULPH2 & DESULPH2 (BETA)							
<i>from 06/05/2013 till 03/07/2013</i>							
						DATA	1
Loss & Emission data for " Desulph1 & Desulph2 " samples @ <180 microns							
<i>Raw and froth floated samples of Desulph 1 and 2 with 1ml teefroth</i>							
SN	Products	Pre- Furnance			Post-Furnance		
		Crucible (g)	Crucible + Product	Product (g)	Crucible + Product (g)	Graphite (g)	Graphite (%)
1	Desulph 1 A: [Raw]	18.4566	18.9831	0.5265	18.8494	0.3928	25.39%
2	Desulph 1 B: [Raw]	13.7587	14.3362	0.5775	14.1895	0.4308	25.40%
3	Desulph 2 A: [Raw]	12.5621	13.0891	0.527	12.9598	0.3977	24.54%
4	Desulph 2 B: [Raw]	22.3282	22.8153	0.4871	22.6945	0.3663	24.80%
5	Desulph 1 A: [<180, FF]	24.9852	25.4984	0.5132	25.228	0.2428	52.69%
6	Desulph 1 B: [<180, FF]	15.2797	15.8327	0.553	15.5697	0.29	47.56%
7	Desulph 2 A: [<180, FF]	24.8982	25.2389	0.3407	25.0702	0.172	49.52%
8	Desulph 2 B: [<180, FF]	17.6072	18.1604	0.5532	17.9049	0.2977	46.19%

						DATA	2
Loss & Emission data for " Desulph1 & Desulph2 " samples @ <180 microns							
<i>Froth floted samples of Desulph 1 and 2 with 1 ml teefroth</i>							
SN	Products	Pre- Furnance			Post-Furnance		
		Crucible (g)	Crucible + Product	Product (g)	Crucible + Product (g)	Graphite (g)	Graphite (%)
1	Desulph 1 A: [FF]	13.748	14.2971	0.5491	13.9965	0.2485	54.74%
2	Desulph 1 B: [FF]	18.4577	18.9558	0.4981	18.6946	0.2369	52.44%
3	Desulph 2 A: [FF]	17.5929	18.1799	0.587	17.9061	0.3132	46.64%
4	Desulph 2 B: [FF]	22.3254	22.8732	0.5478	22.6128	0.2874	47.54%
5	Desulph 1 A: [WASTE]	15.2688	15.8359	0.5671	15.8004	0.5316	6.26%
6	Desulph 1 B: [WASTE]	12.5534	13.1113	0.5579	13.0762	0.5228	6.29%
7	Desulph 2 A: [WASTE]	24.8934	25.4366	0.5432	25.3339	0.4405	18.91%
8	Desulph 2 B: [WASTE]	24.9874	25.4429	0.4555	25.3537	0.3663	19.58%

						DATA	3
<b>Loss &amp; Emission data for " Desulph1 &amp; Desulph2 " samples @ &lt;180 microns</b>							
<i>Froth floated samples of Desulph 1 and 2 with 2 ml teefroth</i>							
		Pre- Furnance			Post-Furnance		
SN	Products	Crucible (g)	Crucible + Product	Product (g)	Crucible + Product (g)	Graphite (g)	Graphite (%)
1	Desulph 1 A: [FF]	18.4543	18.9724	0.5181	18.7035	0.2492	51.90%
2	Desulph 1 B: [FF]	17.5949	18.1049	0.51	17.8503	0.2554	49.92%
3	Desulph 2 A: [FF]	13.723	14.2891	0.5661	14.242	0.519	8.32%
4	Desulph 2 B: [FF]	24.983	25.5445	0.5615	25.4979	0.5149	8.30%
5	Desulph 1 A: [WASTE]	15.2644	15.7539	0.4895	15.5256	0.2612	46.64%
6	Desulph 1 B: [WASTE]	24.8829	25.4123	0.5294	25.1621	0.2792	47.26%
7	Desulph 2 A: [WASTE]	12.5632	13.0764	0.5132	12.9802	0.417	18.75%
						DATE:	18/06/2013

						DATA	4
<b>Loss &amp; Emission data for " Desulph1 " samples @ 150 µm, 125 µm, 90 µm, 63 µm, &lt; 63 µm</b>							
<i>Raw samples of Desulph 1 with 1 ml teefroth</i>							
		Pre- Furnance			Post-Furnance		
SN	Products	Crucible (g)	Crucible + Product	Product (g)	Crucible + Product (g)	Graphite (g)	Graphite (%)
1	Desulph 1 A: [150 µm]	18.4563	19.0174	0.5611	18.602	0.1457	74.03%
2	Desulph 1 B: [150 µm]	12.5655	13.1015	0.536	12.6974	0.1319	75.39%
3	Desulph 1 A: [125 µm]	22.3202	22.8484	0.5282	22.5772	0.257	51.34%
4	Desulph 1 B: [125 µm]	15.2642	15.8421	0.5779	15.5329	0.2687	53.50%
5	Desulph 1 A: [90 µm]	24.9892	25.5596	0.5704	25.2816	0.2924	48.74%
6	Desulph 1 B: [90 µm]	17.5976	18.1572	0.5596	17.882	0.2844	49.18%
7	Desulph 1 A: [63 µm]	13.7234	14.2807	0.5573	14.078	0.3546	36.37%
8	Desulph 1 B: [<63 µm]	24.89	25.4554	0.5654	25.3728	0.4828	14.61%

						DATA	5
Loss & Emission data for " Desulph2 " samples @ 150 µm, 125 µm, 90 µm, < 90 µm							
Raw samples of Desulph 2 with 1 ml teefroth							
SN	Products	Pre- Furnance			Post-Furnance		
		Crucible (g)	Crucible + Product	Product (g)	Crucible + Product (g)	Graphite (g)	Graphite (%)
1	Desulph 2 A: [150 µm]	18.4553	19.2186	0.7633	18.7324	0.2771	63.70%
2	Desulph 2 B: [150 µm]	22.3222	22.8638	0.5416	22.5369	0.2147	60.36%
3	Desulph 2 A: [125 µm]	24.8893	25.4608	0.5715	25.0638	0.1745	69.47%
4	Desulph 2 B: [125 µm]	24.9854	25.5418	0.5564	25.1739	0.1885	66.12%
5	Desulph 2 A: [90 µm]	13.7168	14.1889	0.4721	13.9526	0.2358	50.05%
6	Desulph 2 B: [90 µm]	17.5923	18.1505	0.5582	17.8785	0.2862	48.73%
7	Desulph 2 A: [<90 µm]	15.2571	15.8258	0.5687	15.6997	0.4426	22.17%
8	Desulph 2 B: [<90 µm]	12.5582	13.134	0.5758	13.0066	0.4484	22.13%

						DATA	6
Loss & Emission data for " Desulph1 " samples @ 90 µm, 63 µm, < 63 µm							
Raw samples of Desulph 1 with 1 ml teefroth							
SN	Products	Pre- Furnance			Post-Furnance		
		Crucible (g)	Crucible + Product	Product (g)	Crucible + Product (g)	Graphite (g)	Graphite (%)
1	Desulph 1 A: [90 µm]	12.5657	13.2252	0.6595	12.9239	0.3582	45.69%
2	Desulph 1 B: [90 µm]	24.8812	25.431	0.5498	25.194	0.3128	43.11%
3	Desulph 1 A: [63 µm]	24.9905	25.4229	0.4324	25.3204	0.3299	23.70%
4	Desulph 1 B: [63 µm]	13.7232	14.2838	0.5606	14.1544	0.4312	23.08%
5	Desulph 1 A: [<63 µm]	17.5961	18.1399	0.5438	18.0657	0.4696	13.64%
6	Desulph 1 B: [<63 µm]	15.2664	15.8409	0.5745	15.7619	0.4955	13.75%

						DATE:	20/06/2013
--	--	--	--	--	--	-------	------------

						DATA	7
<b>Loss &amp; Emission data for " Desulph2 (Beta) " samples @ 90 µm, 63 µm, &lt; 63 µm</b>							
<i>Raw samples of Desulph 2 (Beta) with 1 ml teefroth</i>							
		Pre- Furnance			Post-Furnance		
SN	Products	Crucible (g)	Crucible + Product	Product (g)	Crucible + Product (g)	Graphite (g)	Graphite (%)
1	Desulph 2 A: [90 µm]	15.2644	15.8302	0.5658	15.7904	0.526	7.03%
2	Desulph 2 B: [90 µm]	12.5658	13.1564	0.5906	13.1195	0.5537	6.25%
3	Desulph 2 A: [63 µm]	24.9929	25.5311	0.5382	25.4987	0.5058	6.02%
4	Desulph 2 B: [63 µm]	13.721	14.3166	0.5956	14.2804	0.5594	6.08%
5	Desulph 2 A: [<63 µm]	17.5997	18.1555	0.5558	18.127	0.5273	5.13%
6	Desulph 2 B: [<63 µm]	24.8796	25.4573	0.5777	25.4285	0.5489	4.99%
						DATE:	24/06/2013

						DATA	8
<b>Loss &amp; Emission data for " Desulph2 (Beta) " samples @ &lt; 63 µm</b>							
<i>Froth Floated data of Desulph 2 (Beta) with varying ml of teefroth @ &lt;63 µm</i>							
		Pre- Furnance			Post-Furnance		
SN	Products	Crucible (g)	Crucible + Product	Product (g)	Crucible + Product (g)	Graphite (g)	Graphite (%)
1	Sample A [Froth]	15.3018	15.8746	0.5728	15.7957	0.4939	13.77%
2	Sample A [Waste]	12.624	13.18	0.556	13.1283	0.5043	9.30%
3	Sample B [Froth]	25.0018	25.5279	0.5261	25.4678	0.466	11.42%
4	Sample B [Waste]	24.8868	25.3936	0.5068	25.344	0.4572	9.79%
5	Sample C [Froth]	17.6346	18.2074	0.5728	18.1186	0.484	15.50%
6	Sample C [Waste]	13.7499	14.3383	0.5884	14.2825	0.5326	9.48%
7	Sample D [Re-Froth]	18.4538	18.9447	0.4909	18.8937	0.4399	10.39%
8	Sample D [Waste 1]	21.7478	22.2712	0.5234	22.2212	0.4734	9.55%
9	Sample D [Waste 2]	17.9209	18.5293	0.6084	18.4686	0.5477	9.98%
						DATE:	25/06/2013

						<b>DATA</b>	9
<b>Loss &amp; Emission data for " Desulph2 (Beta) " samples @ 63 µm</b>							
<i>Froth Floated data of Desulph 2 (Beta) with varying ml of teefroth @ 63 µm</i>							
SN	Products	Pre- Furnance			Post-Furnance		
		Crucible (g)	Crucible + Product	Product (g)	Crucible + Product (g)	Graphite (g)	Graphite (%)
1	Sample A [Froth]	18.4503	19.0448	0.5945	18.8877	0.4374	26.43%
2	Sample A [Waste]	17.6478	18.1751	0.5273	18.1218	0.474	10.11%
3	Sample B [Froth]	13.7517	14.3112	0.5595	14.1025	0.3508	37.30%
4	Sample B [Waste]	15.2958	15.8341	0.5383	15.7851	0.4893	9.10%
5	Sample C [Froth]	25.0027	25.6167	0.614	25.4307	0.428	30.29%
6	Sample C [Waste]	17.923	18.5242	0.6012	18.4652	0.5422	9.81%
7	Sample D [Re-Froth]	24.8862	25.5002	0.614	25.3047	0.4185	31.84%
8	Sample D [Waste 1]	21.7398	22.3365	0.5967	22.2804	0.5406	9.40%
9	Sample D [Waste 2]	12.6197	13.1431	0.5234	13.0385	0.4188	19.98%
						<b>DATE:</b>	27/06/2013

						<b>DATA</b>	10
<b>Loss &amp; Emission data for " Desulph2 (Beta) " samples @ 90 µm</b>							
<i>Froth Floated data of Desulph 2 (Beta) with varying ml of teefroth @ 90 µm</i>							
SN	Products	Pre- Furnance			Post-Furnance		
		Crucible (g)	Crucible + Product	Product (g)	Crucible + Product (g)	Graphite (g)	Graphite (%)
1	Sample A [Froth]	18.4514	18.9719	0.5205	18.7018	0.2504	51.89%
2	Sample A [Waste]	24.9978	25.5745	0.5767	25.547	0.5492	4.77%
3	Sample B [Froth]	17.6735	18.2265	0.553	17.9354	0.2619	52.64%
4	Sample B [Waste]	13.7525	14.2843	0.5318	14.2632	0.5107	3.97%
5	Sample C [Froth]	17.932	18.4822	0.5502	18.2052	0.2732	50.35%
6	Sample C [Waste]	15.3095	15.9183	0.6088	15.8776	0.5681	6.69%
7	Sample D [Re-Froth]	12.613	13.5813	0.9683	12.9082	0.2952	69.51%
8	Sample D [Waste 1]	24.8828	25.4583	0.5755	25.4379	0.5551	3.54%
8	Sample D [Waste 2]	21.7398	22.2902	0.5504	22.1855	0.4457	19.02%
9	Sample D [Waste 3]	12.8386	13.3556	0.517	13.2827	0.4441	14.10%
						<b>DATE:</b>	03/07/2013

						DATA	11
<b>Loss &amp; Emission data for " Desulph1 " samples @ 90 µm, 63 µm, &lt; 63 µm</b>							
<i>Froth Floated data of Desulph 1 with 1 ml teefroth</i>							
		<b>Pre- Furnance</b>			<b>Post-Furnance</b>		
<b>SN</b>	<b>Products</b>	<b>Crucible (g)</b>	<b>Crucible + Product</b>	<b>Product (g)</b>	<b>Crucible + Product (g)</b>	<b>Graphite (g)</b>	<b>Graphite (%)</b>
1	Desulph 1 A: [90 µm]	24.8896	25.7765	0.8869	25.1521	0.2625	70.40%
2	Desulph 1 B: [90 µm]	13.745	14.312	0.567	14.2765	0.5315	6.26%
3	Desulph 1 A: [63 µm]	17.616	18.2769	0.6609	17.8961	0.2801	57.62%
4	Desulph 1 B: [63 µm]	15.2838	15.7978	0.514	15.7856	0.5018	2.37%
5	Desulph 1 A: [<63 µm]	25.0014	25.8482	0.8468	25.67	0.6686	21.04%
6	Desulph 1 B: [<63 µm]	12.577	13.1278	0.5508	13.0818	0.5048	8.35%
						DATE:	25/06/2013

## **Appendix D: Morgan PLC Data/Communications**

Below is a selection of messages and data pertaining to how the samples performed thermally and electronically when undergoing industrial processing into crucibles (as outlined in the main text) (I am particularly grateful to Alex Daily and his colleagues at Morgan PLC for all of the information below). The full correspondences and presentation slides are available on request.

### **Morgan PLC Processing Notes**

#### Determination of Ash of routine samples

##### Equipment

Platinum lid

Scales (0.1mg resolution)

Muffle Furnace

##### Method

Ignite lid in muffle furnace at 850°C for 10 min

Remove and cool

Weight lid: (A )

Add ~1g kish graphite flakes

Weigh lid + graphite: (B )

Then either:

Place in muffle furnace at 850°C for 24h

Remove and cool

Weigh lid (C )

Or

Place in muffle furnace at 850°C for 2 hours,

Remove and cool,

Weigh lid,

Return lid and sample to furnace for further hour,

Repeat until mass no longer decreases (C )

Calculation:

$$\% \text{ Ash} = \frac{C - A}{B - A} \times 100$$

Notes:

The method is an internal testing procedure, with minor modifications.

The original method suggested cooling the samples in a desiccator however this appears to have negligible effect on the results so was not used.

For the graphite samples received from MIRO (ash content 2.5-8.5%) the samples were usually completed after 4 hours.

24h was used in some cases to reduce the number of steps required

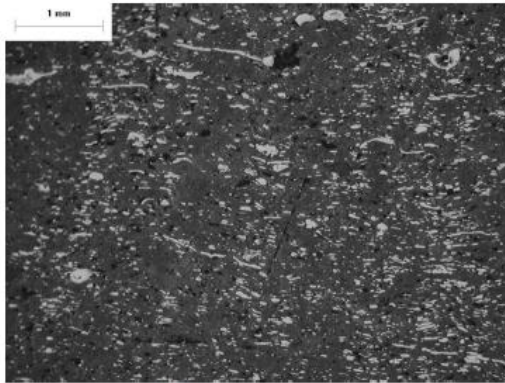
## Copper Impregnation

- The suitability of kish graphite in copper impregnated materials was investigated.
- Both natural and kish graphites based composites were pressed.
- Heat treatment to 1300°C
- Impregnation with liquid copper under pressure

## Copper impregnation micrographs

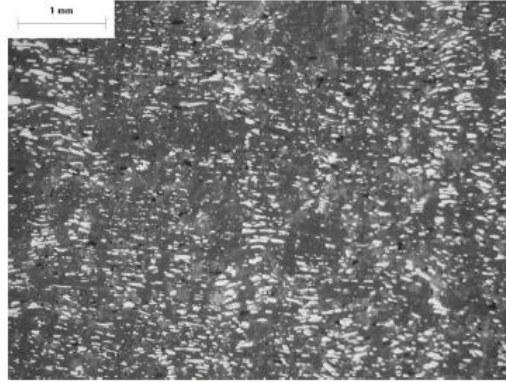
The parts were produced with 7.2% resin,

1mm



Kish Graphite

1mm



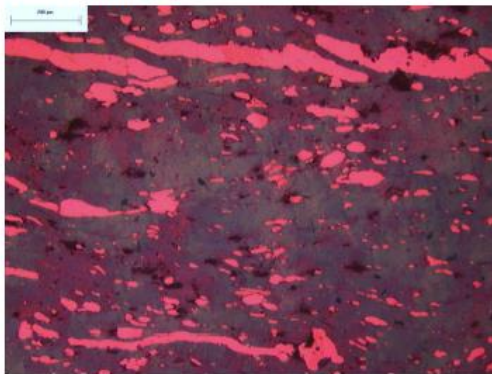
Natural Graphite

- Even distribution of copper throughout the blocks
- No 'letterboxing'

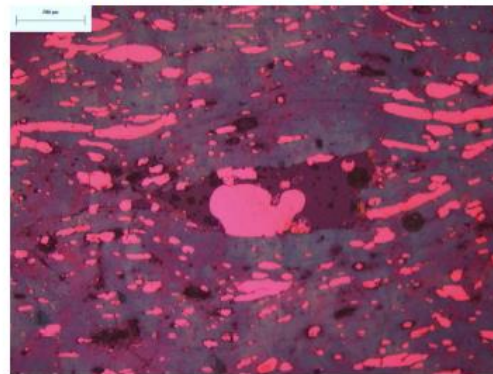


## Copper impregnation micrographs

200um



200um

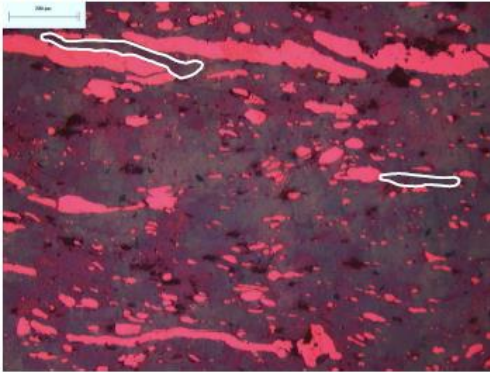


- Kish showed signs of poorer mixing with the resin

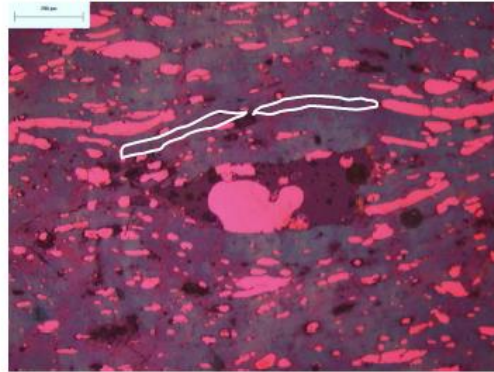


## Copper impregnation micrographs

200um



200um



- Kish showed signs of poorer mixing with the resin

**Appendix E: Lab Safety Documentation**

Please see attached.

**THE UNIVERSITY OF BIRMINGHAM**  
**SCHOOL OF CHEMICAL ENGINEERING**  
**CHEMICAL HAZARD AND RISK ASSESSMENT**

School/Dept

Assessment Number

Assessor   
(Plus Supervisor for Undergraduate Assessor)

Date of Assessment

Notes Guidance on making an assessment is given in *Chemical Hazard and Risk Assessment (GUIDANCE/22/CHRA/03)*.

Guidance is also available from the attached *Guidance on Completing the Chemical Hazard and Risk Assessment Form*.

Substance data is available in HAZDAT. Use a continuation sheet or word processor to expand any section of this form.

**1** **LOCATION OF THE WORK or ACTIVITY**

**2** **PERSONS WHO MAY BE AT RISK**

List names where possible

**3** **ACTIVITY ASSESSED**

State whether specific (the default) or generic

<b>4</b>	<b>MATERIALS INVOLVED</b>	You may wish to attach copies of data sheet(s) or to indicate the source of your information: you are strongly recommended to consult the University <i>Hazdat</i> database, which is kept as up-to-date as possible concerning hazardous chemicals and the like, and with information on correct procedures and methods as appropriate.
----------	---------------------------	--

NAME AND CAS NUMBER OF MATERIAL	AMOUNT and FORM	HAZARD	RISK PHRASES (use text only)	REPORTABLE? (Y/N)
<b>Note:</b> you <i>must</i> check to see whether any of the materials you use are subject to regulations concerning ozone depletion, are covered by Chemical Weapons laws, or are sensitizers or carcinogens. Many such materials are 'reportable' through the University Health and Safety Unit. Consult the HAZDAT database for details.				
Steel waste products from Corus: mainly iron oxides	Kg of fine powder	Avoid dust	Avoid inhalation Avoid contact with skin/eyes	n
Diesel oil	Few ml	irritant	Avoid contact with skin/eyes	n
Alcohol frother	Few ml	-	Avoid contact with skin/eyes	n
Dilute Hydrochloric acid 1%	100 ml	corrosive	Avoid contact with skin/.eyes	n

**If one or more of the materials is reportable, have you notified the University Health and Safety Unit?**      Yes     No  see note

<b>5</b>	<b>INTENDED USE and JUSTIFICATION (where appropriate)</b>
----------	---

Give brief details and attach protocol/instructions. Justification is needed for exceptionally hazardous substances (see note 5)	
Physical separation and dilute HCl leaching will be used to produce kish graphite concentrate from steel waste streams	

6

**RISKS to HEALTH and SAFETY from INTENDED USE**

From personal exposure or hazardous reactions. Refer to OELs, flash points, etc., as appropriate. Are pregnant women, breast-feeding mothers especially at risk?

Good chemical practice

HCl leach will be done in fume cupboard

Graphite analysis will be carried out on furnace- this will be in fume cupboard

7

**CONCLUSIONS ABOUT RISKS**

Is level of risk acceptable? Can risk be prevented or reduced by change of substance/procedure? Are control measures necessary?

Acceptable

8

**CONTROL MEASURES**

*In addition* to Good Chemical Practice, eg., fume cupboard, etc. Any special requirements, eg., glove type, etc.

**Engineering controls:** indicate that in your view, the risk is acceptable if the procedure is carried out in: **1)** the open laboratory (**n.b. this is now rare**); **2)** a recirculating fume cupboard; **3)** a ducted fume cupboard; **4)** a glove box; **5)** only in a purpose built facility; **6)** Another specialised enclosure (please specify what you intend) You must select at least one of these, and use at least that level of containment, or not conduct the procedure.

These options represent an increasing level of containment. For further guidance on deciding the appropriate control measures to use consult Hazardous Substances Policy Schedule 3.11 and 3.13

**1**       **2**       **3**       **4**       **5**   
**6**  Specify .....

<b>SPECIAL REQUIREMENTS:</b>	<i>e.g.</i> special glassware; no vibration; Fluoro-plastic apparatus; no dry chemicals on heated surfaces; must be in the dark.
None	

**9**      **INSTRUCTION/TRAINING**

Specify course(s) and/or special arrangements.	Will be given by NAR
<b>LOCAL WARNINGS:</b> On occasion a procedure will necessitate warning workers nearby, and instructing them in particular or special emergency actions which may be required.	
Is this necessary for this procedure?      Yes <input type="checkbox"/> No <input checked="" type="checkbox"/>	

**10**      **MONITORING**

Performance of control measures, <i>eg</i> fume hood flow rates required			
Personal exposure	<b>If in doubt, seek advice from the University Health and Safety unit</b>	Health Surveillance	<b>Specify measures agreed with the Health and Safety Unit</b>

11

**WASTE DISPOSAL PROCEDURE**

**HAZARDOUS WASTES REQUIRING SPECIAL MEASURES FOR DISPOSAL** (specify waste and disposal method see Hazardous Sustances Policy Schedule 7) Include name, 6 digit code and H numbers if to be sent away for disposal.

N/A

*DISPOSAL OF WASTE SOLVENTS (The School Code of Practice for the Disposal of Waste Solvents must be observed)*

Halogenated

Non-Halogenated

12

**REVIEW**

Enter the date or circumstances for review of assessment (maximum review interval is now 1 year)

AFTER ONE MONTH

13

**EMERGENCY ACTION**

**TO CONTROL HAZARDS**

To stabilize situation eg spread absorbant on liquid spill; eliminate sources of ignition, etc.

<b>TO PROTECT PERSONNEL</b>	Evacuation, protection for personnel involved in clean-up, Special First Aid
-----------------------------	--

<b>TO RENDER SITE OF EMERGENCY SAFE</b>	Clean-up/decontamination requirements and protocols
---	---

<b>14</b>	<b>EMERGENCY CONTACT</b>	NAME(S)	NEIL ROWSON	PHONE(S)	X45298
				(Home and School contacts, please)	

Signed ..... (Assessor) Date  
 .....

Signed .....NEIL ROWSON..... (Supervisor) Date  
 .....8/11/12.....